Supporting Information

Multinuclear Silver(I) XPhos Complexes with Cyclooctatetraene: Photochemical C-C bond cleavage of Acetonitrile and Cyanide bridged Ag clusters formation

A. Grirrane,*[a] E. Álvarez,[b] J. Albero,[a] H. García*[a] and A. Corma*[a]

[a] Instituto Universitario de Tecnología Química CSIC-UPV, Universidad Politécnica de Valencia, Av. De los Naranjos s/n, 46022 Valencia (Spain), E-mail: grirrane@itq.upv.es, hgarcia@qim.upv.es, acorma@itq.upv.es, joalsan6@upvnet.upv.es

[b] Instituto de Investigaciones Químicas IIQ-CSIC-US, Consejo Superior de Investigaciones Científicas – Universidad de Sevilla. Av. Américo Vespucio 49, 41092 Sevilla (Spain), E-mail: ealvarez@iiq.csic.es

Contents:

Experimental Section: Details of preparation, isolation and full characterization of new silver (I) complexes **1, 2, 3** and **4**, including NMR spectroscopy, ESI-MS spectra, combustion analysis and X-ray structure analysis data for: **1** (CCDC-1443116), **2** (1443117), **2a** (1443118) and **5** (1443119) contain the supplementary crystallographic data for this paper. These data can also be obtained free of charge from The Cambridge Crystallographic Data centre via http//www.ccdc.cam.ac.uk/data_request/cif. All reactions were carried out under Ar atmosphere in dried solvent using a commercial solvent purification system. ^{1}H NMR spectra were recorded on a Bruker AV300 (300 MHz) spectrometer. Chemical shifts of ^{1}H signals are reported in ppm using the solvent peak as the internal standard ($CHDCl_2$: 5.27 ppm). Data are reported as follows: chemical shift, integral, multiplicity (s = singlet, br = broad, d = doublet, dd = doublet of doublets, t = triplet, tt = triplet of triplets, sept = septuplet, m = multiplet), coupling constants (Hz) and assignment. Chemical shifts of ^{13}C are reported also in ppm using the solvent peak as the internal standard (CD_2Cl_2: 53.84 ppm). ^{31}P spectra were recorded on a Bruker 300 MHz spectrometer. Chemical shifts are reported in ppm and coupling constants in Hz. ESI-MS were performed on an Agilent Esquire 6000 instrument. HRESI-MS were performed on an Waters (XEVO QTOF MS) instrument equipped with ACQUIM UPLC BEH C18 (1,7 mm x 2,1 mm x 100 mm) column to obtain the exact mass for the corresponding compounds. Elemental analyses were performed on an EuroEA Elemental Analyser Eurovector. HR-TEM was acquired using a JEOL JEM-2100F with the field emission gun operating at 200 kV and the images were recorded using a GATAN Orius SC600A. Cyclic voltametries provided by the VersaSTAT 3 apparatus of the Ag complexes, carried out in CH_2Cl_2 at 1 mM concentration and the scan rate was 0.1 V/s and a Ag/AgCl KCl sat. electrode was used as reference electrode, the electrolyte was prepared in CH_2Cl_2 and consisted in a tert-butylammonium perchloride dissolution at 0.1 M and the counter electrode consisted in a Pt wire electrode and as working electrode a round Pt electrode of 2mm^2 was used. The measurements were carried out under N_2 atmosphere.

Isolation of cationic [(XPhos-Ag)(η^4-cot)][SbF$_6$] complex (1): A mixture of $[Ag]^+[SbF_6]^-$ (**1**) salt (0.086 g, 0.25 mmol), 2-di-tert-butylphosphinobiphenyl (XPhos) (0.075 g, 0.25 mmol) and cyclooctatetraene (0.028 g, 0.27 mmol) was dissolved in dried-dichloromethane (2 ml). The solution was stirred at RT under argon atmosphere for 24 h. Then, the resulting transparent pal yellow mixture was diluted with additional 2 ml of CH_2Cl_2, filtered and the supernatant was covered carefully with a layer of 2 ml of n-hexane. Pal yellow crystals of **1** suitable for X-ray crystallography (see Table S1 and Fig. S1 for details) were obtained by standing for 48 h at -8 ºC, which were collected by filtration, washed with cold n-hexane and dried under vacuum to yield the corresponding complex silver(I)(2-biphenyl)di-*tert*-butylphosphane-cyclooctatetraene hexafluoroantimonate complex (**1**) (0.175 g, 94 % yield). ^{1}H NMR (300 MHz, CD_2Cl_2, 25ºC): δ (ppm) = 7.91 (m, 1 H; ArH); 7.60-7.41 (m, 5 H; ArH), 7.32 (dd, 2 H; ArH), 7.26-7.17 (m, 1 H; ArH), 5.98 (s, 8 H; COT), 1.28 (s, 9 H; *tert*-butyl CH_3), 1.23 (s, 9 H; *tert*-butyl CH_3) (see Fig. S2 for details). ^{13}C NMR (75 MHz, CD_2Cl_2, 25ºC): δ (ppm) = 149.09 (d, ^{3}J(Ag-^{13}C) = 1.122 Hz), 148.84 (d, ^{3}J(Ag-^{13}C) = 1.391 Hz), 143.185 (d, ^{4}J(Ag-^{13}C) = 1.151 Hz), 143.06 (d, ^{4}J(Ag-^{13}C) = 1.398 Hz), 134.61 (d), 133.09 (d), 132.61 (s, 8C, COT), 131.63 (d), 131.01, 128.68, 128.29 (dd, ^{5}J(Ag-^{13}C) = 1.679 Hz and ^{5}J(Ag-^{13}C) = 1.633 Hz), 128.01 (t), 126.54 (d, ^{2}J(Ag-^{13}C) = 4.261 Hz), 126.19 (d, ^{2}J(Ag-^{13}C) = 4.138 Hz), 35.83 (d, ^{2}J(Ag-^{13}C) = 4.403 Hz), 35.70 (d, ^{2}J(Ag-^{13}C) = 4.430 Hz), 30.81 (d, ^{3}J(Ag-^{13}C) = 1.727 Hz), 30.69 (d, ^{3}J(Ag-^{13}C) = 1.711 Hz) (see Fig. S3 for details). ^{13}C DEPT-135 NMR (75 MHz, CD_2Cl_2): δ (ppm) = Negative Signals: none; Positive Signals: 134.61 (d), 133.09 (d), 132.60 (s, 8C, COT), 131.62 (d), 131.62, 128.68, 128.31 (d), 128.26 (d), 127.96 (t), 30.80 (d), 30.68 (d) (see fig. S4). ^{31}P NMR (CD_2Cl_2): δ (ppm) = 42.01 (dd, ^{1}J(^{107}Ag-^{31}P) = 573.98 Hz and ^{1}J(^{109}Ag-^{31}P) = 662.38 Hz). (see Fig. S5 for details). ESI-MS (+MS) *m/z*: 549.1 amu for [$C_{28}H_{35}AgF_6PSb$ (**1**) -

$SbF_6^- + K]^{2+}$ and 405.1 amu for $[C_{28}H_{35}AgF_6PSb$ (**1**) - SbF_6^- - COT$]^+$ with the ^{107}Ag and ^{109}Ag isotopes (see Fig. S6 for details). ESI-MS (-MS) *m/z*: 234.9 and 236.7 amu for counter anion $[SbF_6]^-$ of complex **1** with the ^{121}Sb and ^{123}Sb isotopes (see Fig. S6 for details). ^{1}H NMR (300 MHz, CD_2Cl_2, - 80 ºC): δ (ppm) = 7.83 (m, 1 H; ArH); 7.55-7.32 (m, 5 H; ArH), 7.25 (d, 2 H; ArH), 7.20-7.12 (m, 1 H; ArH), 5.94 (d, 8 H; COT), 1.15 (s, 9 H; *tert*-butyl CH_3), 1.10 (s, 9 H; *tert*-butyl CH_3) (see Fig. S7 for details). ^{13}C NMR (75 MHz, CD_2Cl_2, - 80 ºC): δ (ppm) = 148.68, 148.43, 143.19, 143.07, 134.95 (d), 133.08 (d), 132.86 (s, 4C, COT), 132.18 (s, 4C, COT), 131.49, 131.39, 128.37, 127.23, 126.27 (d), 125.94 (d), 35.43 (d), 35.30 (d), 30.52, 30.42 (see Fig. S8 for details). Elemental analysis, calc. for $C_{28}H_{35}AgF_6PSb$ (**1**) (%): C, 45.07; H, 4.73. Found: C, 45.27; H, 5.02.

Isolation of cationic $[(XPhos\text{-}Ag)_2\ \mu_2\text{-}(\eta^4{:}\eta^2\text{-cot})][SbF_6]_2$ complex (2): A mixture of $[Ag]^+[SbF_6]^-$ (**1**) salt (0.086 g, 0.25 mmol), 2-di-tert-butylphosphinobiphenyl (XPhos) (0.075 g, 0.25 mmol) and cyclooctatetraene (0.013 g, 0.125 mmol) was dissolved in dried-dichloromethane (2 ml). The solution was stirred at RT under argon atmosphere for 24 h. Then, the resulting transparent pal yellow mixture was diluted with additional 2 ml of CH_2Cl_2, filtered and the supernatant was covered carefully with a layer of 2 ml of n-hexane. Colorless crystals of **2** suitable for X-ray crystallography (see Table S2 and Fig. S9 for details) were obtained by standing for 48 h at -2 ºC, which were collected by filtration, washed with cold n-hexane and dried under vacuum to yield the corresponding complex [silver(I)(2-biphenyl)di-*tert*-butylphosphane]$_2$[cyclooctatetraene] hexafluoroantimonate complex (**2**) (0.160 g, 92 % yield). ^{1}H NMR (300 MHz, CD_2Cl_2, 25ºC): δ (ppm) = 7.90 (m, 2 H; ArH); 7.59-7.44 (m, 10 H; ArH), 7.29 (d, 4 H; ArH), 7.27-7.21 (m, 2 H; ArH), 5.99 (br, 8 H; COT), 1.29 (s, 18 H; *tert*-butyl CH_3), 1.23 (s, 18 H; *tert*-butyl CH_3) (see Fig. S10 for details). ^{13}C NMR (75 MHz, CD_2Cl_2, 25ºC): δ (ppm) = 149.26 (d, ^3J(Ag-^{13}C) = 1.653 Hz), 149.01 (d, ^3J(Ag-^{13}C) = 1.690 Hz), 142.88 (d, ^4J(Ag-^{13}C) = 1.451 Hz), 142.76 (d, ^4J(Ag-^{13}C) = 1.378 Hz), 134.34 (d), 132.77 (d), 132.63 (s, 8C, COT), 131.52 (d), 130.43, 128.57 (d), 128.50 (t), 128.24 (dd, ^5J(Ag-^{13}C) = 2.023 Hz and ^5J(Ag-^{13}C) = 2.000 Hz), 126.66 (d, ^2J(Ag-^{13}C) = 4.729 Hz), 126.29 (d, ^2J(Ag-^{13}C) = 4.501 Hz), 35.79 (d, ^2J(Ag-^{13}C) = 4.622 Hz), 35.65 (d, ^2J(Ag-^{13}C) = 4.756 Hz), 30.89 (d, ^3J(Ag-^{13}C) = 1.922 Hz), 30.76 (d, ^3J(Ag-^{13}C) = 2.010 Hz) (see Fig. S11 for details). ^{13}C DEPT-135 NMR (75 MHz, CD_2Cl_2): δ (ppm) = Negative Signals: none; Positive Signals: 134.34 (d), 132.78 (d), 132.63 (s, 8C, COT), 131.52 (d), 130.44, 128.57, 128.49 (t), 128.265 (d), 128.21 (d), 30.89 (d), 30.76 (d) (see fig. S12). ^{31}P NMR (CD_2Cl_2): δ (ppm) = 43.54 (dd, ^1J(^{107}Ag-^{31}P) = 626.59 Hz and ^1J(^{109}Ag-^{31}P) = 723.63 Hz) (see Fig. S13 for details). ESI-MS (+MS) *m/z*: 938.9 amu for $[C_{48}H_{62}Ag_2F_{12}P_2Sb_2$ (**2**) - 2 SbF_6^- + Na$]^+$ with the ^{107}Ag and ^{109}Ag isotopes (see Fig. S14 for details). Elemental analysis, calc. for $C_{48}H_{62}Ag_2F_{12}P_2Sb_2$ (**2**) (%): C, 41.53; H, 4.50. Found: C, 41.50; H, 4.69.

Isolation of cationic $[(XPhos\text{-}Ag)_3(\mu_3\text{-cot})][SbF_6]_3$ complex (3): A mixture of $[Ag]^+[SbF_6]^-$ (**1**) salt (0.086 g, 0.25 mmol), 2-di-tert-butylphosphinobiphenyl (XPhos) (0.075 g, 0.25 mmol) and cyclooctatetraene (0.0087 g, 0.083 mmol) was dissolved in dried-dichloromethane (2 ml). The solution was stirred at RT under argon atmosphere for 24 h. Then, the resulting transparent pal yellow mixture was diluted with additional 2 ml of CH_2Cl_2, filtered and the supernatant was covered carefully with a layer of 2 ml

of n-hexane. Colorless micro crystals of **3** were obtained by standing for 48 h at -8 ºC, which were collected by filtration, washed with cold n-hexane and dried under vacuum to yield the corresponding complex [silver(I)(2-biphenyl)di-*tert*-butylphosphane]$_3$[cyclooctatetraene] hexafluoroantimonate complex (**3**) (0.151 g, 90 % yield). ^{1}H NMR (300 MHz, CD_2Cl_2, 25ºC): δ (ppm) = 7.89 (m, 3 H; ArH); 7.60-7.48 (m, 15 H; ArH), 7.27 (d, 9 H; ArH), 6.01 (s, 8 H; COT), 1.28 (s, 27 H; *tert*-butyl CH_3), 1.23 (s, 27 H; *tert*-butyl CH_3) (see Fig. S15 for details). ^{13}C NMR (75 MHz, CD_2Cl_2, 25ºC): δ (ppm) = 149.31 (d, ^3J(Ag-^{13}C) = 1.749 Hz), 149.06 (d, ^3J(Ag-^{13}C) = 1.779 Hz), 142.78 (d, ^4J(Ag-^{13}C) = 1.756 Hz), 142.65 (d, ^4J(Ag-^{13}C) = 1.580 Hz), 134.27 (d), 132.70, 132.65 (s, 8C, COT), 131.48 (d), 130.24, 128.64 (t), 128.54, 128.21 (dd, ^5J(Ag-^{13}C) = 2.161 Hz and ^5J(Ag-^{13}C) = 2.152 Hz), 126.72 (d, ^2J(Ag-^{13}C) = 4.755 Hz), 126.34 (d, ^2J(Ag-^{13}C) = 4.808 Hz), 35.77 (d, ^2J(Ag-^{13}C) = 4.752 Hz), 35.63 (d, ^2J(Ag-^{13}C) = 4.733 Hz), 30.91 (d, ^3J(Ag-^{13}C) = 2.068 Hz), 30.78 (d, ^3J(Ag-^{13}C) = 2.085 Hz) (see Fig. S16 for details). ^{13}C DEPT-135 NMR (75 MHz, CD_2Cl_2): δ (ppm) = Negative Signals: none; Positive Signals: 134.26 (d), 132.70, 132.64 (s, 8C, COT), 131.47 (d), 130.24, 128.64 (t), 128.54 (d), 128.22 (dd), 30.91 (d), 30.78 (d) (see fig. S17). ^{31}P NMR (CD_2Cl_2): δ (ppm) = 44.82 (dd, ^1J(^{107}Ag-^{31}P) = 670.40 Hz and ^1J(^{109}Ag-^{31}P) = 773.86 Hz) (see Fig. S18 for details). ESI-MS (+MS) *m/z*: 1347.5 amu for [$C_{68}H_{89}Ag_3F_{18}P_3Sb_3$ (**3**) - 3 SbF_6^- + Na]$^+$ with the ^{107}Ag and ^{109}Ag isotopes (see Fig. S23 for details). Elemental analysis, calc. for $C_{68}H_{89}Ag_3F_{18}P_3Sb_3$ (**3**) (%): C, 40.23; H, 4.42. Found: C, 40.30; H, 4.54.

Isolation of cationic [(XPhos-Ag)$_4$(μ$_4$-(cot)][SbF$_6$]$_4$ complex (4): A mixture of [Ag]$^+$[SbF_6]$^-$ (**1**) salt (0.086 g, 0.25 mmol), 2-di-tert-butylphosphinobiphenyl (XPhos) (0.075 g, 0.25 mmol) and cyclooctatetraene (0.0066 g, 0.063 mmol) was dissolved in dried-dichloromethane (2 ml). The solution was stirred at RT under argon atmosphere for 24 h. Then, the resulting transparent pal yellow mixture was diluted with additional 2 ml of CH_2Cl_2, filtered and the supernatant was covered carefully with a layer of 2 ml of n-hexane. Colorless micro crystals of **4** were obtained by standing for 48 h at -8 ºC, which were collected by filtration, washed with cold n-hexane and dried under vacuum to yield the corresponding complex [silver(I)(2-biphenyl)di-*tert*-butylphosphane]$_4$[cyclooctatetraene] hexafluoroantimonate complex (**4**) (0.155 g, 92 % yield). ^{1}H NMR (300 MHz, CD_2Cl_2, 25ºC): δ (ppm) = 7.89 (m, 4 H; ArH); 7.59-7.47 (m, 20 H; ArH), 7.32-7.21 (m, 12 H; ArH), 6.00 (s, 8 H; COT), 1.29 (s, 36 H; *tert*-butyl CH_3), 1.24 (s, 36 H; *tert*-butyl CH_3) (see Fig. S19 for details). ^{13}C NMR (75 MHz, CD_2Cl_2, 25ºC): δ (ppm) = 149.30 (d, ^3J(Ag-^{13}C) = 1.952 Hz), 149.05 (d, ^3J(Ag-^{13}C) = 1.705 Hz), 142.79 (d, ^4J(Ag-^{13}C) = 1.881 Hz), 142.66 (d, ^4J(Ag-^{13}C) = 1.560 Hz), 134.25 (d), 132.71, 132.64 (s, 8C, COT), 131.49 (d), 130.23, 128.65 (t), 128.54, 128.23 (dd, ^5J(Ag-^{13}C) = 2.178 Hz and ^5J(Ag-^{13}C) = 2.195 Hz), 126.71 (d, ^2J(Ag-^{13}C) = 4.767 Hz), 126.33 (d, ^2J(Ag-^{13}C) = 4.792 Hz), 35.79 (d, ^2J(Ag-^{13}C) = 4.831 Hz), 35.65 (d, ^2J(Ag-^{13}C) = 4.803 Hz), 30.92 (d, ^3J(Ag-^{13}C) = 2.066 Hz), 30.79 (d, ^3J(Ag-^{13}C) = 2.090 Hz) (see Fig. S20 for details). ^{13}C DEPT-135 NMR (75 MHz, CD_2Cl_2): δ (ppm) = Negative Signals: none; Positive Signals: 134.25 (d), 132.71, 132.64 (s, 8C, COT), 131.49 (d), 130.23, 128.66 (t), 128.54, 128.23 (dd), 30.92 (d), 30.79 (d) (see fig. S21). ^{31}P NMR (CD_2Cl_2): δ (ppm) = 45.21 (dd, ^1J(^{107}Ag-^{31}P) = 682.47 Hz and ^1J(^{109}Ag-^{31}P) = 788.01 Hz) (see Fig. S22 for details). Elemental analysis, calc. for $C_{88}H_{116}Ag_4F_{24}P_4Sb_4$ (**4**) (%): C, 39.55; H, 4.38. Found: C, 40.01; H, 4.43.

Crystal X-Ray structure analysis for 1, 2, 2a and 5.

Crystals of suitable size for X-ray diffraction analysis were coated with dry perfluoropolyether and mounted on glass fibers and fixed in a cold nitrogen stream (T = 193 K) to the goniometer head. Data collection was performed on a Bruker-Nonius X8Apex-II CCD diffractometer, using monochromatic radiation λ(Mo K_α) = 0.71073 Å, by means of ω and φ scans with a width of 0.50 degree. The data were reduced (SAINT) [1] and corrected for absorption effects by the multi-scan method (SADABS) [2]. The structures were solved by direct methods (SIR-2002) [3] and refined against all F^2 data by full-matrix least-squares techniques (SHELXTL-6.12) [4] minimizing $w[F_o^2-F_c^2]^2$. All the non-hydrogen atoms were refined anisotropically, while C-H hydrogen atoms were placed in geometrically calculated positions using a riding model. Some geometric restraints (DFIX command), the ADP restraint SIMU and the rigid bond restraint DELU were used to make the geometric and ADP values of the disordered atoms more reasonable.

[1] Bruker (**2007**). *APEX2*. Bruker AXS Inc., Madison, Wisconsin, USA.

[2] Bruker (**2001**). *APEX2*. Bruker AXS Inc., Madison, Wisconsin, USA.

[3] C. M. Burla, M. Camalli, B. Carrozzini, G. L. Cascarano, C. Giacovazzo, G. Poliori, R. Spagna, *SIR2002*: the program; (**2003**). *J. Appl. Cryst.* **36**, 1103–1103.

[4] G. M. Sheldrick, Acta Crystallogr., Sect. A: Found. Crystallogr., **2008**, 64, 112-122.

Table S1: Crystal data and structure refining for **1**:

Empirical formula	$C_{28}H_{35}AgF_6PSb$	
	$[C_{28}H_{35}AgP, F_6Sb]$	
Formula weight	746.15	
Temperature	193(2) K	
Wavelength	0.71073 Å	
Crystal system	Monoclinic	
Space group	$P\ 2_1/n$	
Unit cell dimensions	a = 9.1981(4) Å	α= 90°.
	b = 11.3126(5) Å	β= 94.618(3)°.
	c = 27.9588(13) Å	γ = 90°.
Volume	2899.8(2) $Å^3$	
Z	4	
Density (calculated)	1.709 Mg/m^3	
Absorption coefficient	1.716 mm^{-1}	
F(000)	1480	
Crystal size	0.50 x 0.43 x 0.25 mm^3	
Theta range for data collection	2.32 to 25.25°.	
Index ranges	-11<=h<=11, -11<=k<=13, -30<=l<=33	
Reflections collected	28254	
Independent reflections	5196 [R(int) = 0.0480]	
Completeness to theta = 25.25°	98.9 %	
Absorption correction	Semi-empirical from equivalents	
Max. and min. transmission	0.6536 and 0.4267	
Refinement method	Full-matrix least-squares on F^2	
Data / restraints / parameters	5196 / 36 / 340	
Goodness-of-fit on F^2	1.105	
Final R indices [I>2sigma(I)]	R1 = 0.0411, wR2 = 0.1086	
R indices (all data)	R1 = 0.0529, wR2 = 0.1148	
Largest diff. peak and hole	1.153 and -1.521 e.$Å^{-3}$	

Ag(1)-P(1): 2.4137(11) Å Ag(1)-C(22): 2.432(4) Å Ag(1)-C(21): 2.465(4) Å

Ag(1)-C(25): 2.921(4) Å Ag(1)-C(26): 2.972(5) Å

Ag(1)-C7(ipso): 2.910 Å Ag(1)-C12(nearest): 2.872 Å

Fig. S1: ORTEP drawing of **1**:

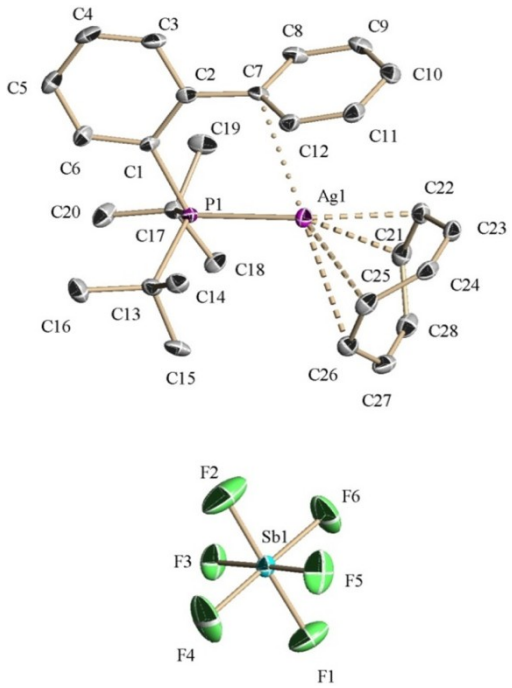

(Left) Crystal packing detail of **1** viewed along the a-axis, hydrogen atoms are omitted for clarity. (Right) Crystal packing detail of **1** viewed along the a-axis, showing the presence of inter- and intramolecular hydrogen bonds.

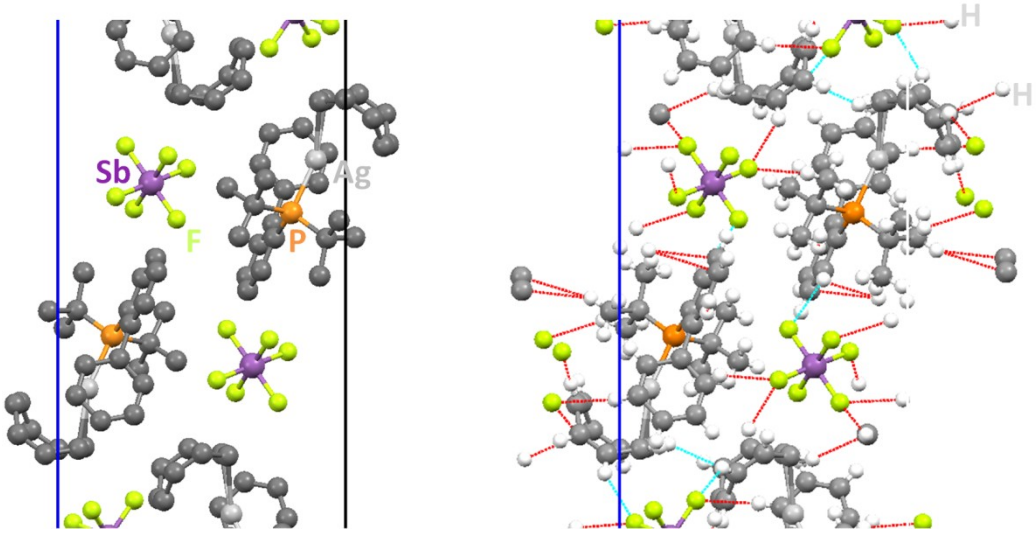

Fig. S2: ^{1}H NMR spectrum in CD_2Cl_2 for isolated complex **1**.

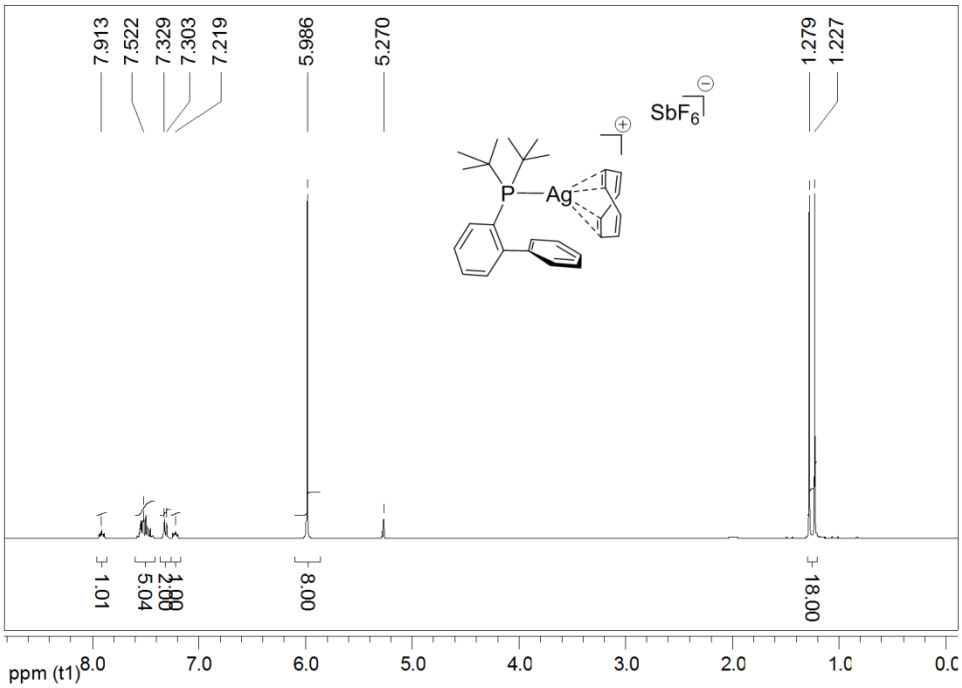

Magnification of the ^{1}H NMR peaks (**1**):

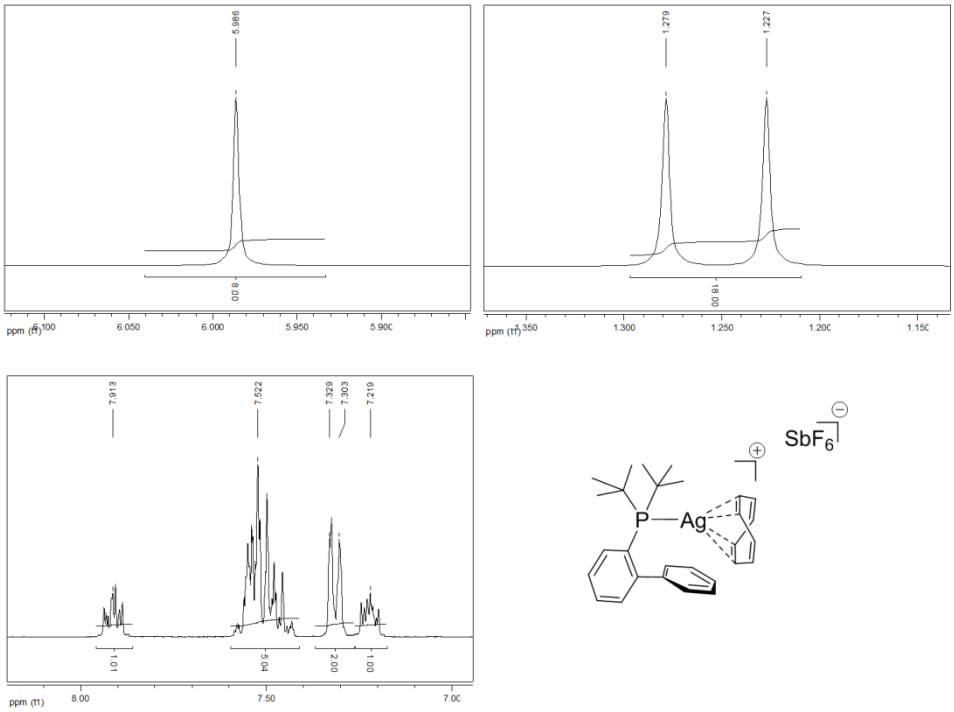

Fig. S3: ^{13}C NMR spectrum in CD_2Cl_2 for isolated complex (**1**).

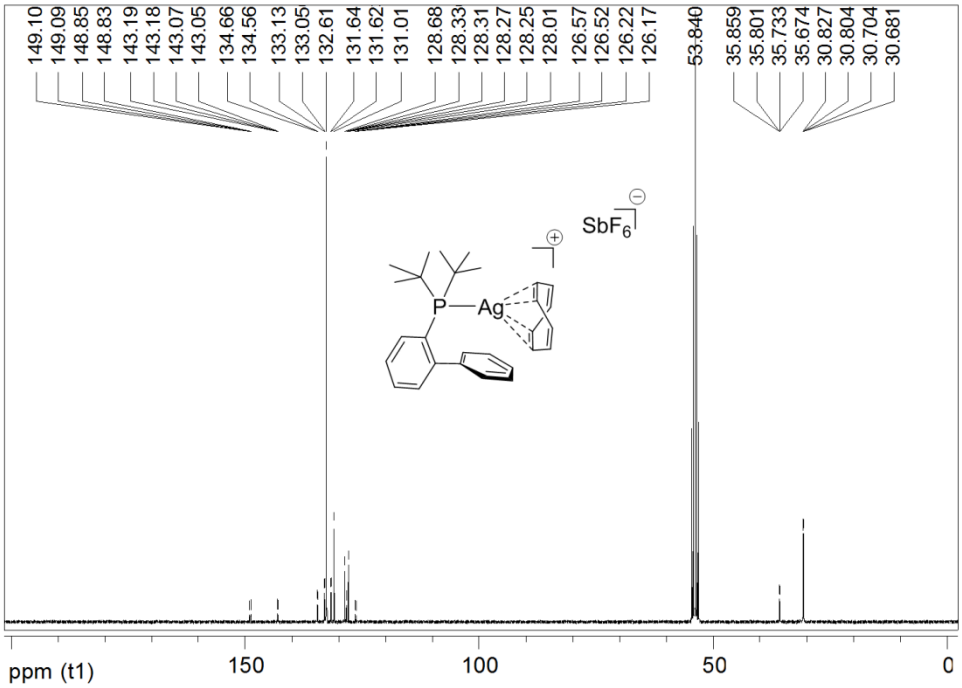

Magnification of the ^{13}C NMR peaks (**1**):

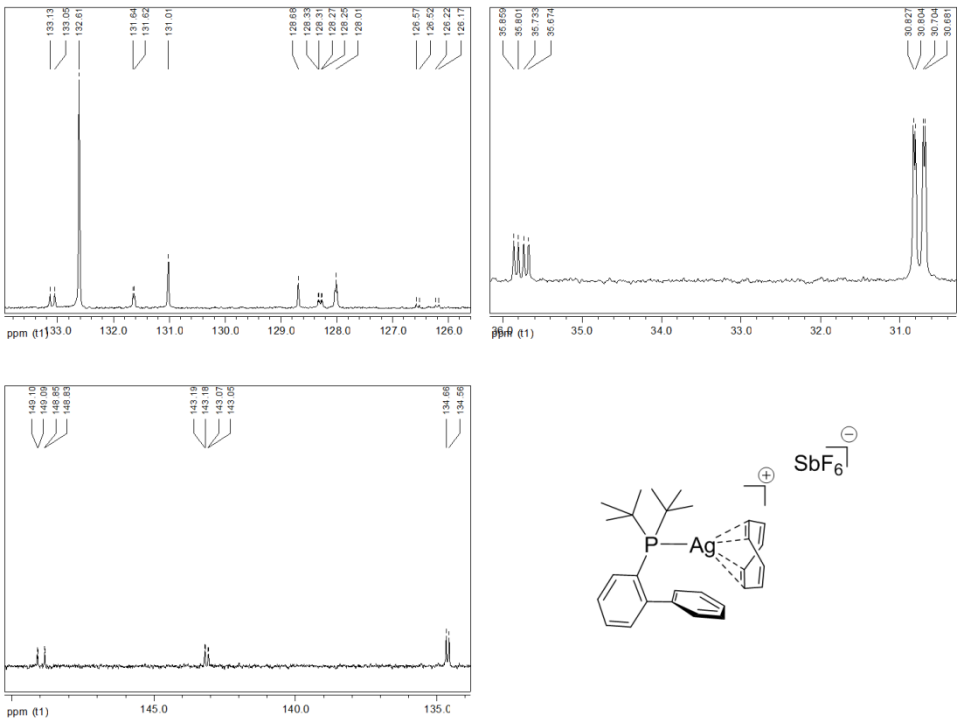

Fig. S4: DEPT. 135 spectrum in CD_2Cl_2 for isolated complex **1**.

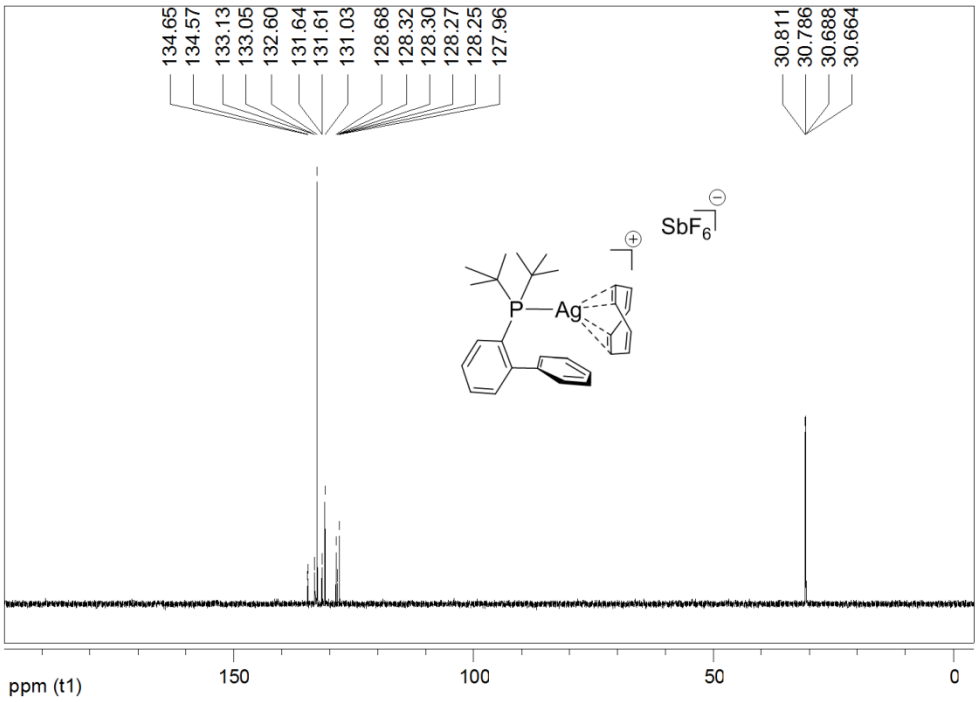

Magnification of the DEPT. 135 NMR peaks (**1**):

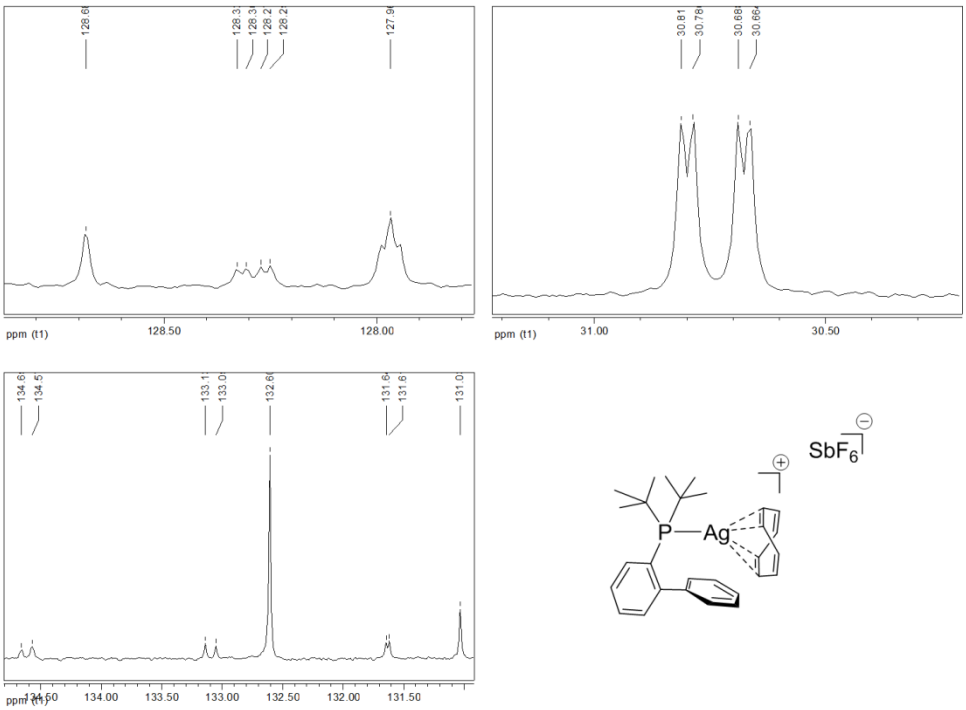

Fig. S5: ^{31}P NMR spectrum in CD_2Cl_2 for isolated complex **1**.

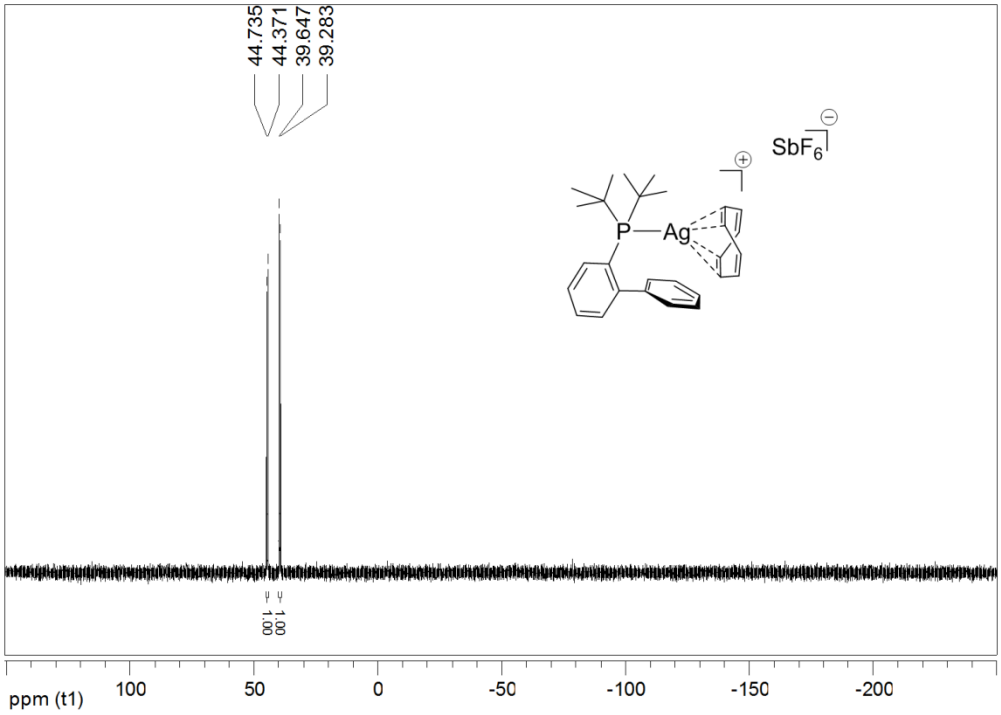

Magnification of the ^{31}P NMR peaks (**1**):

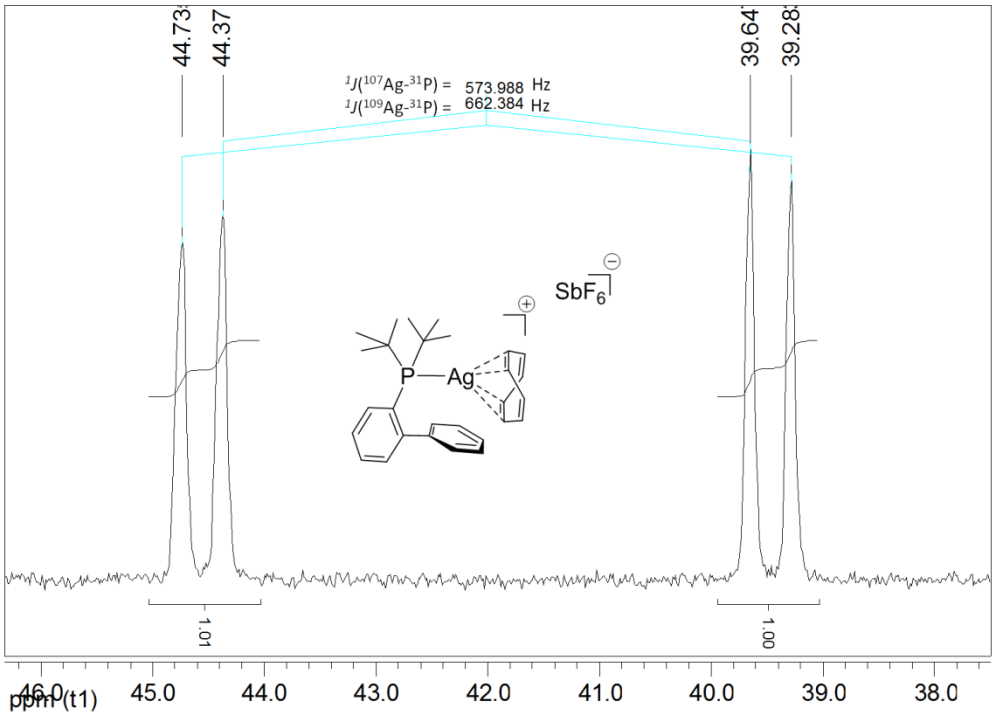

Fig. S6: ESI-MS data for **1**.

Acquisition Parameter:
Comment: 1/1000 CH_2Cl_2 1/500 CH_3CN
Instrument: esquire6000

Ion Source Type	ESI	Ion Polarity	Positive	Alternating Ion Polarity	off
Mass Range Mode	Std/Normal	Scan Begin	65 m/z	Scan End	2000 m/z
Capillary Exit	128.5 Volt	Skim 1	40.0 Volt	Trap Drive	55.0
Accumulation Time	362 µs	Averages	8 Spectra	Auto MS/MS	off

- ESI-MS (+MS) *m/z*: 549.1 amu for $[C_{28}H_{35}AgF_6PSb$ (**1**) - SbF_6^- and + K$]^{2+}$:
- ESI-MS (+MS) *m/z*: 405.1 amu for $[C_{28}H_{35}AgF_6PSb$ (**1**) - SbF_6^- and - C_8H_8 ring$]^+$:

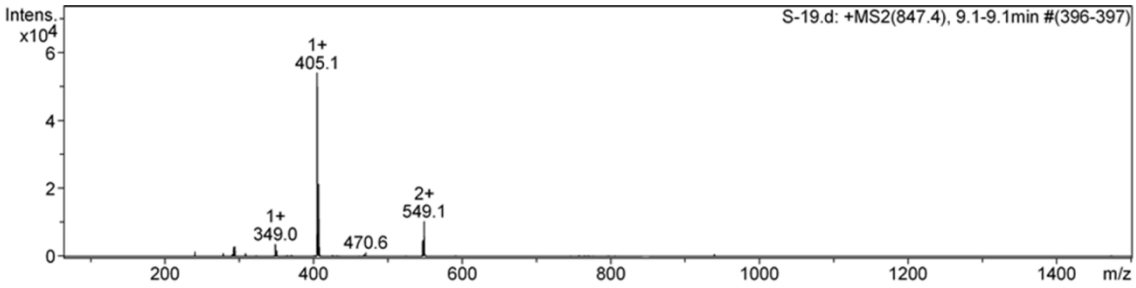

- ESI-MS (-MS) *m/z*: 234.9 and 236.7 amu for counter anion $[SbF_6]^-$ of complex **1**:

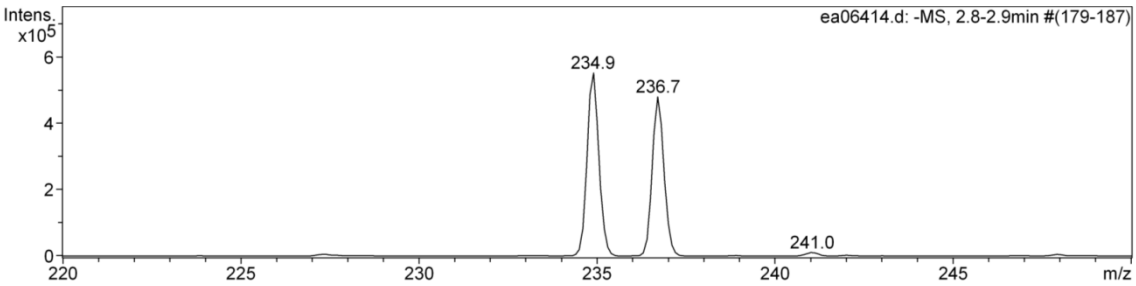

Fig. S7: ^{1}H NMR spectrum in CD_2Cl_2 for isolated complex **1** recorded at -80 ºC.

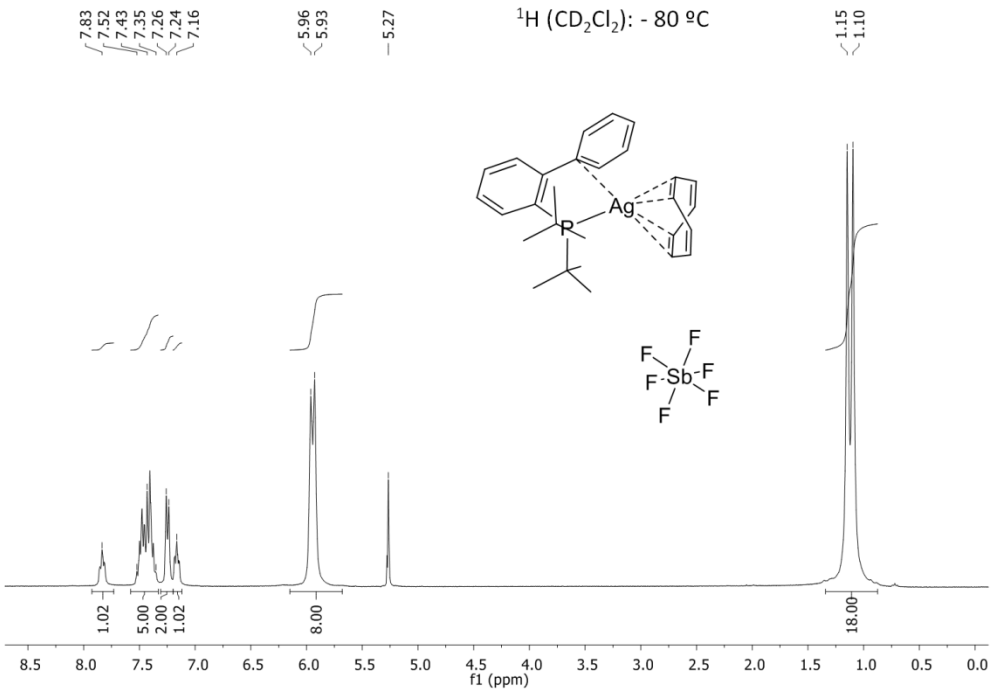

Magnification of the ^{1}H NMR peaks (**1**) at -80 ºC:

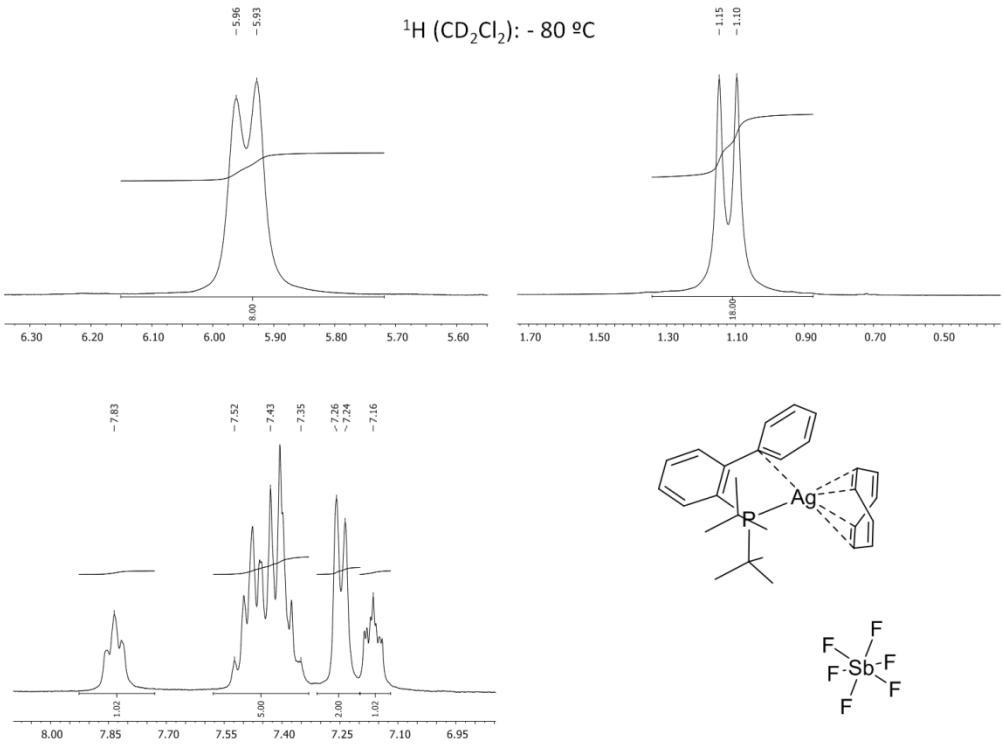

Fig. S8: ^{13}C NMR spectrum in CD_2Cl_2 for isolated complex **1** recorded at -80 ºC.

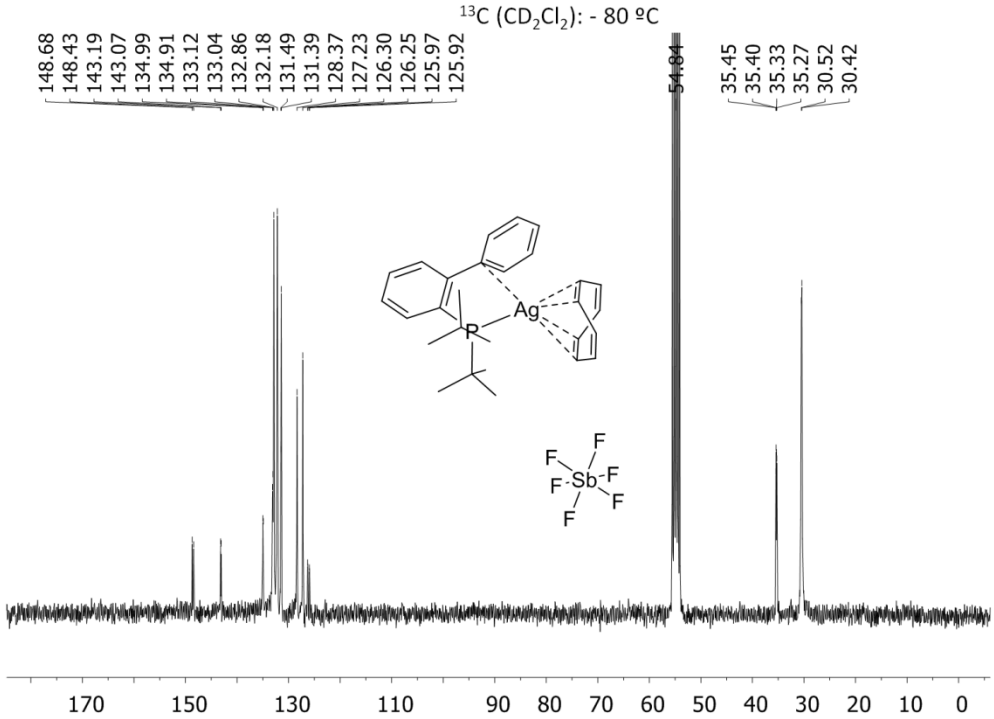

Magnification of the ^{13}C NMR peaks (**1**) at -80 ºC:

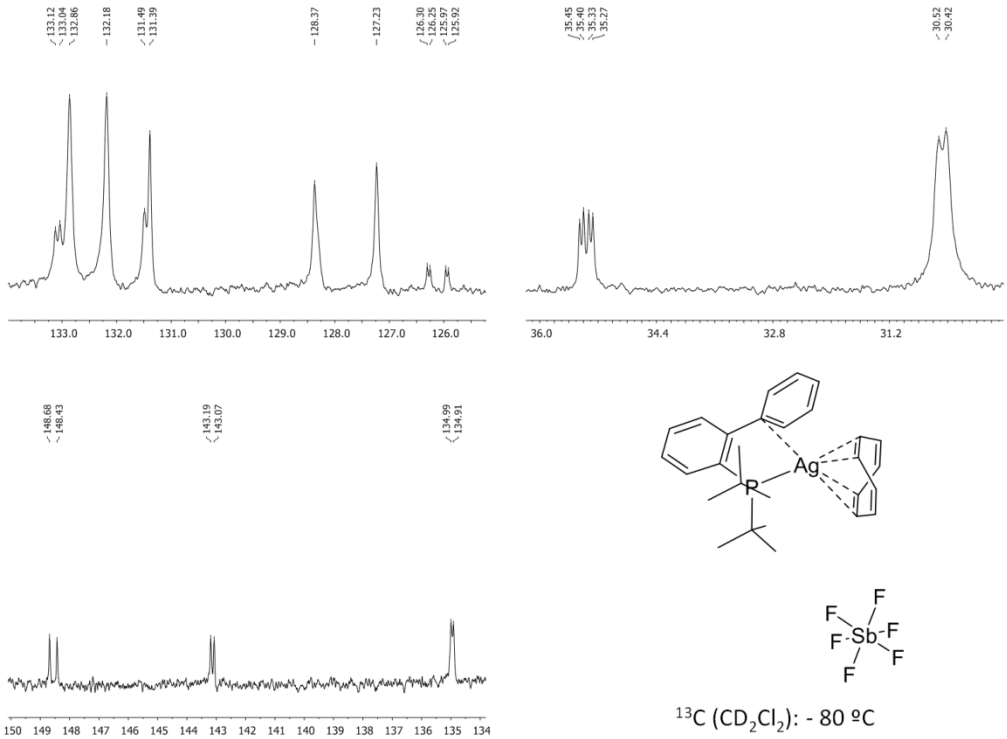

Table S2: Crystal data and structure refining for **2**:

Empirical formula	$C_{49}H_{64}Ag_2Cl_2F_{12}P_2Sb_2$	
	$[C_{48}H_{62}Ag_2P_2, 2(F_6Sb), CH_2Cl_2]$	
Formula weight	1473.08	
Temperature	193(2) K	
Wavelength	0.71073 Å	
Crystal system	Monoclinic	
Space group	P 2_1/n	
Unit cell dimensions	a = 21.7571(19) Å	α= 90°.
	b = 10.1105(9) Å	β= 100.802(2)°.
	c = 26.215(2) Å	γ = 90°.
Volume	5664.6(9) $Å^3$	
Z	4	
Density (calculated)	1.727 Mg/m^3	
Absorption coefficient	1.847 mm^{-1}	
F(000)	2904	
Crystal size	0.50 x 0.45 x 0.40 mm^3	
Theta range for data collection	3.92 to 25.25°.	
Index ranges	-26<=h<=26, -12<=k<=11, -25<=l<=31	
Reflections collected	54881	
Independent reflections	10203 [R(int) = 0.0184]	
Completeness to theta = 25.25°	99.5 %	
Absorption correction	Semi-empirical from equivalents	
Max. and min. transmission	0.4853 and 0.4186	
Refinement method	Full-matrix least-squares on F^2	
Data / restraints / parameters	10203 / 214 / 670	
Goodness-of-fit on F^2	1.147	
Final R indices [I>2sigma(I)]	R1 = 0.0330, wR2 = 0.0777	
R indices (all data)	R1 = 0.0346, wR2 = 0.0784	
Largest diff. peak and hole	0.991 and -0.829 e.$Å^{-3}$	

Ag(1)-P(1) : 2.4286(11) Å Ag(1)-C(45) : 2.596(4) Å Ag(1)-C(46) : 2.614(4) Å
Ag(1)-C(41) : 2.677(4) Å Ag(1)-C(42) : 2.690(4) Å

Ag(2)-P(2): 2.4303(10) Å Ag(2)-C(48): 2.442(4) Å Ag(2)-C(47): 2.490(4) Å

Fig. S9: ORTEP drawing of **2**:

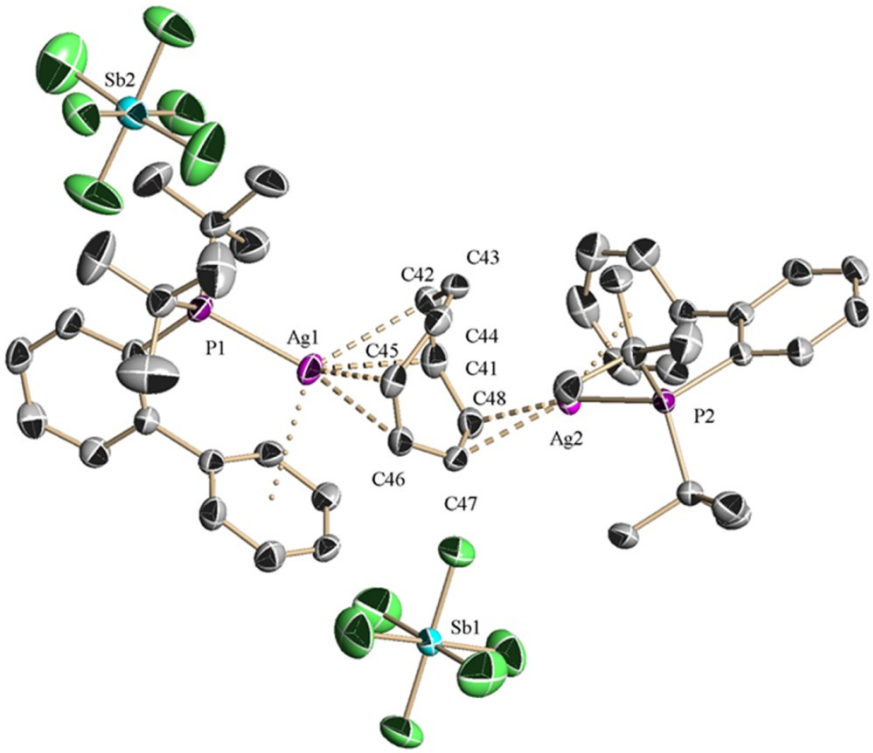

Crystal packing detail of **2** viewed along the b-axis, hydrogen atoms are omitted for clarity:

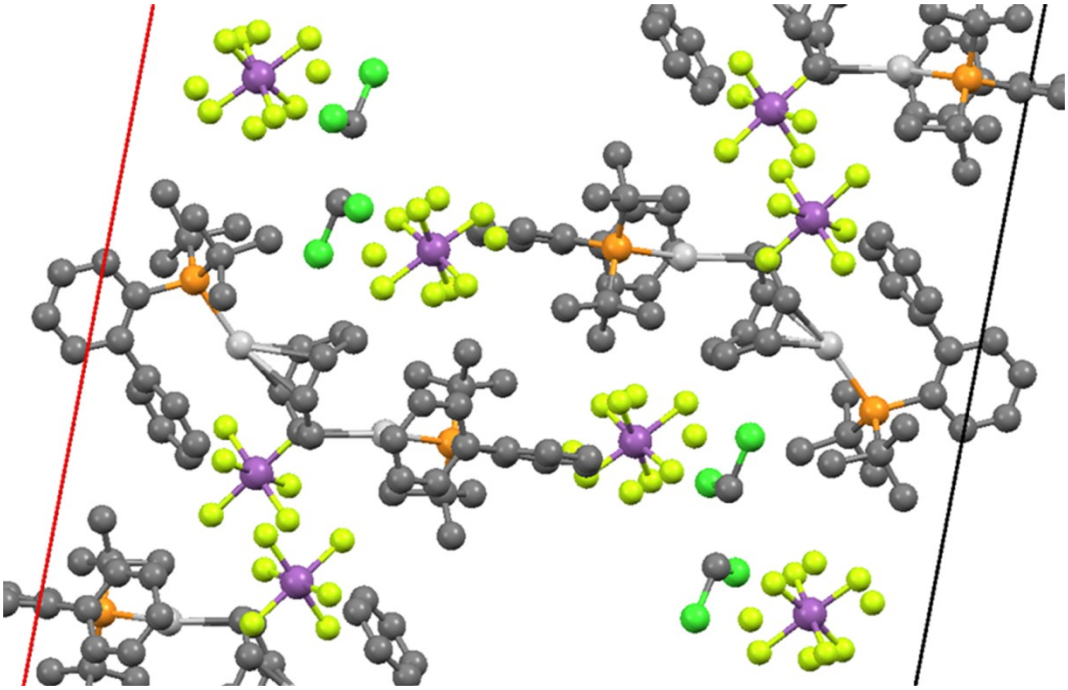

Fig. S10: ^{1}H NMR spectrum in CD_2Cl_2 for isolated complex **2**.

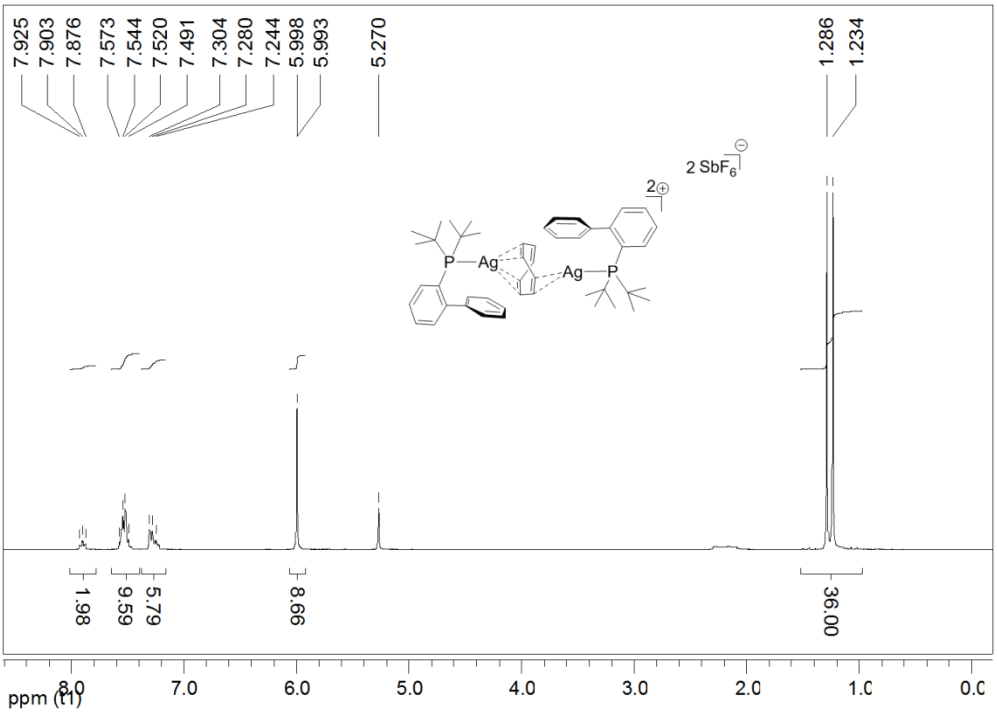

Magnification of the ^{1}H NMR peaks (**2**):

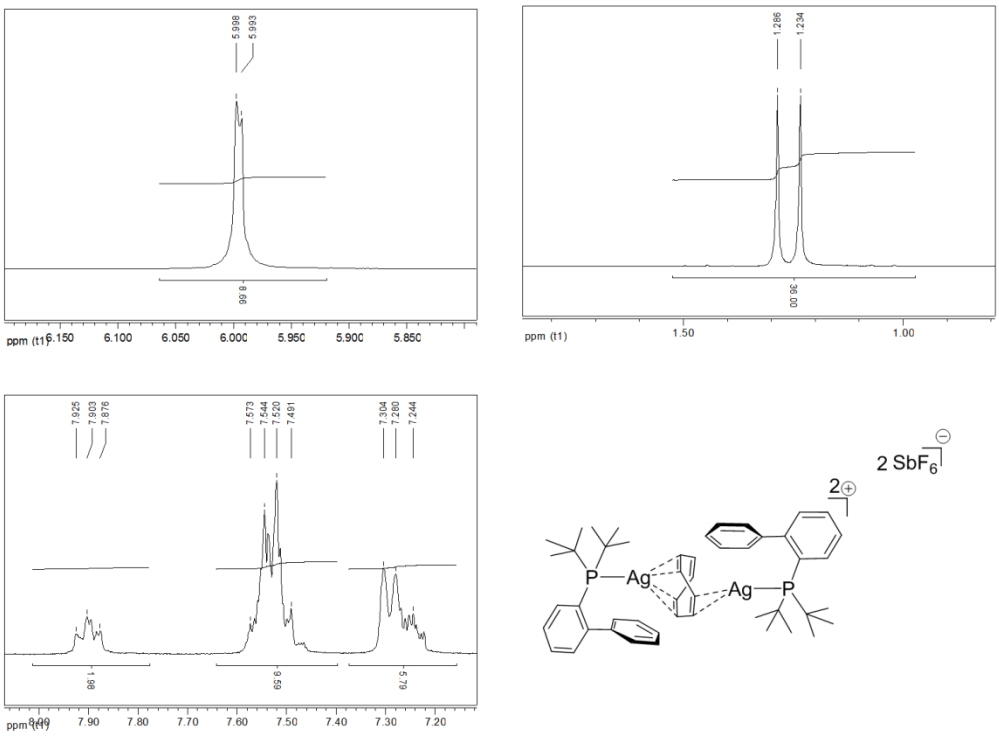

Fig. S11: ^{13}C NMR spectrum in CD_2Cl_2 for isolated complex (**2**).

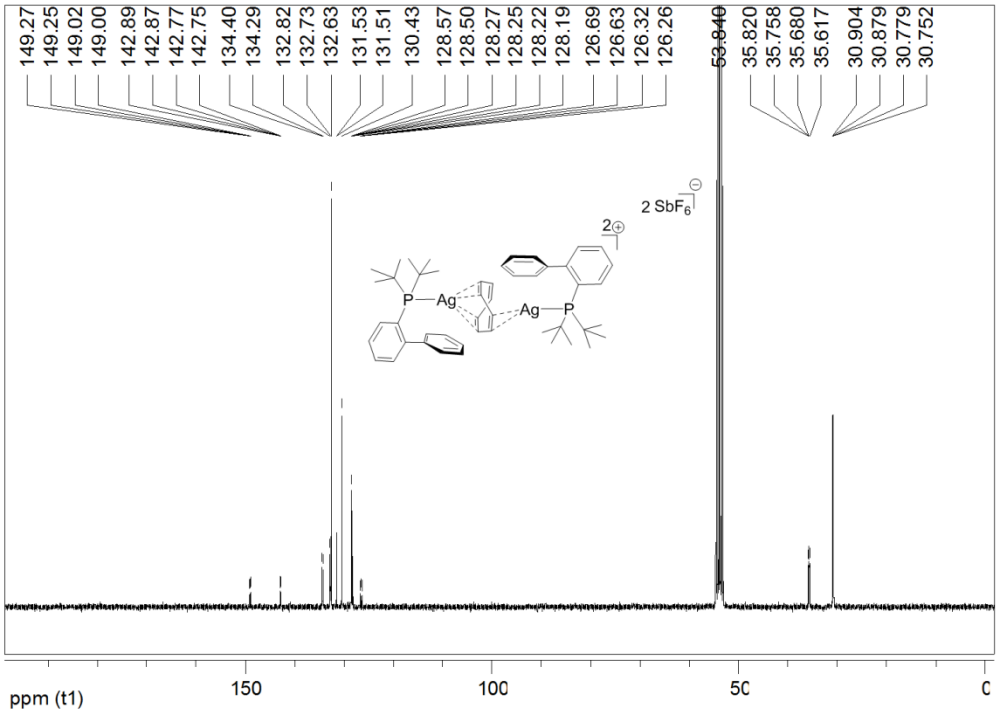

Magnification of the ^{13}C NMR peaks (**2**):

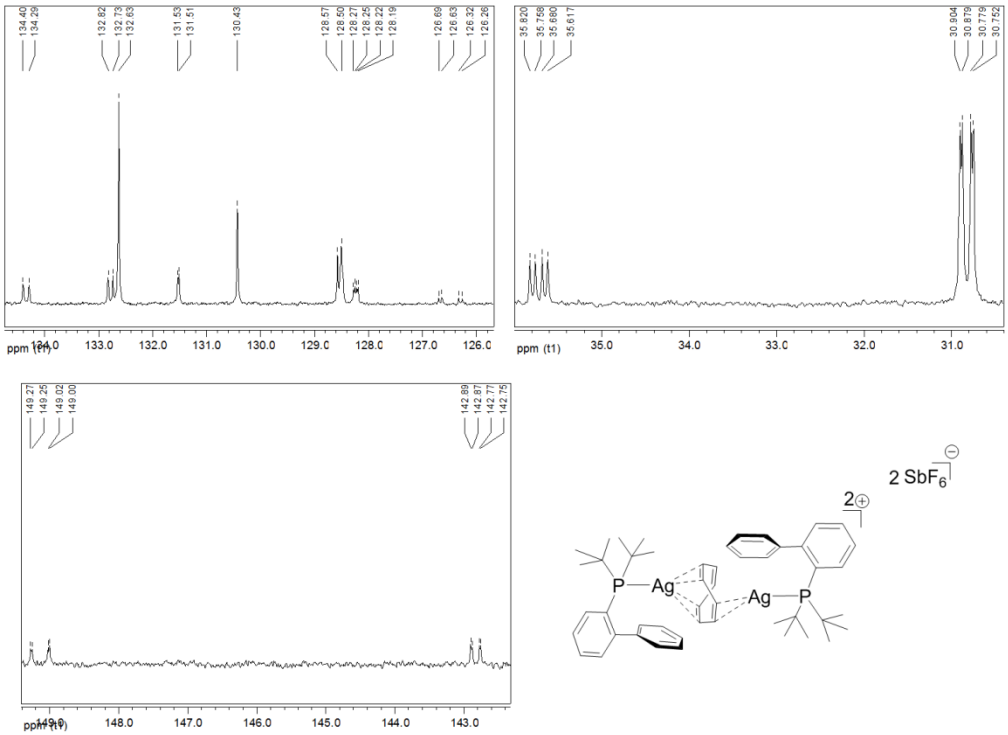

Fig. S12: DEPT. 135 spectrum in CD_2Cl_2 for isolated complex **2**.

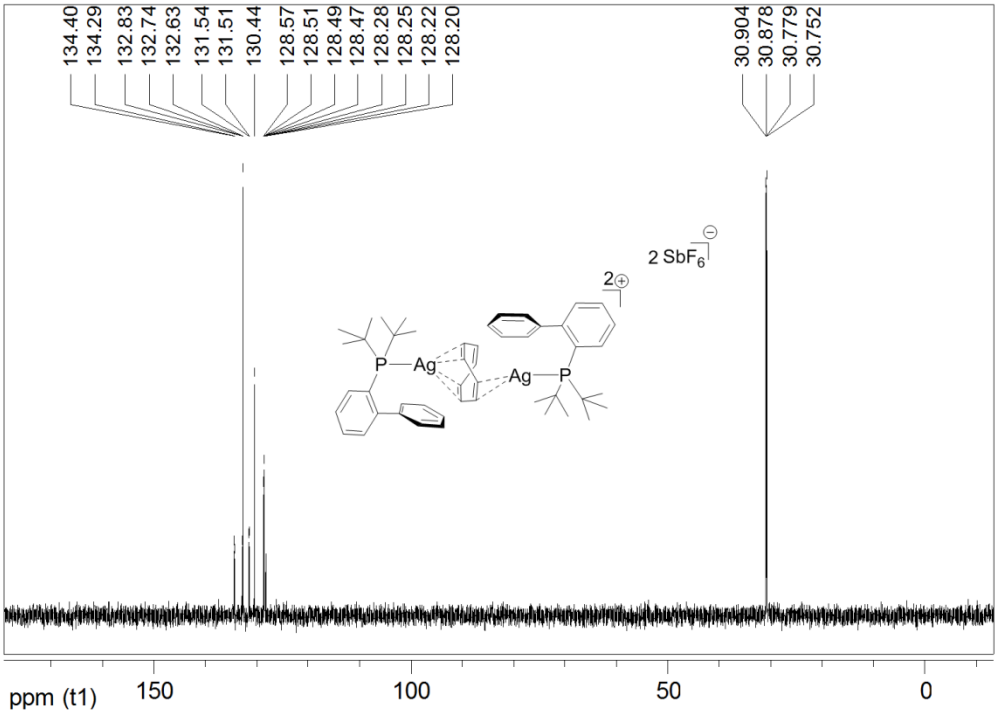

Magnification of the DEPT. 135 NMR peaks (**2**):

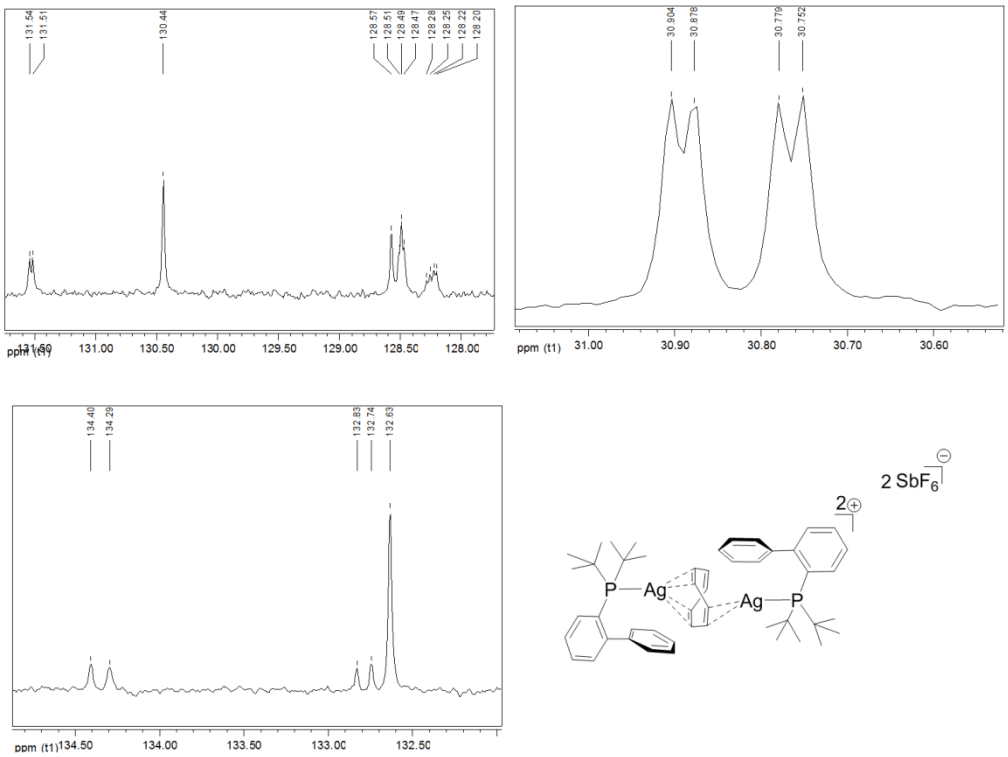

Fig. S13: ^{31}P NMR spectrum in CD_2Cl_2 for isolated complex **2**.

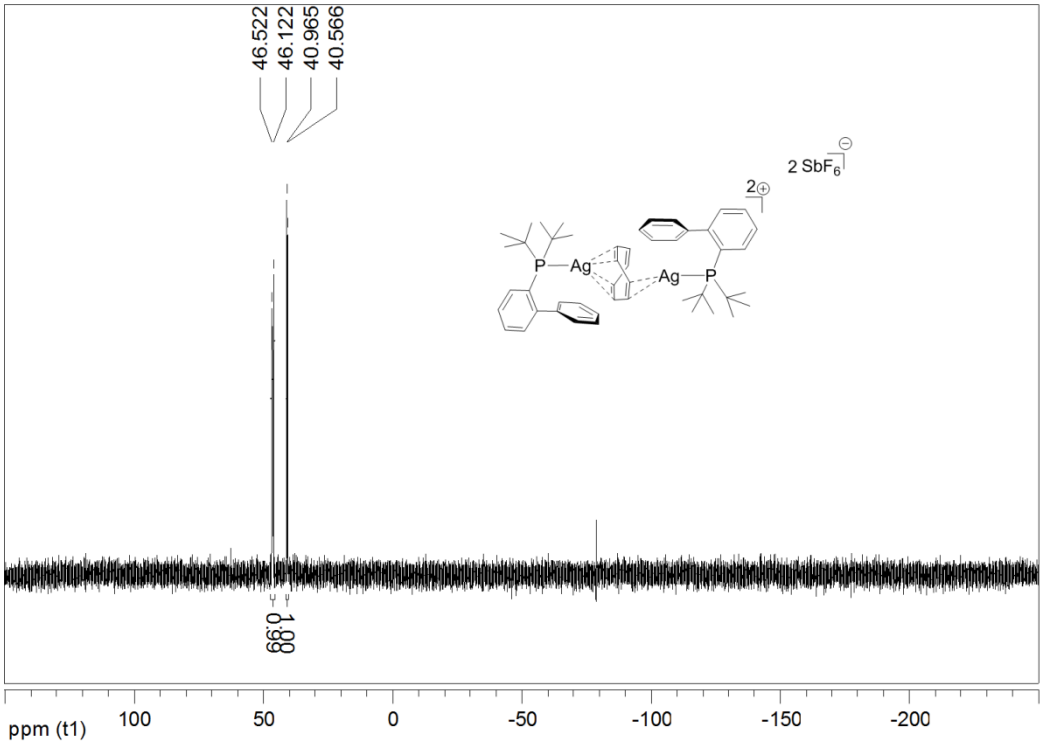

Magnification of the ^{31}P NMR peaks (**2**):

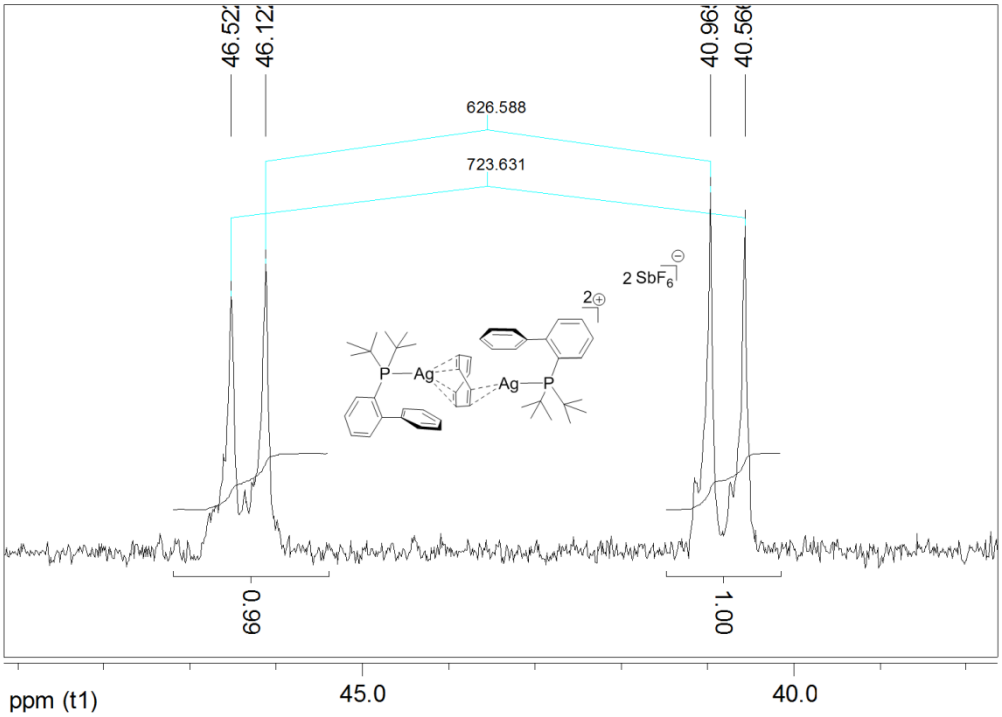

Fig. S14: ESI-MS data for **2**.

Acquisition Parameter:
Comment: 1/1000 1/1000 CH_2Cl_2
Instrument: esquire 6000

Ion Source Type	ESI	Ion Polarity	Positive	Alternating Ion Polarity	off
Mass Range Mode	Std/Normal	Scan Begin	65 m/z	Scan End	2000 m/z
Capillary Exit	159.1 Volt	Skim 1	40.0 Volt	Trap Drive	84.3
Accumulation Time	200000 µs	Averages	8 Spectra	Auto MS/MS	off

- ESI-MS (+MS) *m/z*: 938.9 amu for $[C_{48}H_{62}Ag_2P_2, 2(F_6Sb)]$ (**2**) – $2SbF_6^-$ and + $Na]^+$:
- ESI-MS (+MS) *m/z*: 847.0 amu for $[C_{48}H_{62}Ag_2P_2, 2(F_6Sb)]$ (**2**) – $2SbF_6$ - C_8H_8 and + $Cl]^+$:

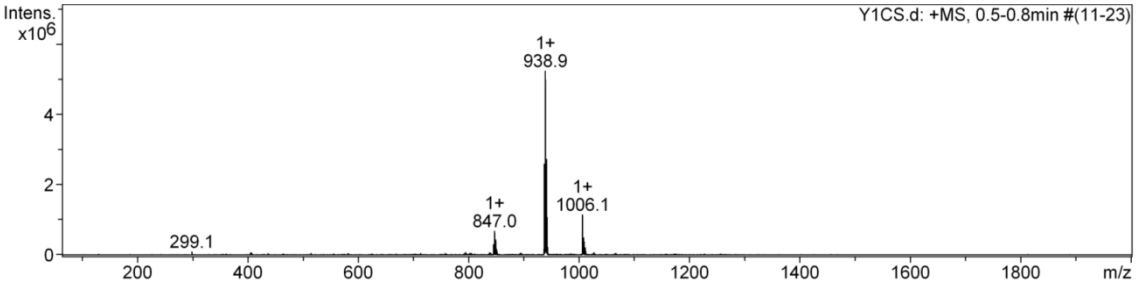

- Peak at 938.9 m/z expanded to show the cluster of ions composition:

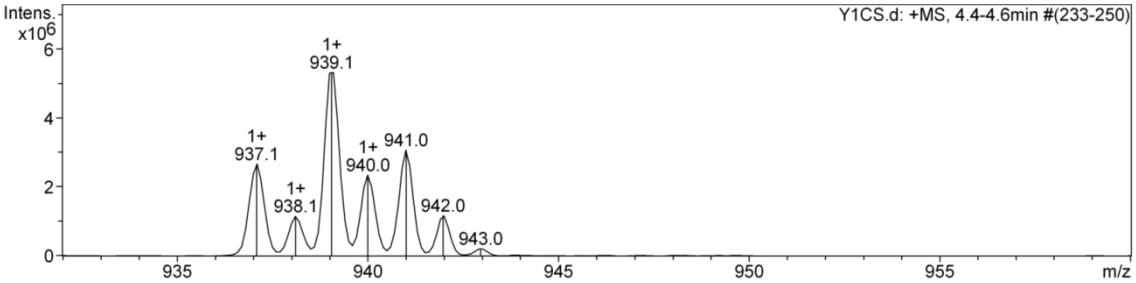

- Plot of the isotopic distribution for this $C_{48}H_{62}Ag_2P_2Na$ chemical elements formula:

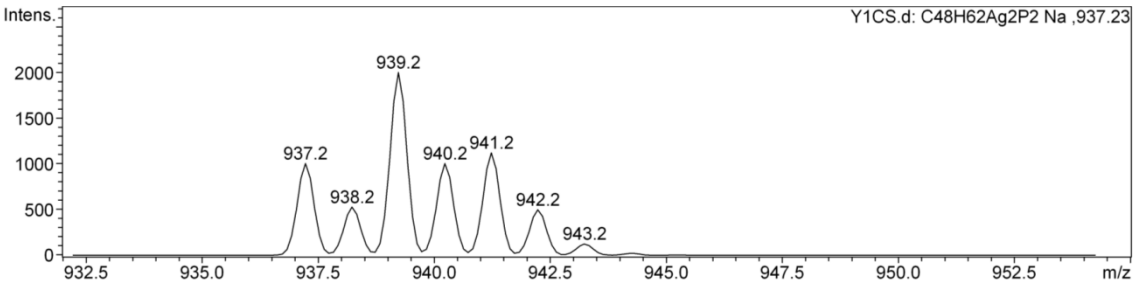

Fig. S15: ^{1}H NMR spectrum in CD_2Cl_2 for isolated complex **3**.

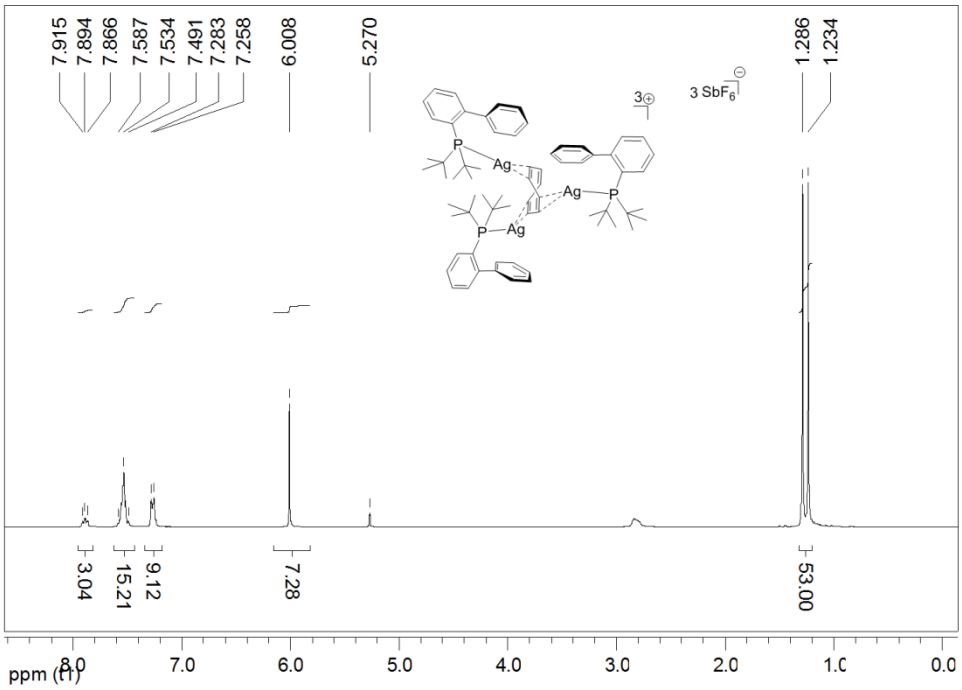

Magnification of the ^{1}H NMR peaks (**3**):

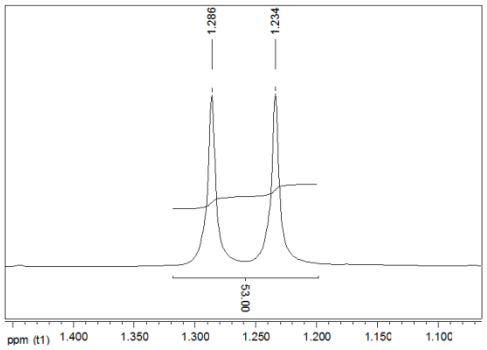

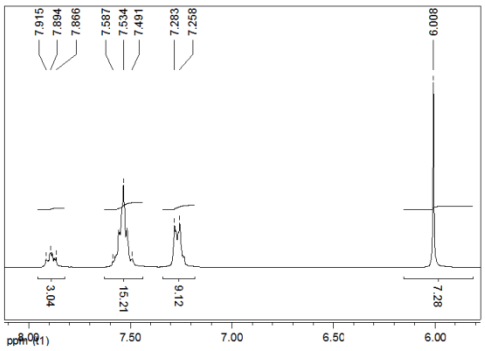

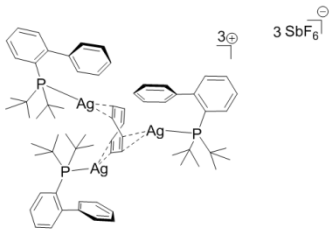

Fig. S16: ^{13}C NMR spectrum in CD_2Cl_2 for isolated complex (**3**).

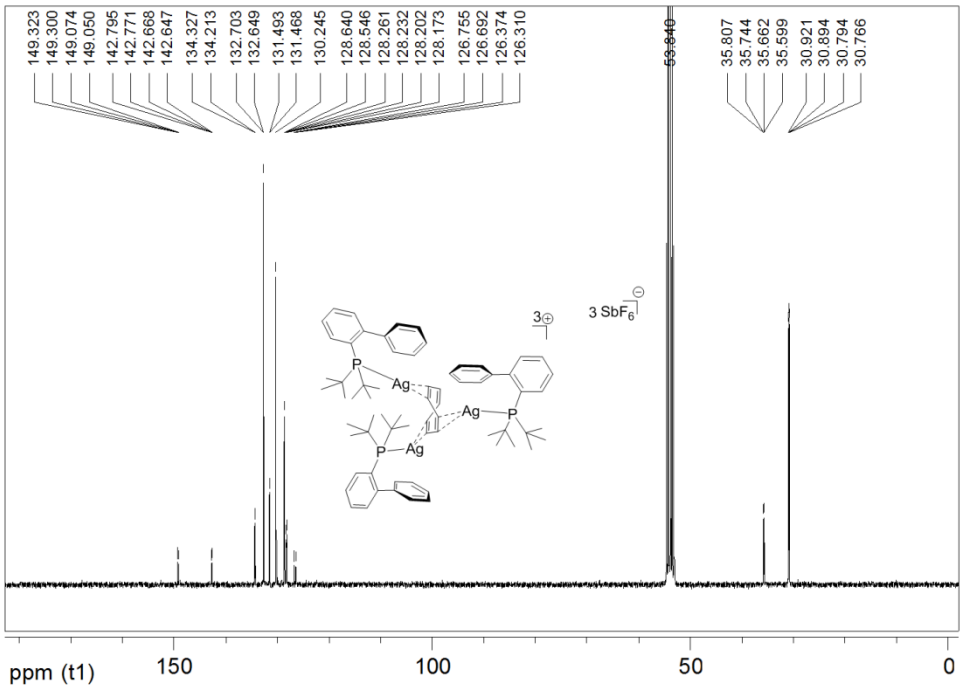

Magnification of the ^{13}C NMR peaks (**3**):

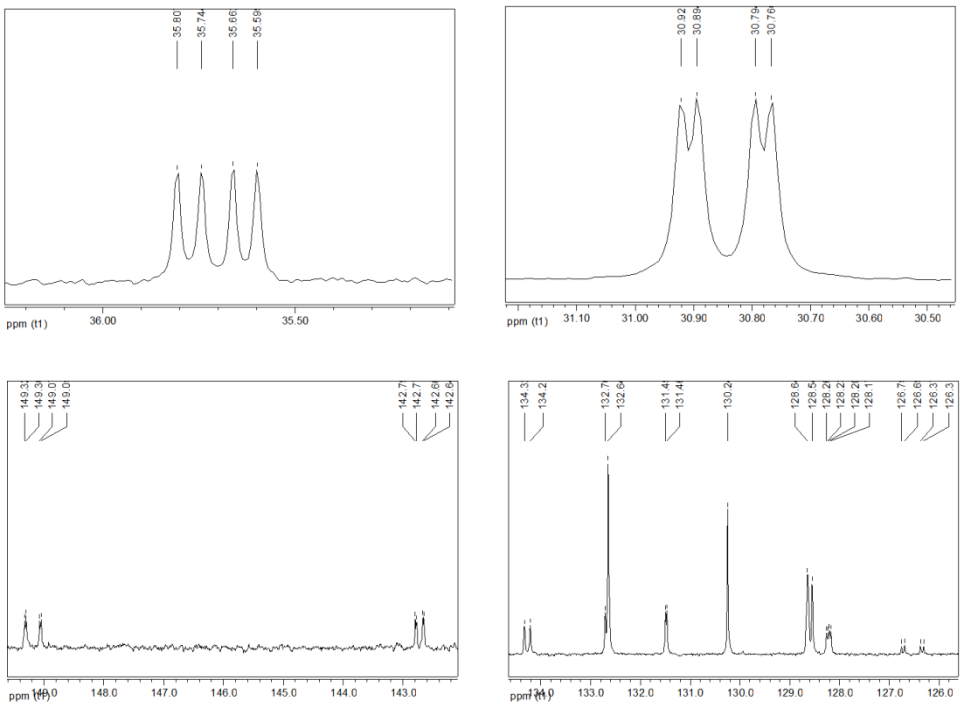

Fig. S17: DEPT-135 spectrum in CD_2Cl_2 for isolated complex (**3**).

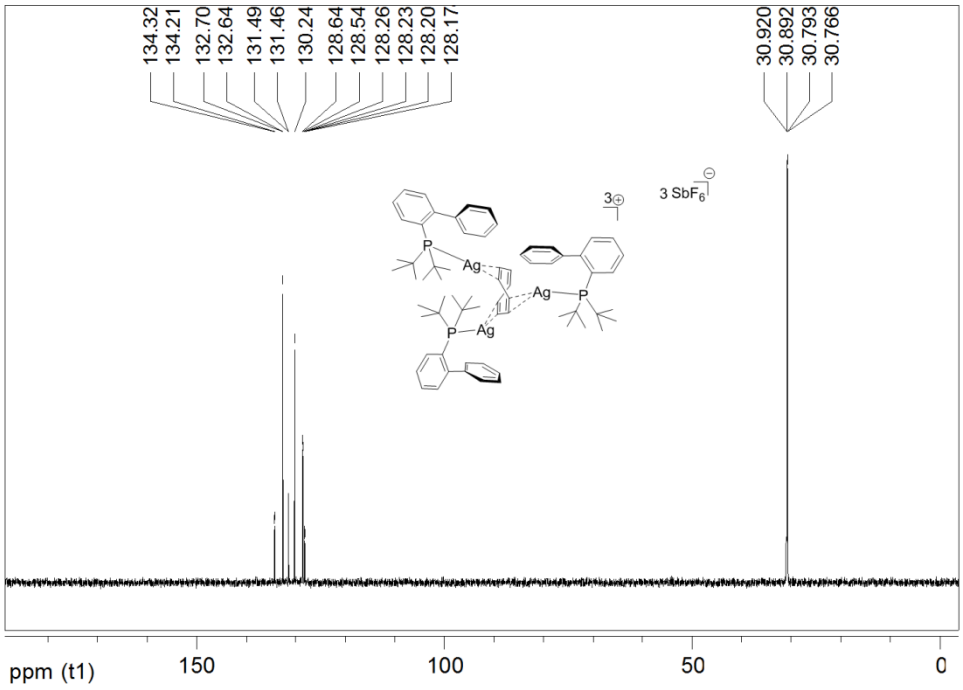

Magnification of the DEPT-135 NMR peaks (**3**):

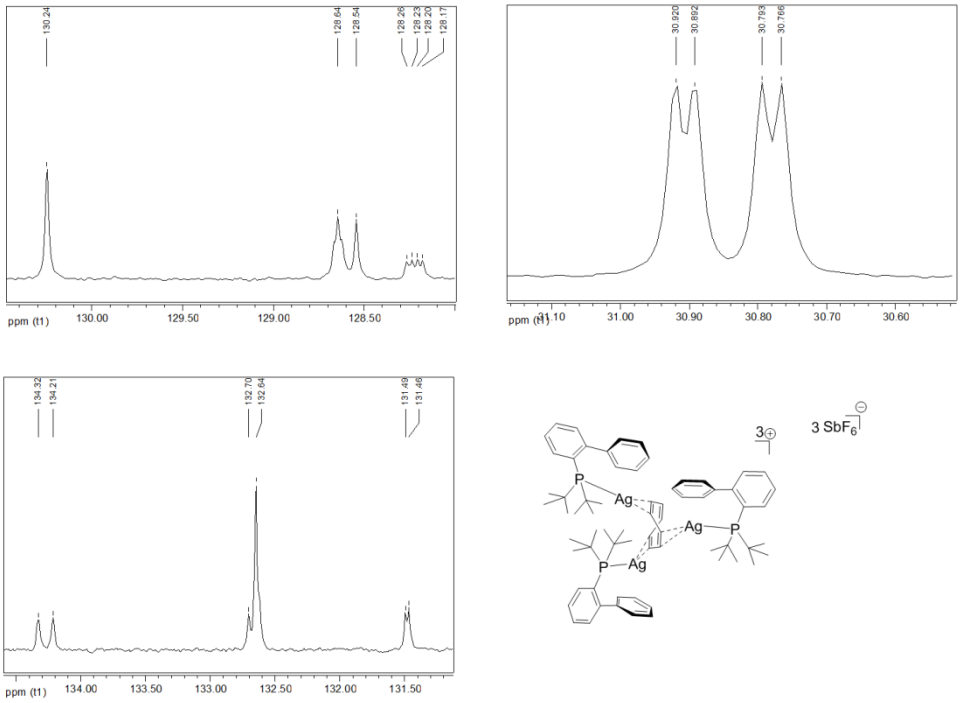

Fig. S18: ^{31}P NMR spectrum in CD_2Cl_2 for isolated complex **3**.

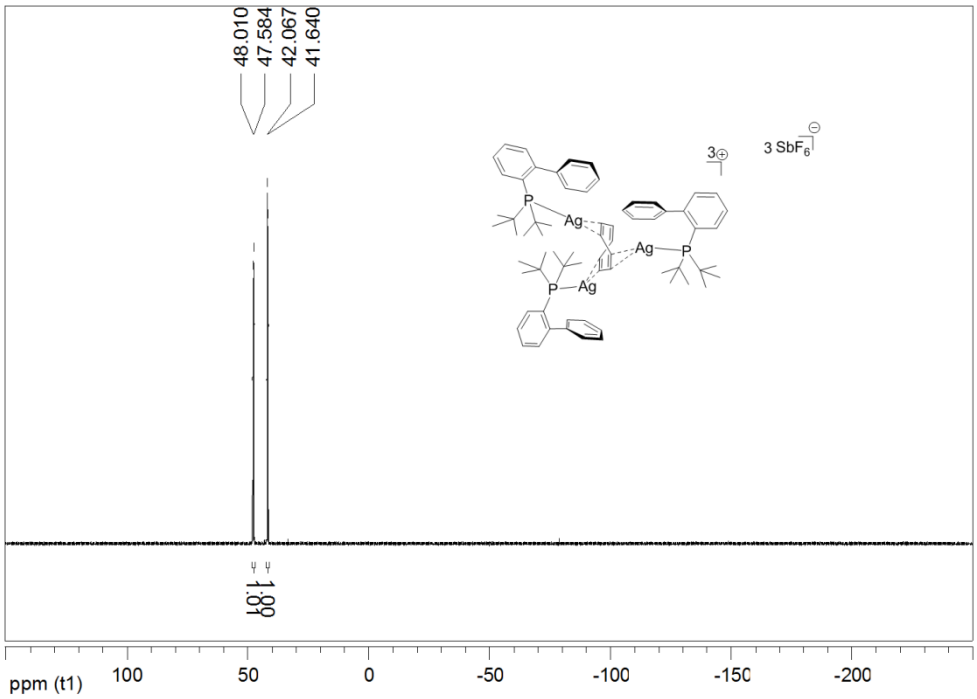

Magnification of the ^{31}P NMR peaks (**3**):

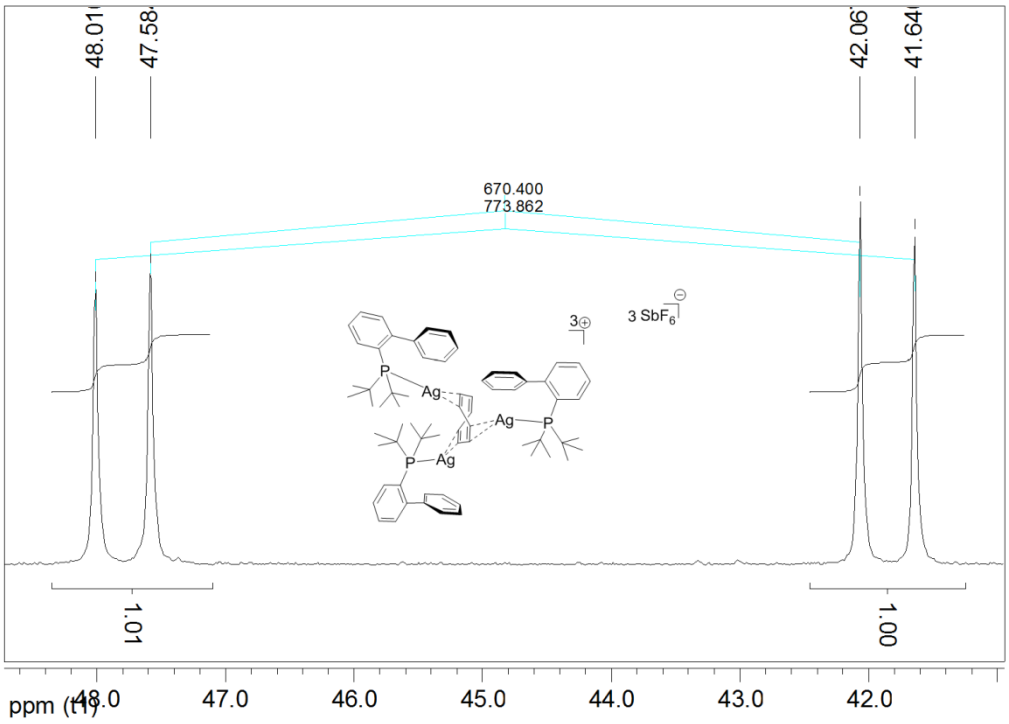

Fig. S19: ^{1}H NMR spectrum in CD_2Cl_2 for isolated complex **4**.

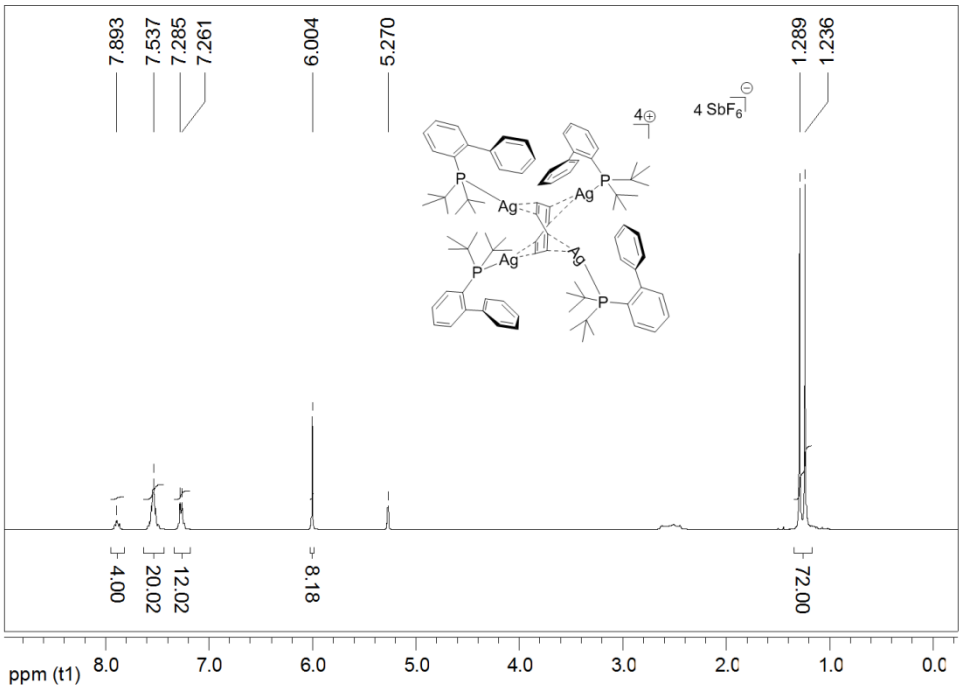

Magnification of the ^{1}H NMR peaks (**4**):

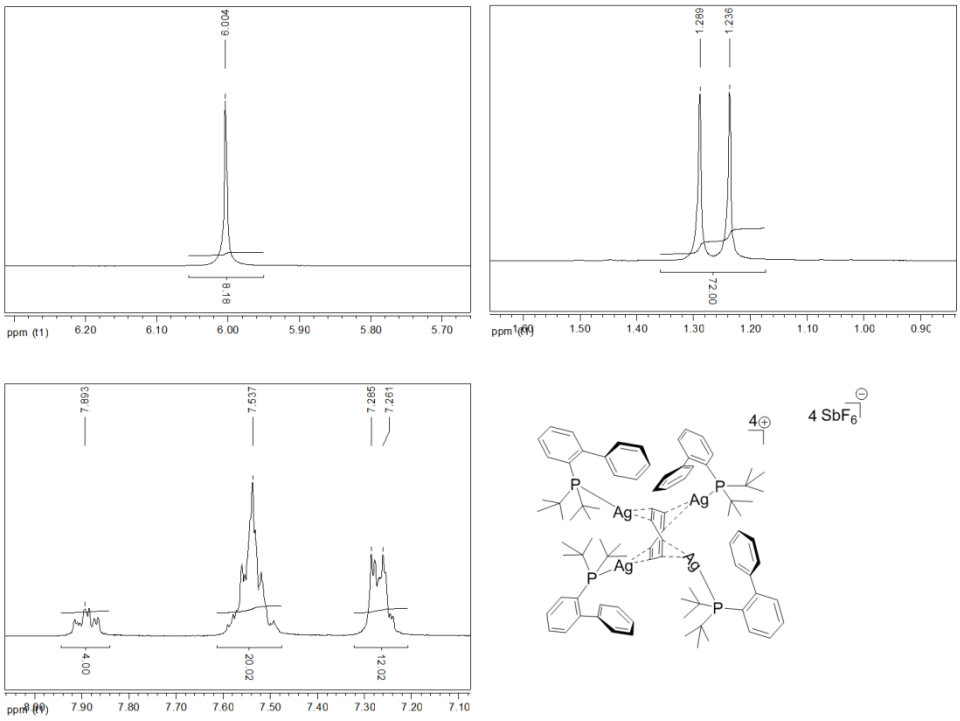

Fig. S20: ^{13}C NMR spectrum in CD_2Cl_2 for isolated complex (**4**).

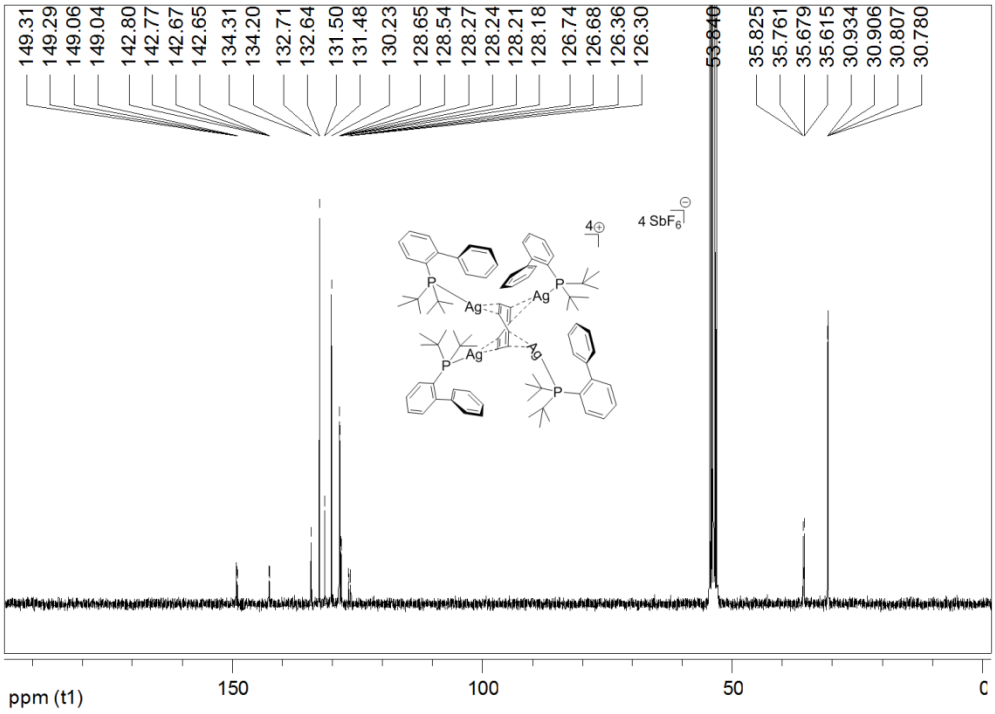

Magnification of the ^{13}C NMR peaks (**4**):

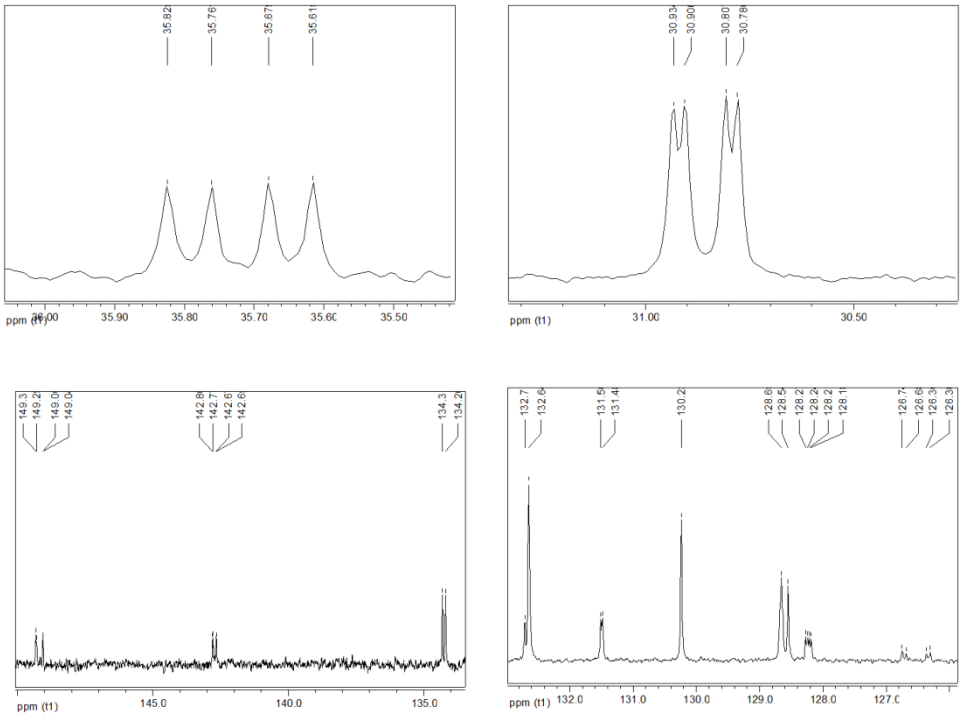

Fig. S21: DEPT-135 spectrum in CD_2Cl_2 for isolated complex (**4**).

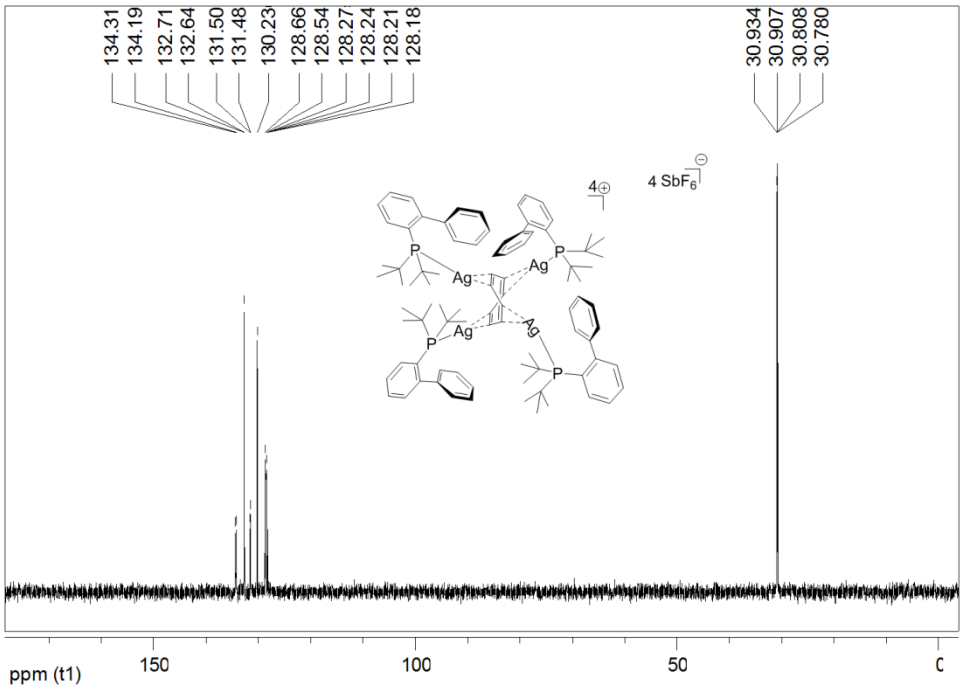

Magnification of the DEPT-135 NMR peaks (**4**):

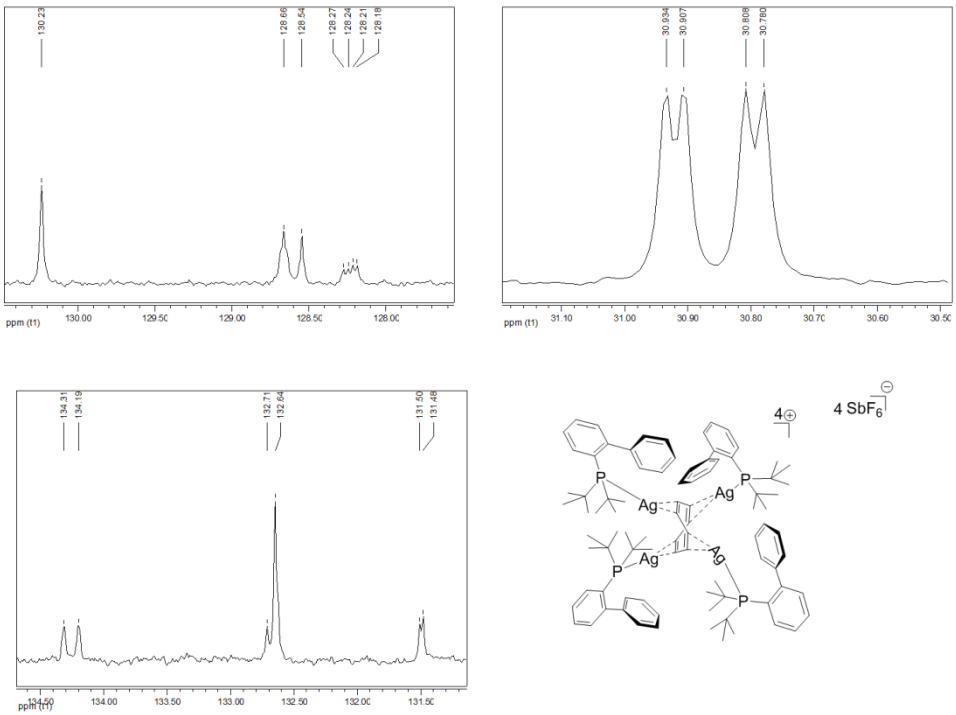

Fig. S22: ^{31}P NMR spectrum in CD_2Cl_2 for isolated complex **4**.

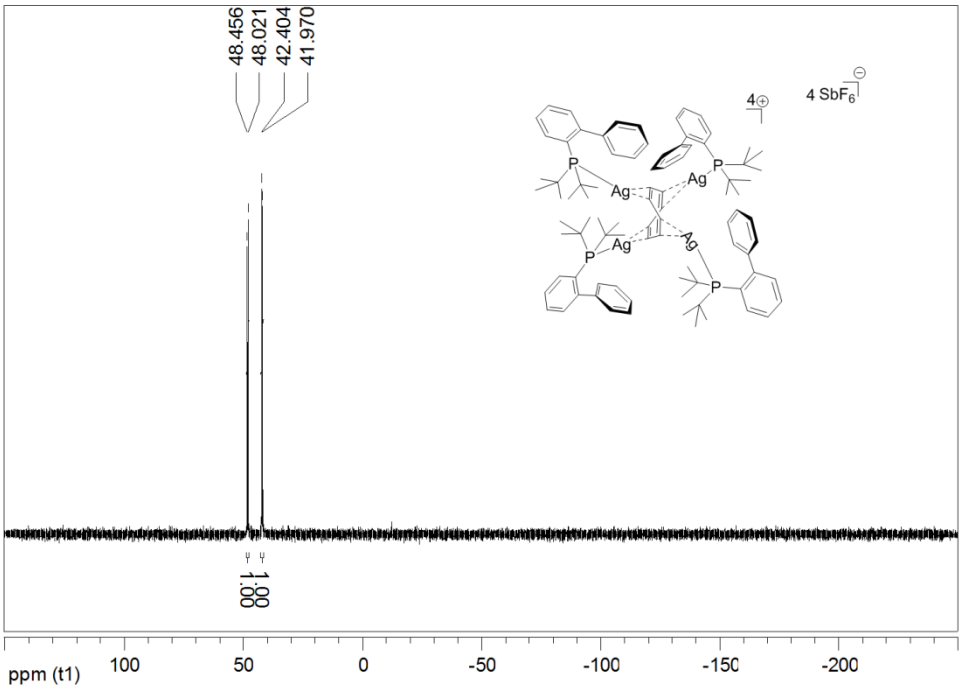

Magnification of the ^{31}P NMR peaks (**4**):

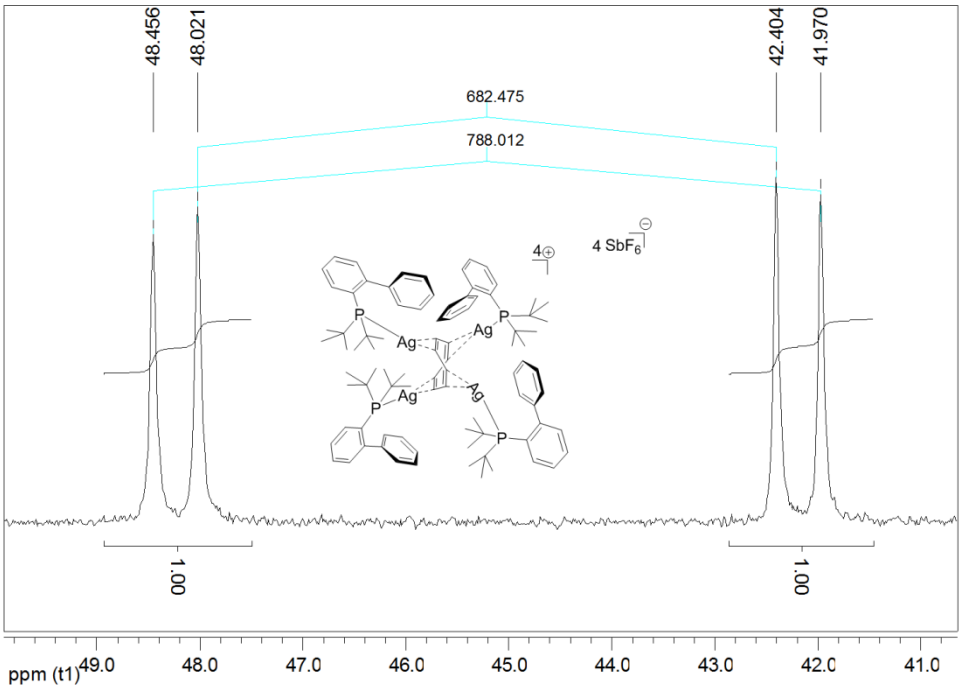

Fig. S23: ESI-MS data for **4**.

Acquisition Parameter:
Comment: 1/1000 CH_2Cl_2 1/1000 Toluene
Instrument: esquire 6000

Ion Source Type	ESI	Ion Polarity	Positive	Alternating Ion Polarity	off
Mass Range Mode	Std/Normal	Scan Begin	65 m/z	Scan End	2000 m/z
Capillary Exit	125.3 Volt	Skim 1	40.0 Volt	Trap Drive	52.1
Accumulation Time	1597 µs	Averages	8 Spectra	Auto MS/MS	off

- ESI-MS (+MS) *m/z*: 1347.5 amu for $[C_{68}H_{89}Ag_3P_3, 3(F_6Sb)]$ (**3**) – $3SbF_6$ and + Na]$^+$:
- ESI-MS (+MS) *m/z*: 938.9 amu for $[C_{48}H_{62}Ag_2P_2, 2(F_6Sb)]$ (**2**) – $2SbF_6^-$ and + Na]$^+$:

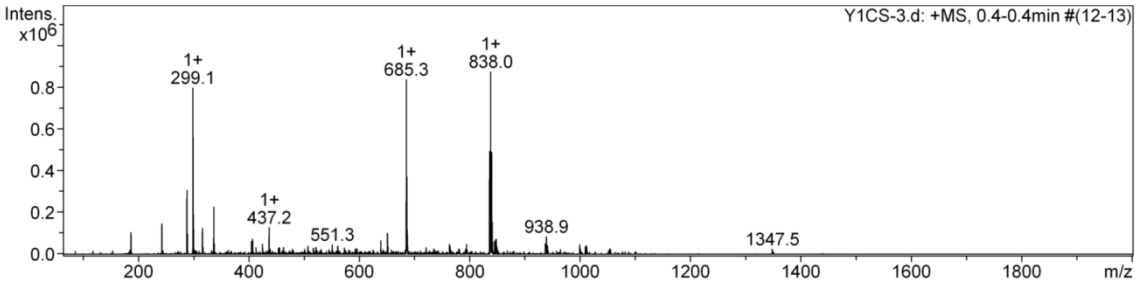

- Peak at 938.9 m/z expanded to show the cluster of ions composition:

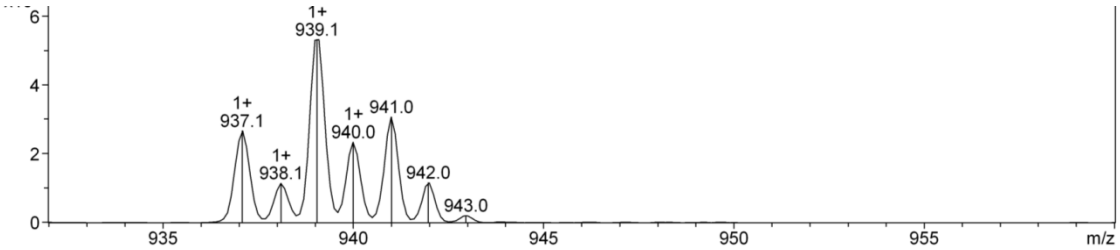

- Plot of the isotopic distribution for this $C_{48}H_{62}Ag_2P_2Na$ chemical elements formula:

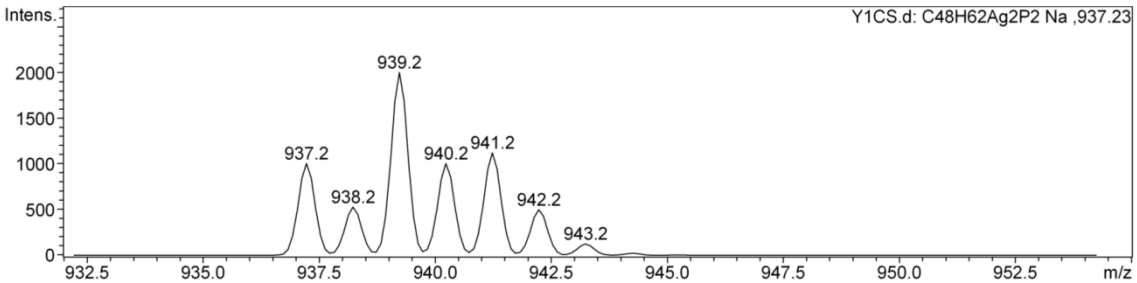

Fig. S24: Solid state ^{31}P NMR spectrum for crude complex **1**.

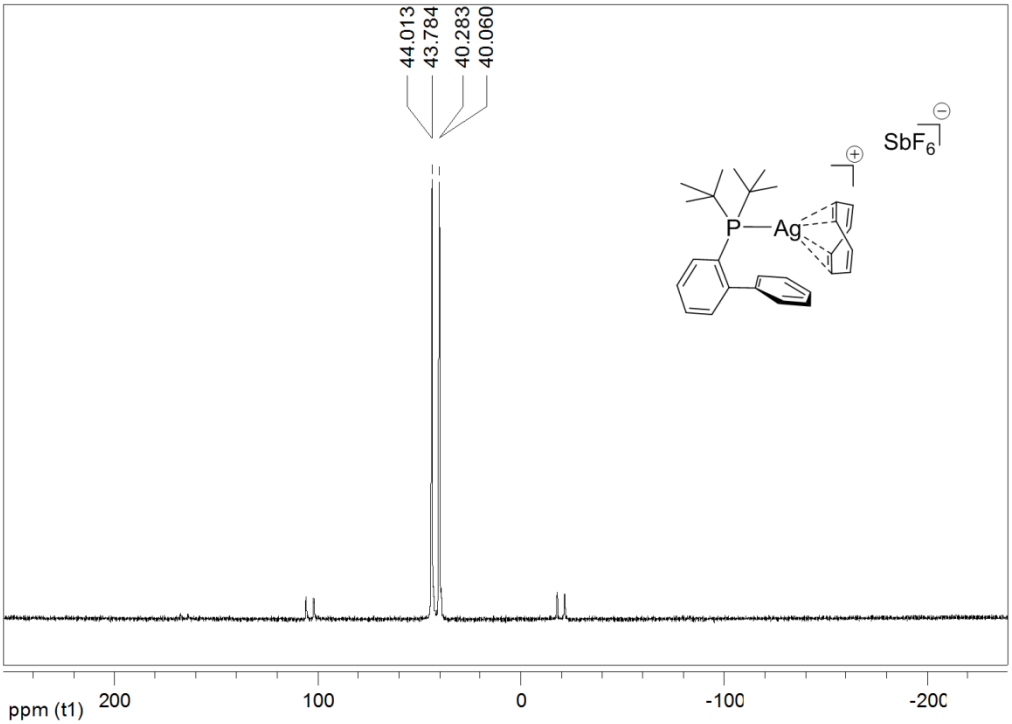

Magnification of the solid state ^{31}P NMR peaks (**1**):

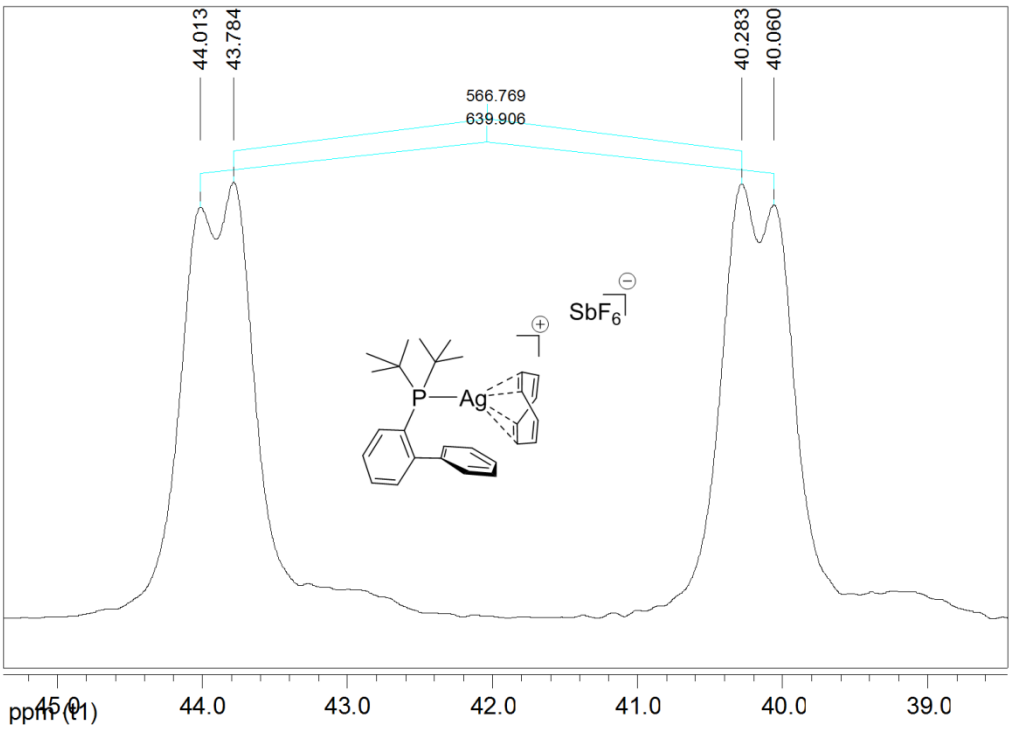

Fig. S25: Solid state ^{31}P NMR spectrum for crude complex **4**.

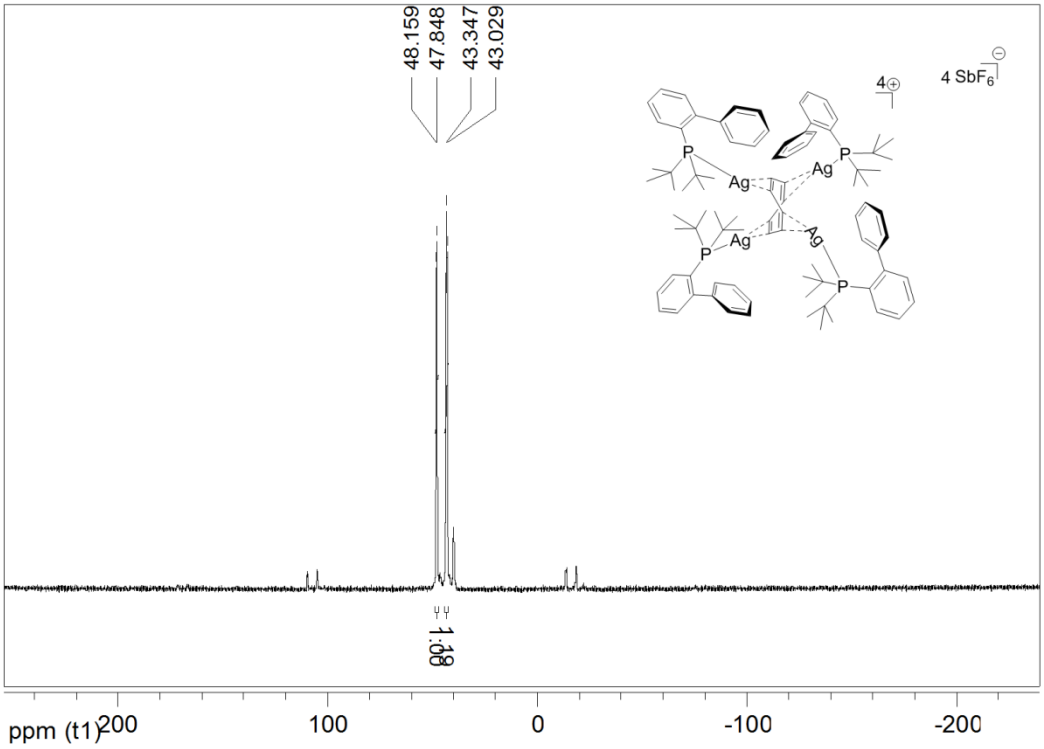

Magnification of the solid state ^{31}P NMR peaks (**4**):

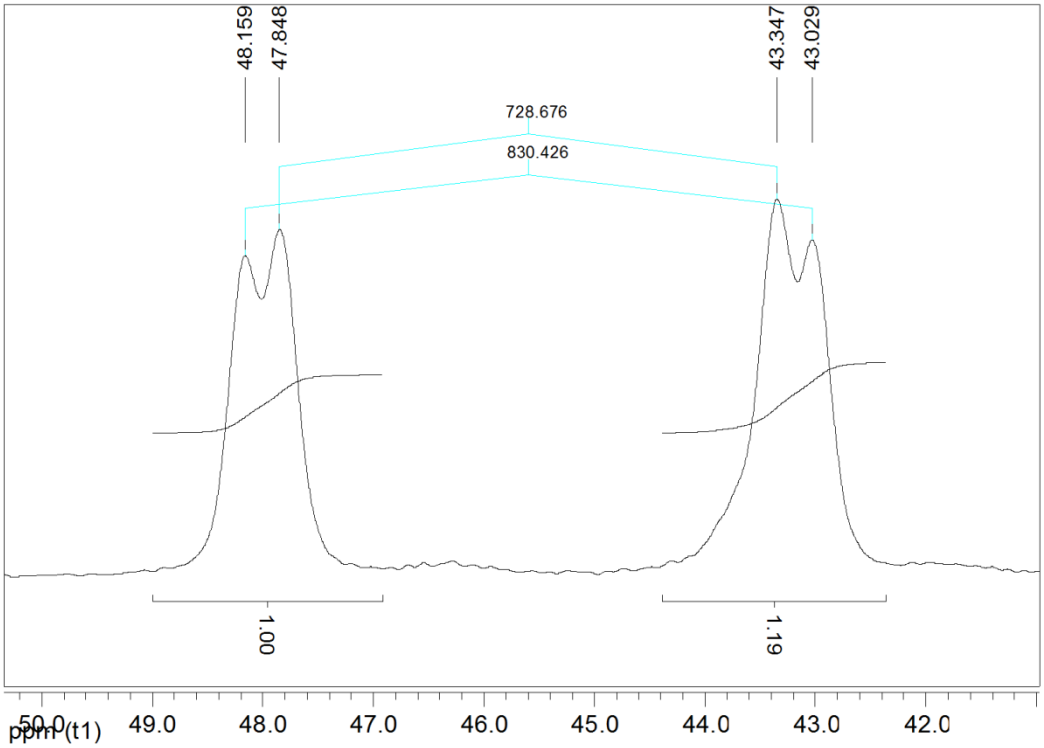

Fig. S26: Solid state ^{31}P NMR spectrum of complex **2** obtained by fast evaporation.

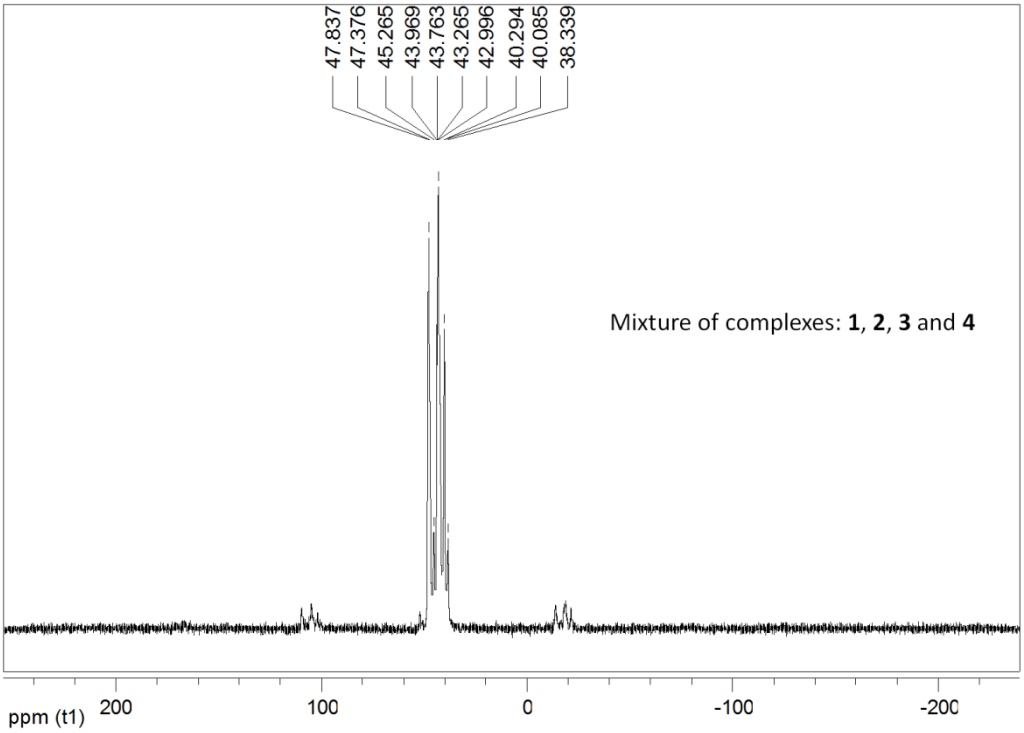

Magnification of the solid state ^{31}P NMR peaks mixture of complexes **1**, **2**, **3** and **4**:

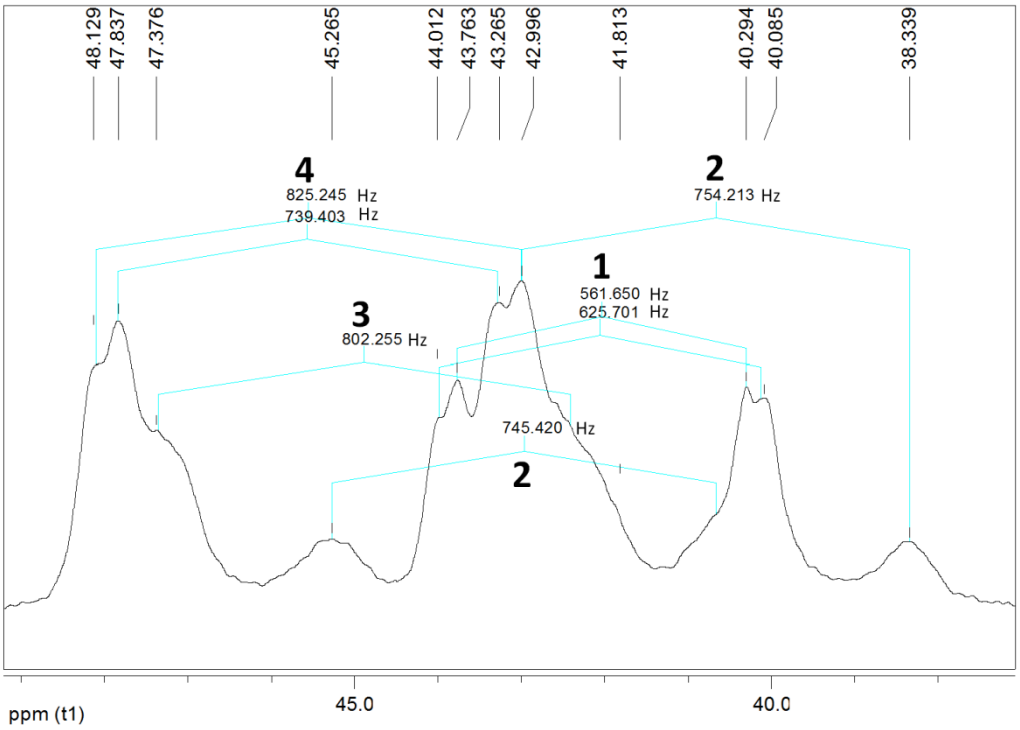

Fig. S27: Deconvolution of the solid state ^{31}P NMR spectrum (b).

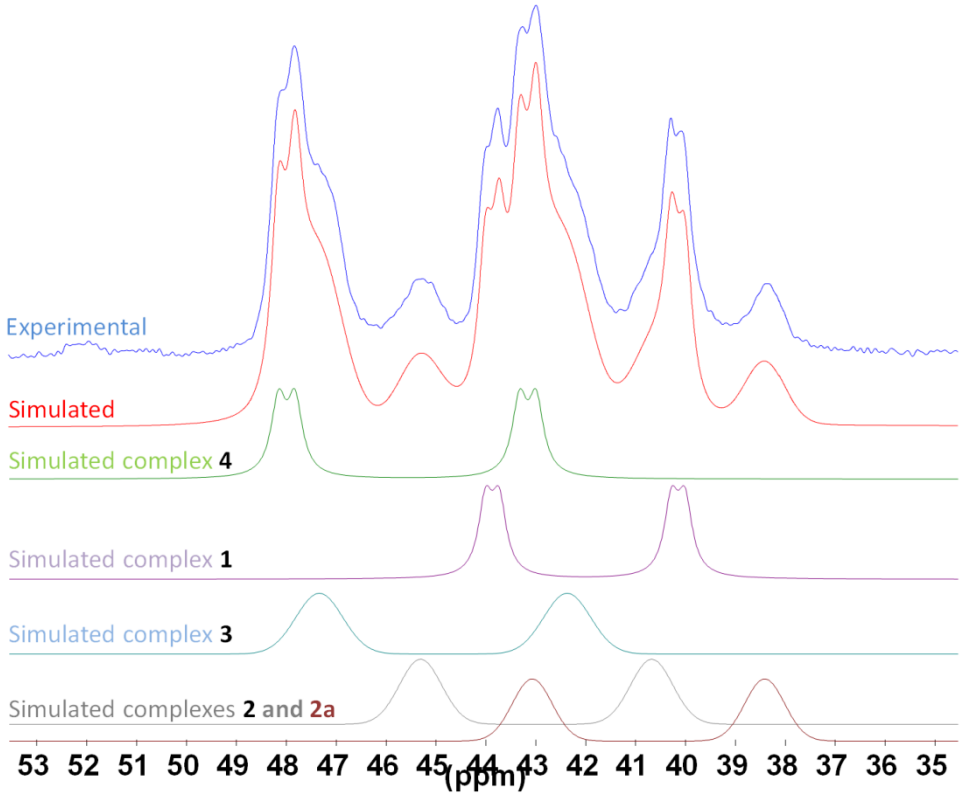

"Complexes"

"4"	"Jmultiplet"	"amp"	137.77	"pos(ppm)"	45.58	"wid(ppm)"	0.36	"gl"	0.00
	"T2(ms)"	5.43	J1: 782.10 / 1		J2: 53.66 / 1				
"1"	"Jmultiplet"	"amp"	109.98	"pos(ppm)"	42.01	"wid(ppm)"	0.35	"gl"	0.00
	"T2(ms)"	5.62	J1: 602.94 / 1		J2: 43.92 / 1				
"3"	"Jmultiplet"	"amp"	81.80	"pos(ppm)"	44.85	"wid(ppm)"	1.10	"gl"	1.00
	"T2(ms)"	1.78	J1: 804.07 / 1						
"2"	"Jmultiplet"	"amp"	34.48	"pos(ppm)"	42.99	"wid(ppm)"	0.99	"gl"	1.00
	"T2(ms)"	1.98	J1: 750.00 / 1						
"2a"	"Jmultiplet"	"amp"	32.90	"pos(ppm)"	40.74	"wid(ppm)"	0.94	"gl"	1.00
	"T2(ms)"	2.10	J1: 754.00 / 1						

Model Integration:

complexes		Name	Peak Model %		Intens
4	""	"Jmultiplet"	30.45	25042.62	
1	""	"Jmultiplet"	23.50	19323.64	
3	""	"Jmultiplet"	26.76	22004.95	
2	""	"Jmultiplet"	10.16	8355.14	
2a	""	"Jmultiplet"	9.13	7505.69	

Fig. S28: ^{1}H NMR spectrum in CD_2Cl_2 for the crude solid of complex **2**.

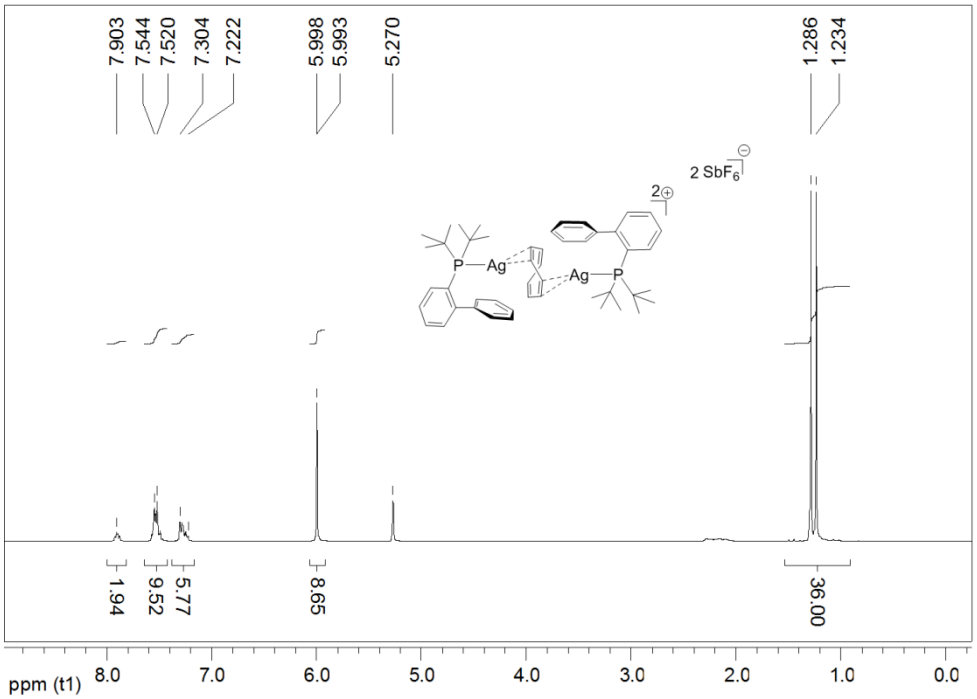

Fig. S29: ^{31}P NMR spectrum in CD_2Cl_2 for the crude solid of complex **2**.

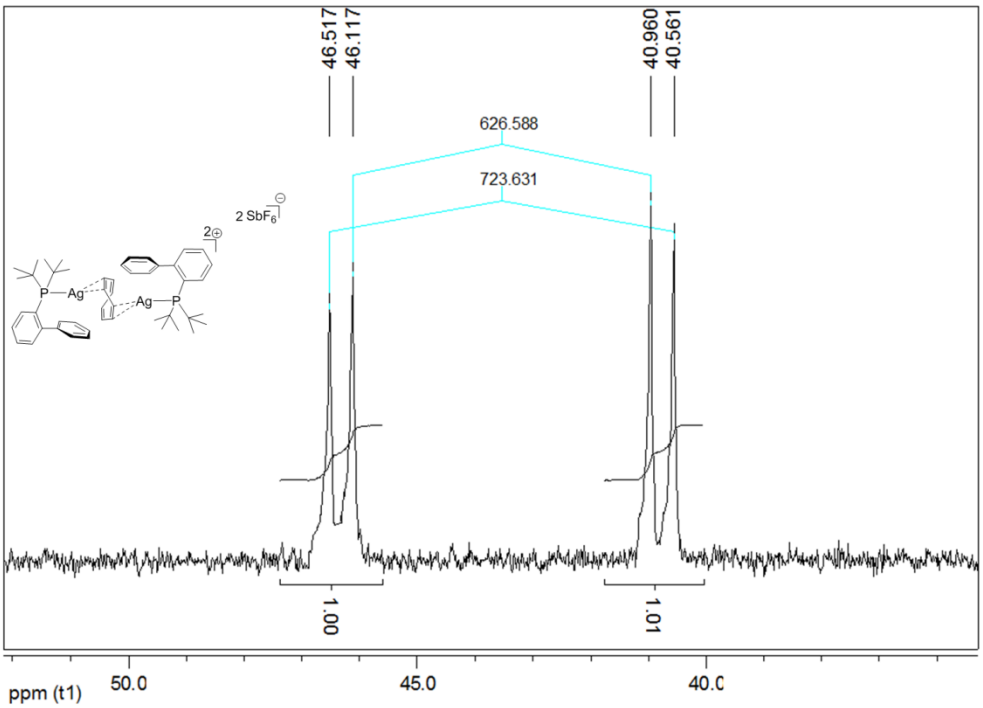

Table S3: Crystal data and structure refining for **2a**:

Empirical formula	$C_{50}H_{66}Ag_2Cl_4F_{12}P_2Sb_2$	
	$[C_{48}H_{62}Ag_2P_2, 2(F_6Sb), 2(CH_2Cl_2)]$	
Formula weight	1558.01	
Temperature	193(2) K	
Wavelength	0.71073 Å	
Crystal system	Orthorhombic	
Space group	P b c a	
Unit cell dimensions	a = 24.389(4) Å	α= 90°.
	b = 15.102(3) Å	β= 90°.
	c = 32.963(6) Å	γ = 90°.
Volume	12141(4) $Å^3$	
Z	8	
Density (calculated)	1.705 Mg/m^3	
Absorption coefficient	1.814 mm^{-1}	
F(000)	6144	
Crystal size	0.50 x 0.40 x 0.30 mm^3	
Theta range for data collection	1.70 to 25.00°.	
Index ranges	0<=h<=28, 0<=k<=17, 0<=l<=39	
Reflections collected	10632	
Independent reflections	10632 [R(int) = 0.0835]	
Completeness to theta = 25.00°	99.6 %	
Absorption correction	Semi-empirical from equivalents	
Max. and min. transmission	0.6122 and 0.4641	
Refinement method	Full-matrix least-squares on F^2	
Data / restraints / parameters	10632 / 146 / 688	
Goodness-of-fit on F^2	1.102	
Final R indices [I>2sigma(I)]	R1 = 0.0738, wR2 = 0.2210	
R indices (all data)	R1 = 0.1170, wR2 = 0.2574	
Largest diff. peak and hole	3.825 and -2.716 e.$Å^{-3}$	

Ag(1)-P(1) : 2.430(2) Å	Ag(1)-C(41) : 2.484(9) Å	Ag(1)-C(42) : 2.484(9) Å
Ag(2)-P(2): 2.426(2) Å	Ag(2)-C(48): 2.426(9) Å	Ag(2)-C(47): 2.455(8) Å

Fig. S30: ORTEP drawing of **2a**:

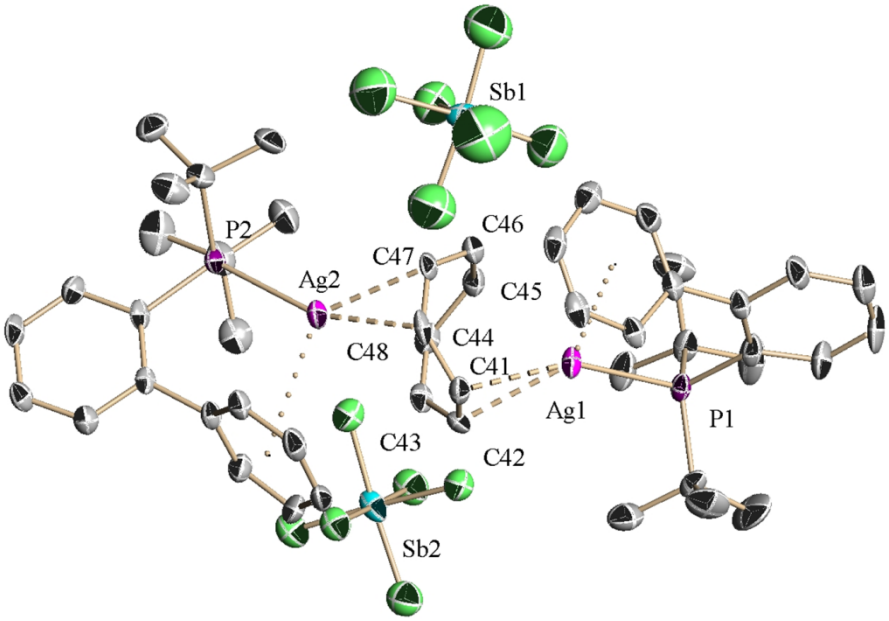

Crystal packing detail of **2a** viewed along the b-axis, hydrogen atoms are omitted for clarity:

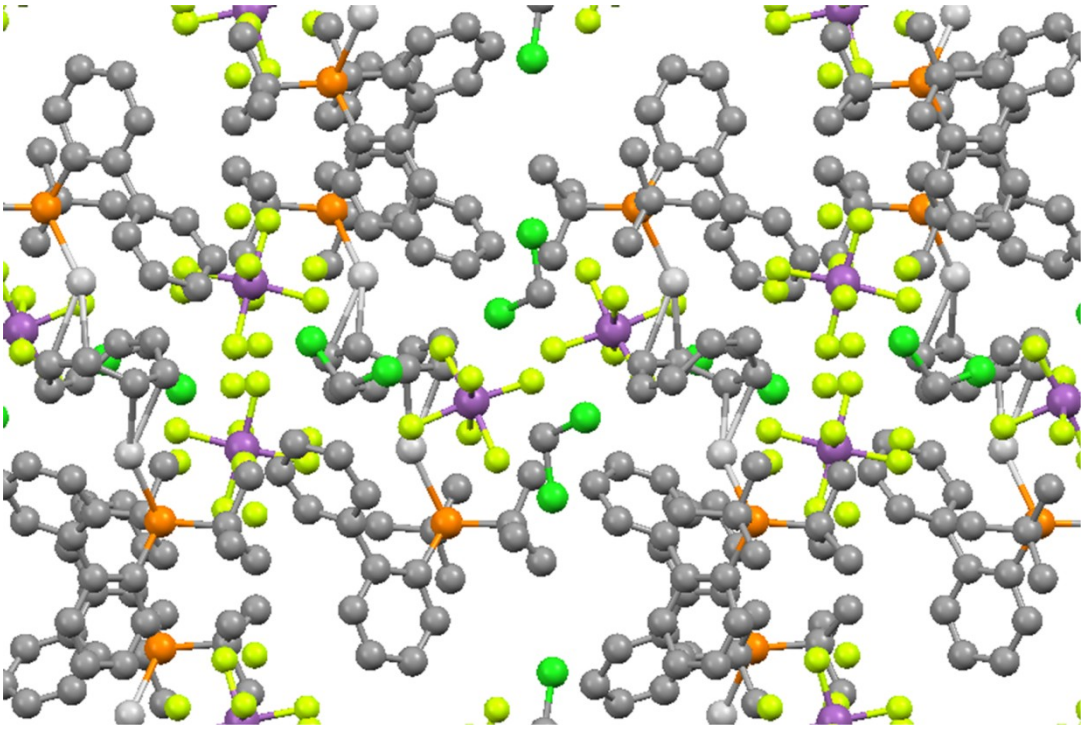

Fig. S31: ^{1}H NMR spectrum in CD_2Cl_2 for isolated complex **2** recorded at -80 ºC.

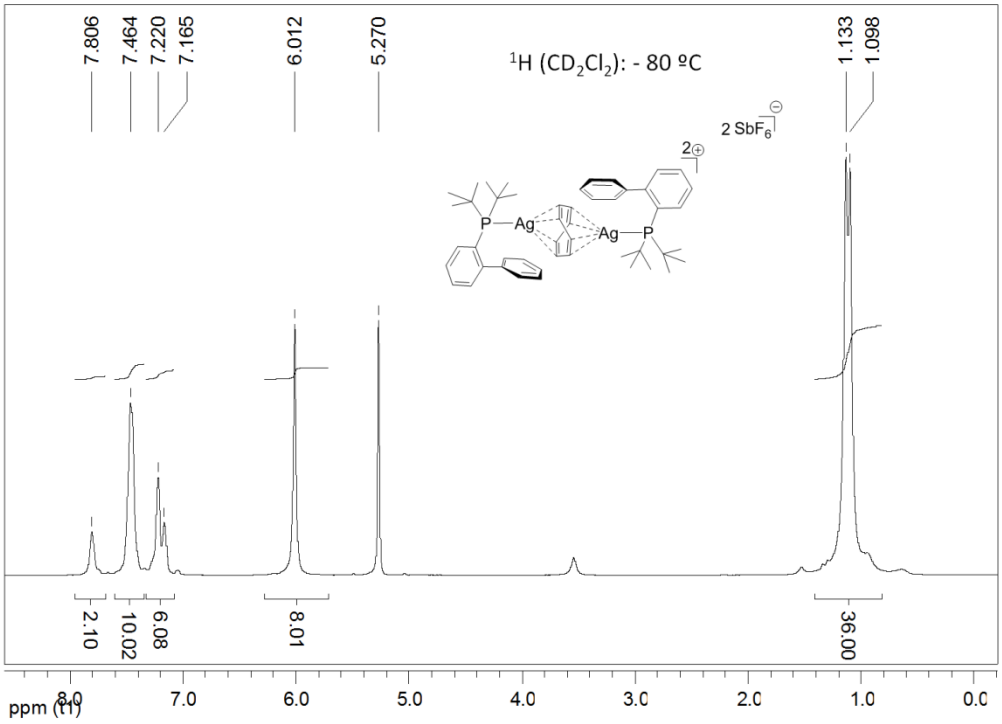

Magnification of the ^{1}H NMR peaks (**2**) at -80 ºC:

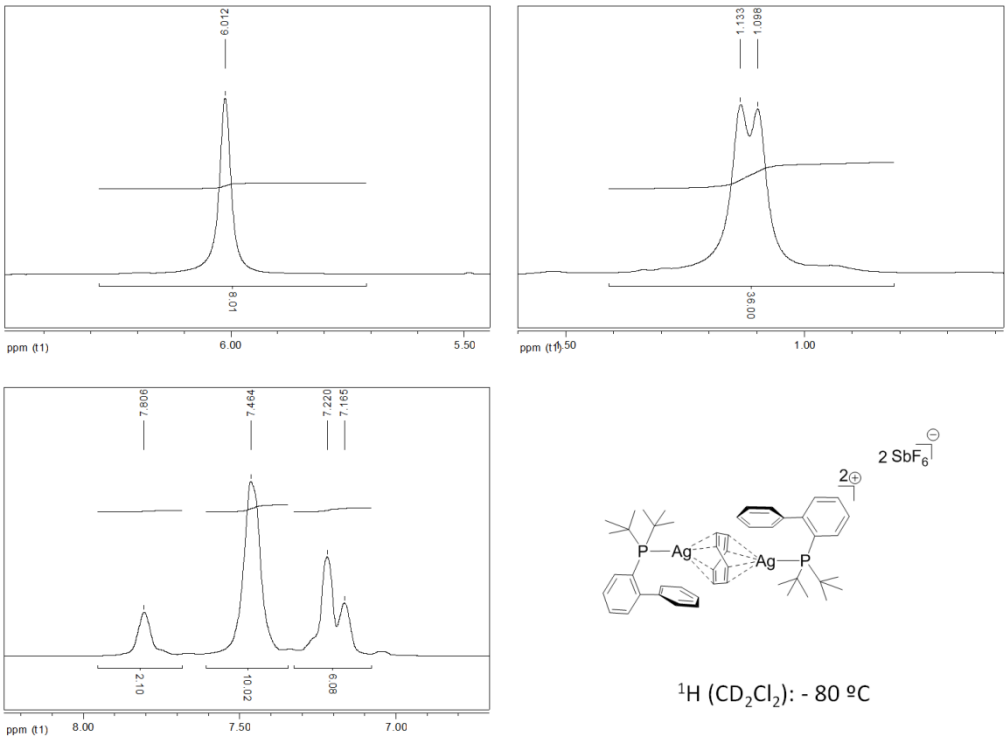

Fig. S32: ^{13}C NMR spectrum in CD_2Cl_2 for isolated complex **2** recorded at -80 ºC.

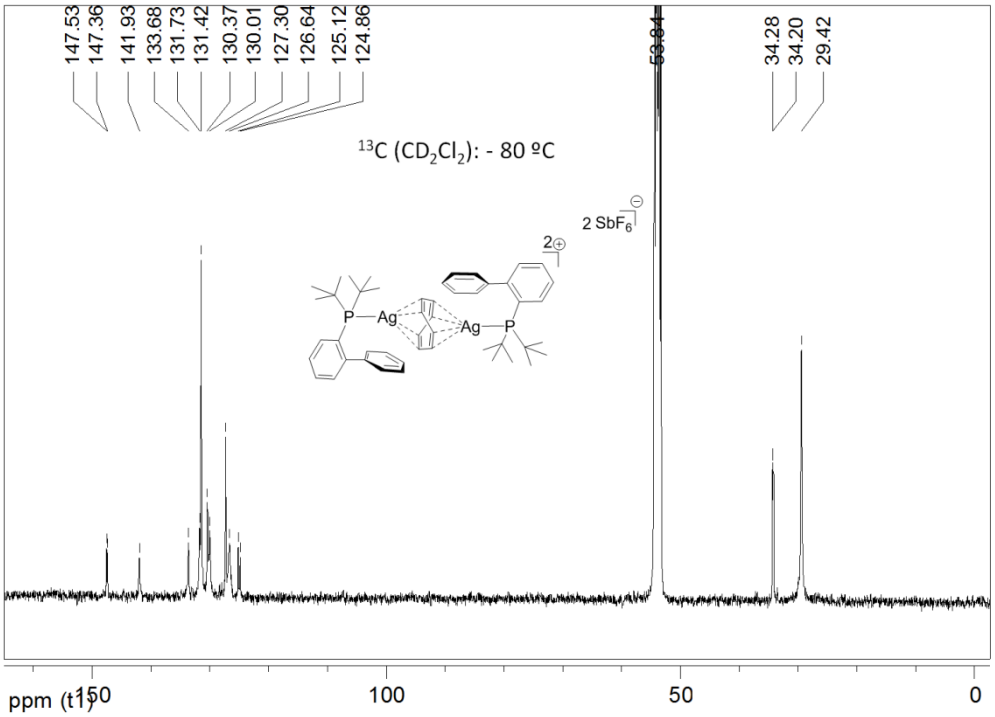

Magnification of the ^{13}C NMR peaks (**2**) at -80 ºC:

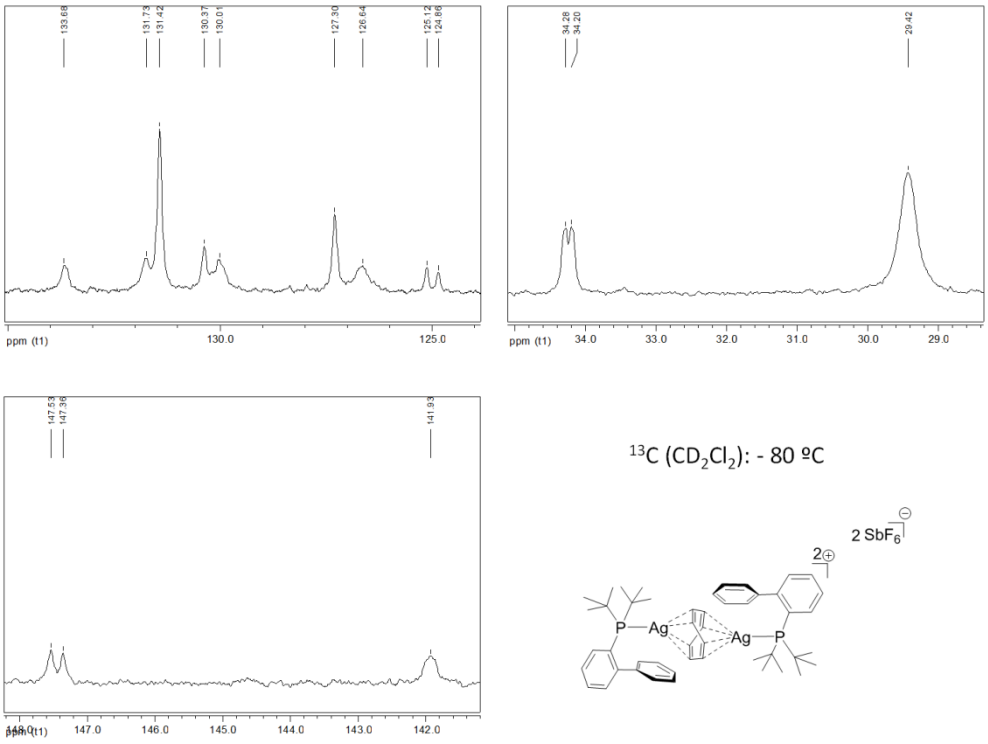

Table S4: Crystal data and structure refining for Silver aquo-complex **5**:

Empirical formula	$C_{20}H_{29}AgF_6OPSb$	
	$[C_{20}H_{29}AgOP, F_6Sb]$	
Formula weight	660.02	
Temperature	193(2) K	
Wavelength	0.71073 Å	
Crystal system	Monoclinic	
Space group	$P\ 2_1/c$	
Unit cell dimensions	a = 7.6971(13) Å	α= 90°.
	b = 22.120(3) Å	β= 103.508(4)°.
	c = 14.649(2) Å	γ = 90°.
Volume	2425.1(6) $Å^3$	
Z	4	
Density (calculated)	1.808 Mg/m^3	
Absorption coefficient	2.042 mm^{-1}	
F(000)	1296	
Crystal size	0.50 x 0.40 x 0.25 mm^3	
Theta range for data collection	1.70 to 25.25°.	
Index ranges	-9<=h<=9, -21<=k<=26, -17<=l<=11	
Reflections collected	22569	
Independent reflections	4369 [R(int) = 0.0401]	
Completeness to theta = 25.25°	99.4 %	
Absorption correction	Semi-empirical from equivalents	
Max. and min. transmission	0.6293 and 0.4283	
Refinement method	Full-matrix least-squares on F^2	
Data / restraints / parameters	4369 / 36 / 277	
Goodness-of-fit on F^2	1.013	
Final R indices [I>2sigma(I)]	R1 = 0.0480, wR2 = 0.1388	
R indices (all data)	R1 = 0.0532, wR2 = 0.1435	
Largest diff. peak and hole	1.273 and -1.277 $e.Å^{-3}$	

Fig. S33: ORTEP drawing of Silver aquo-complex **5**:

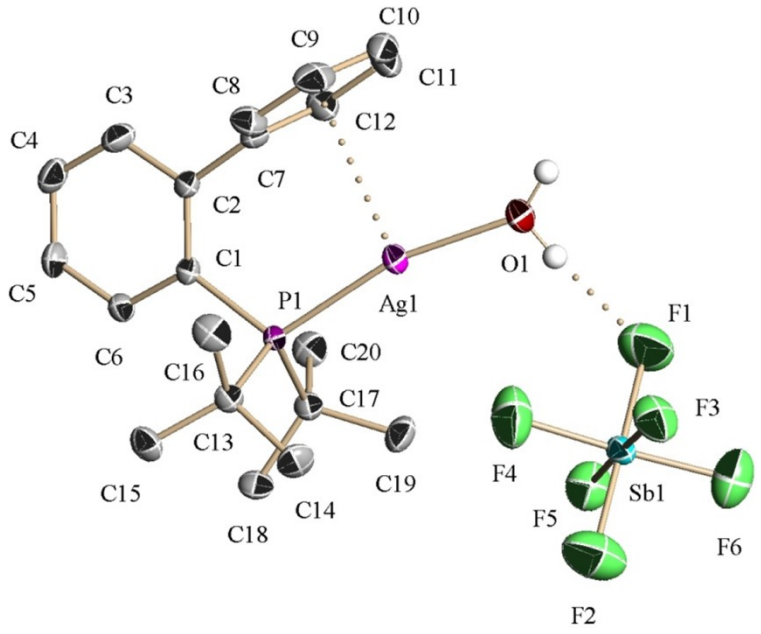

Crystal packing detail of Silver acuo-complex **5** viewed along the b-axis, hydrogen atoms are omitted for clarity:

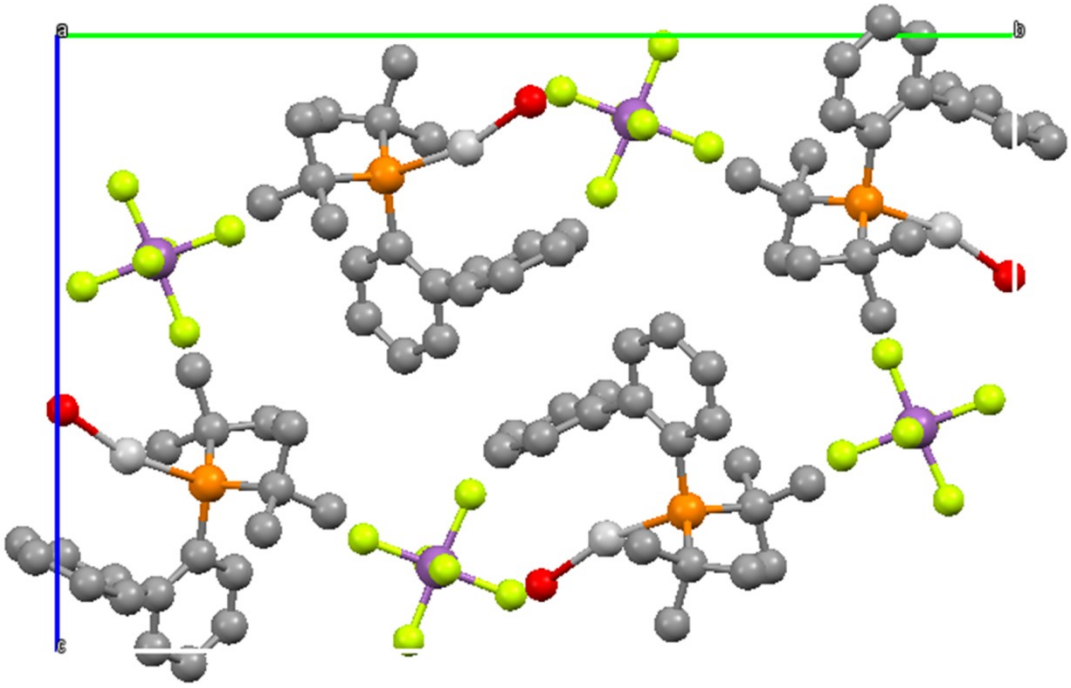

Fig. S34: Time-dependent UV/Vis spectra of acetonitrile solution of complex **1**.

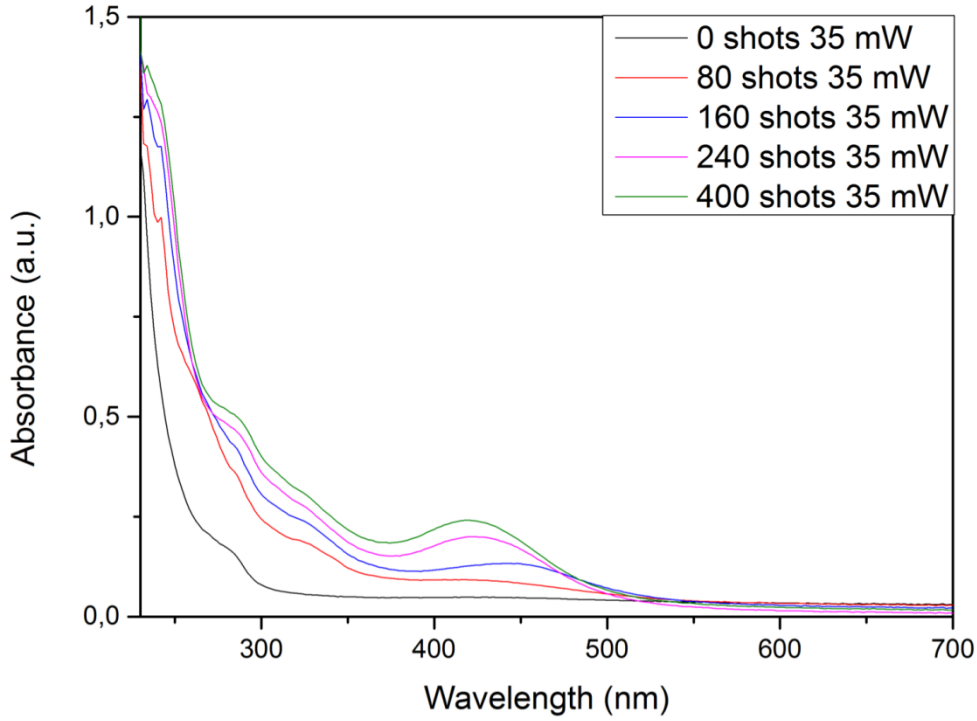

Fig. S35: Time-UV/Vis spectra of acetonitrile solution blanks of **1**, **4**, COT and Xphos.

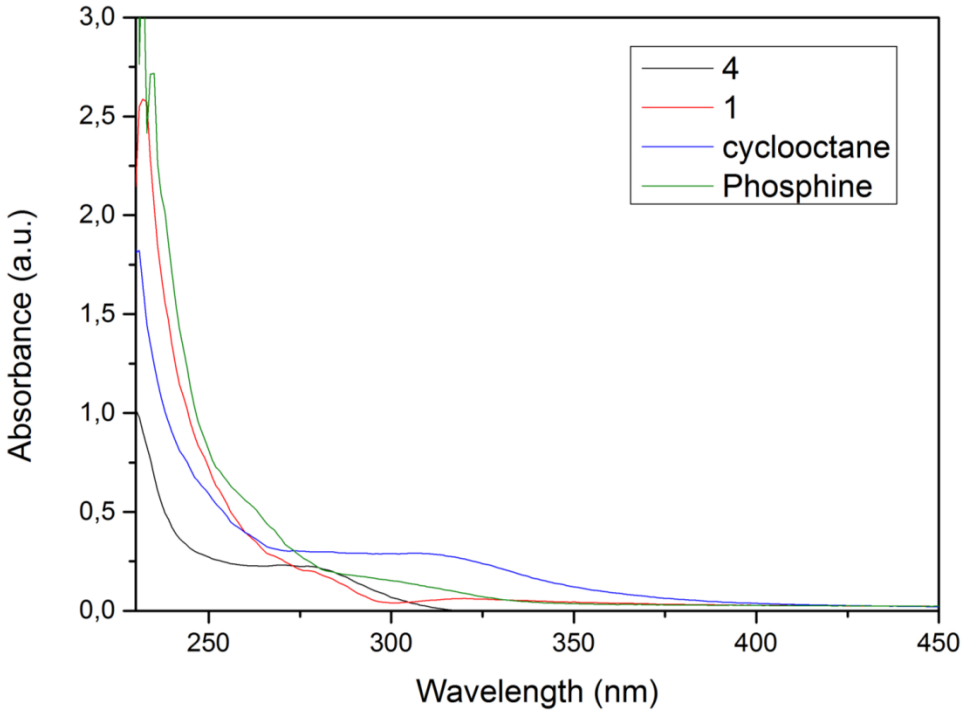

Fig. S36: Transient absorption spectroscopy of acetonitrile solution of complex **1** (5µs).

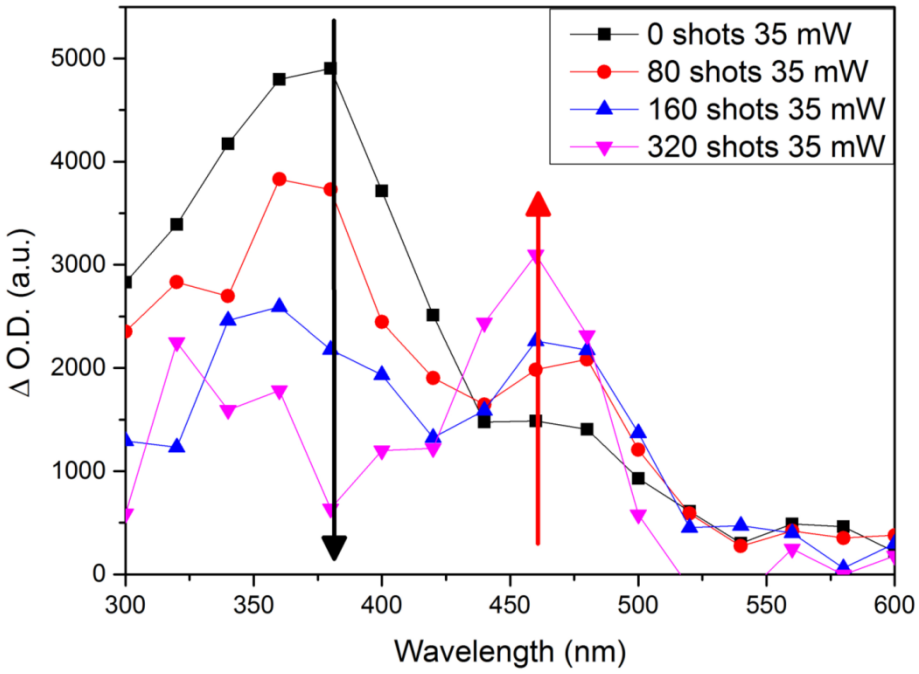

Fig. S37: Kinetics decay of 380 and 460 nm bands.

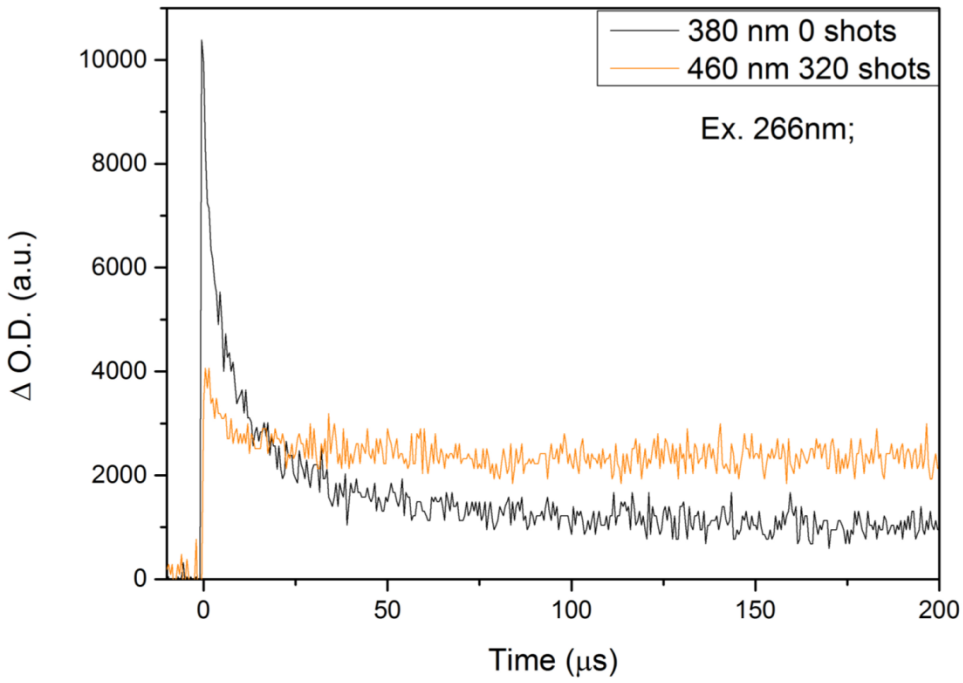

Fig. S38: Kinetics decay of 380 nm band.

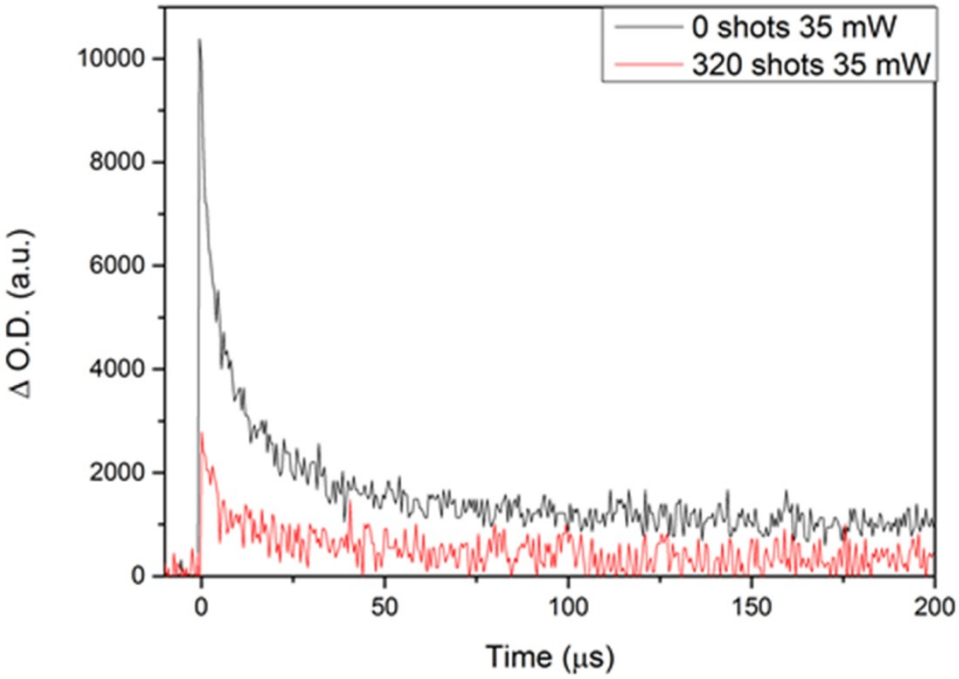

Fig. S39: Kinetics decay of 460 nm band.

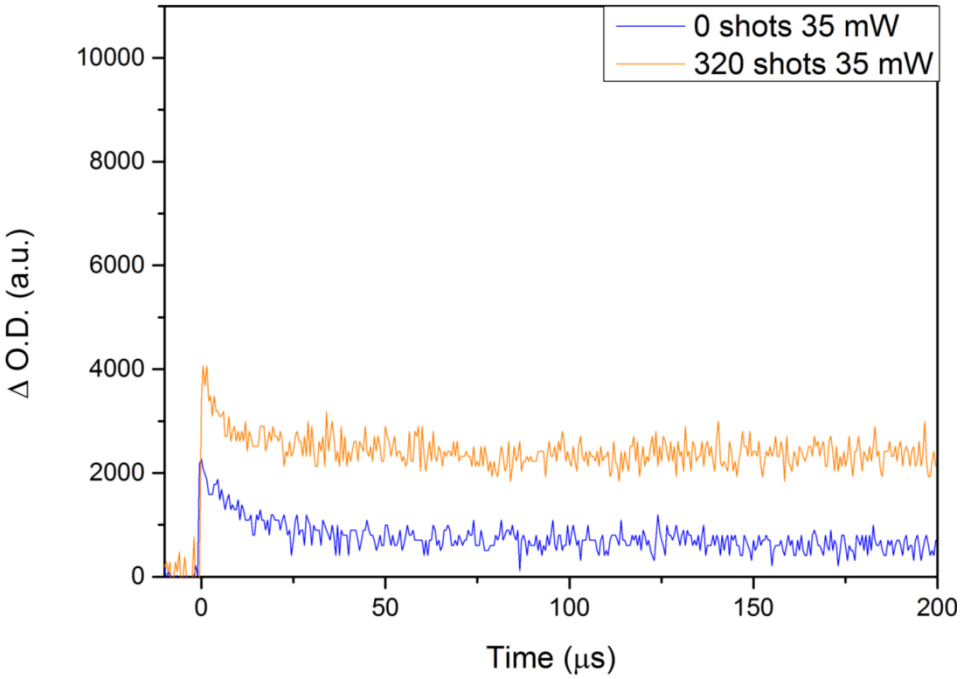

Fig. S40: HR-TEM of complex 4 after 360 shots at 30 mw.

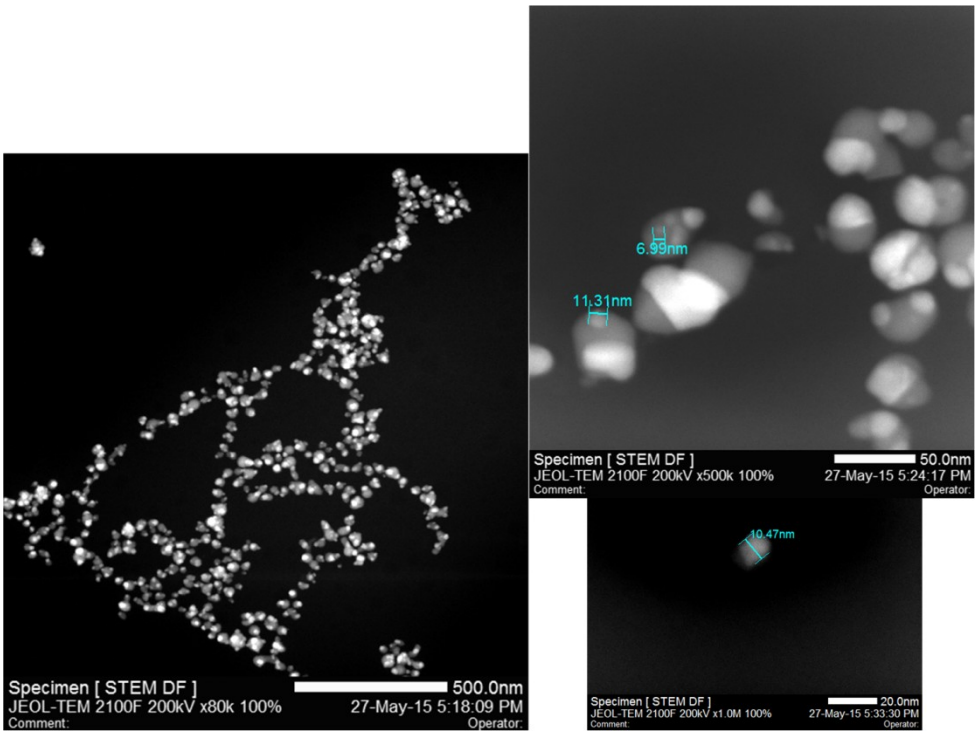

Fig. S41: HR-TEM of complex 4 after 720 shots at 30 mw.

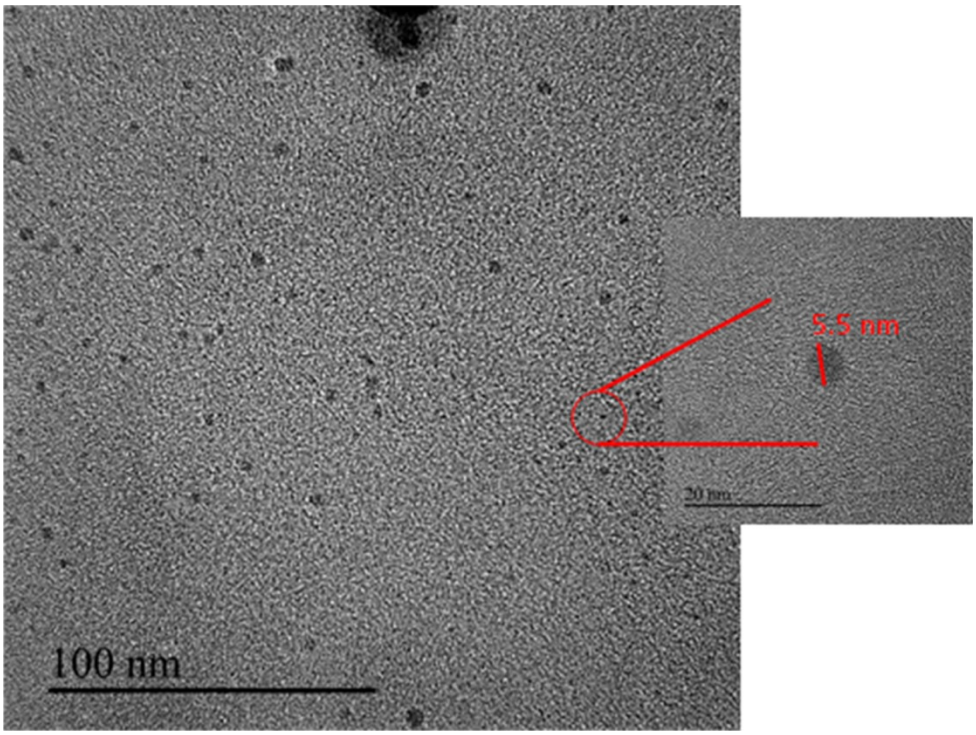

Fig. S42: HR-TEM of complex 4 after 720 shots at 30 mw.

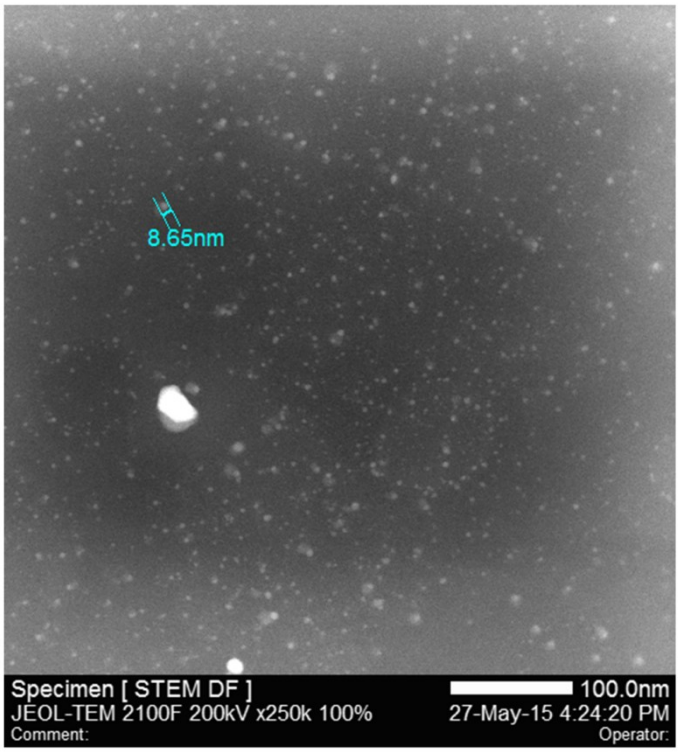

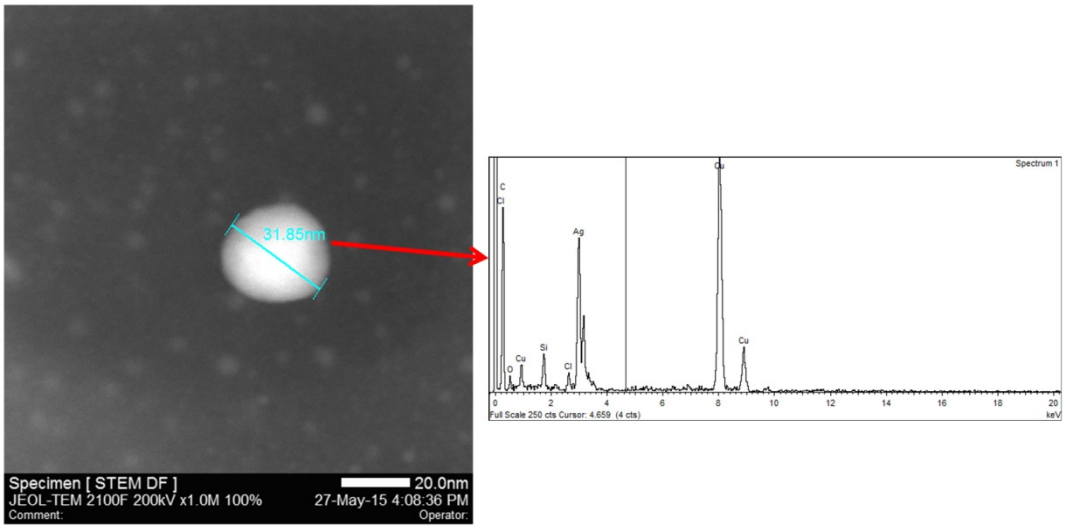

Fig. S43: HRESI-MS of cationic $[XPhos\text{-}Ag]^+$ fragment with the ^{107}Ag and ^{109}Ag isomers:

- Peak at 405.0717 m/z expanded to show the cluster of ions composition:

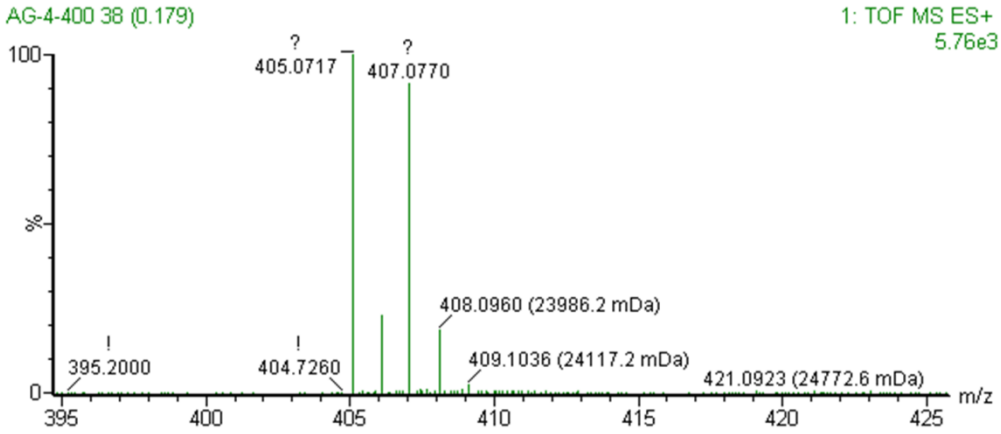

- Plot of the isotopic distribution for this $C_{20}H_{27}AgP$ chemical elements formula:

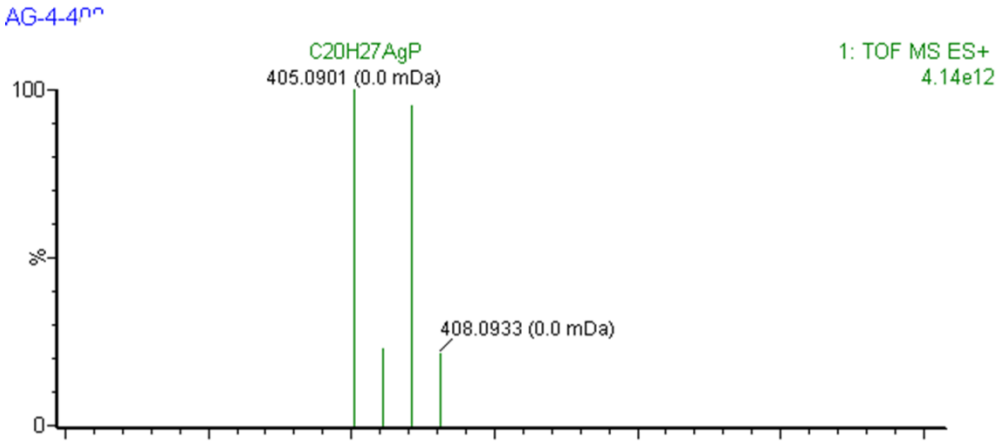

Fig. S44: HRESI-MS of [XPhos-Ag][$NCCH_3$] complex with the ^{107}Ag and ^{109}Ag isomers:

- Peak at 446.1163 m/z expanded to show the cluster of ions composition:

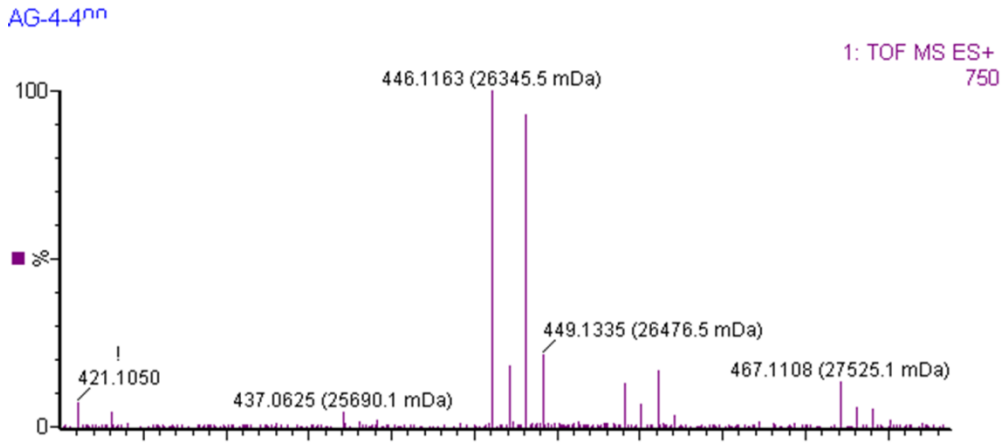

- Plot of the isotopic distribution for this $C_{22}H_{30}AgNP$ chemical elements formula:

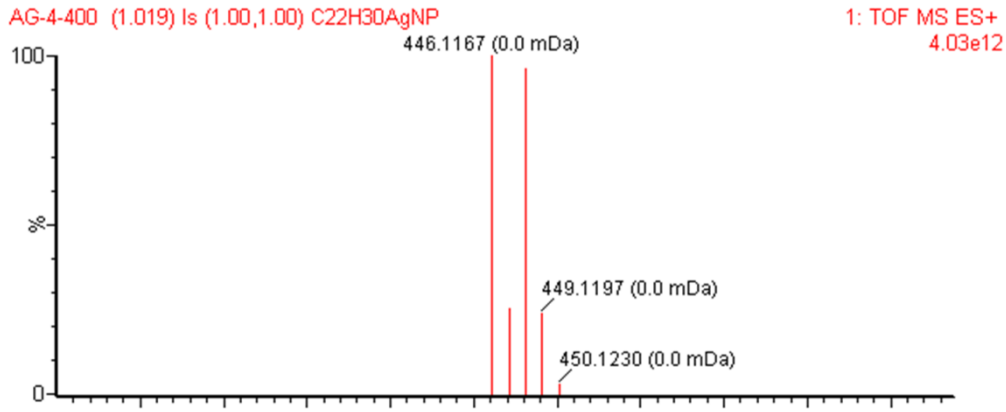

Fig. S45: HRESI-MS spectra of acetonitrile solution of complex **1** or **4** after 90 laser shots.

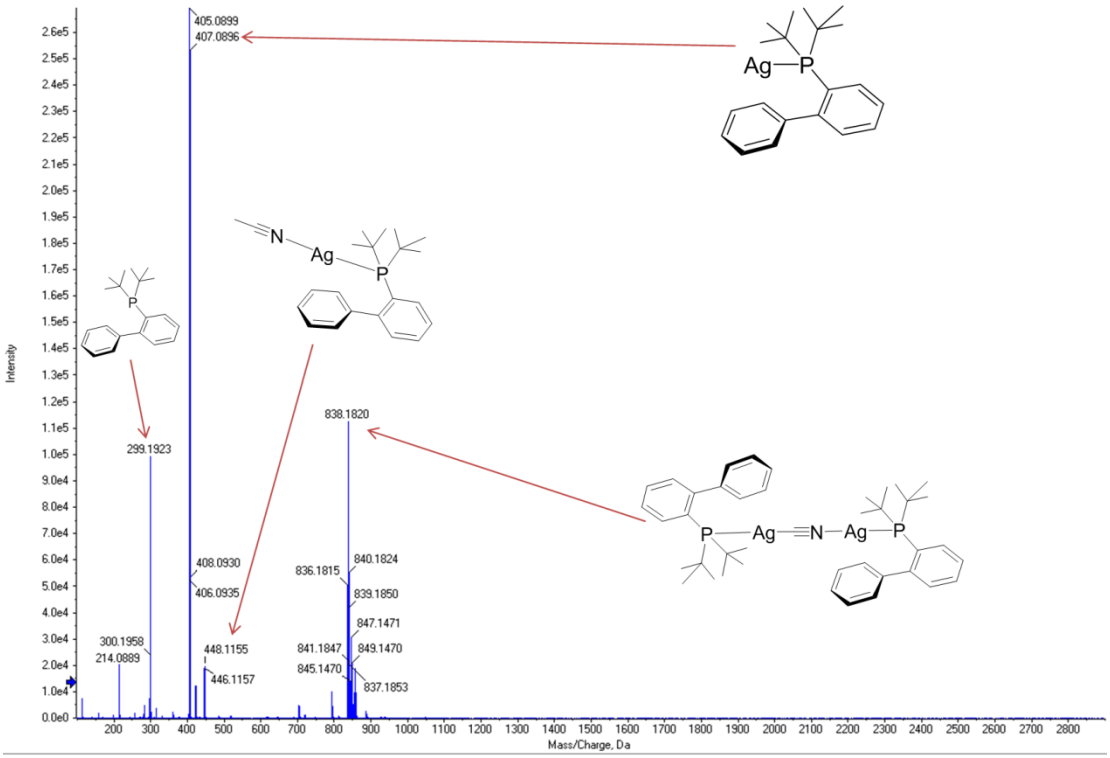

Fig. S46: HRESI-MS spectra of acetonitrile solution of complex **1** or **4** after 180 laser shots.

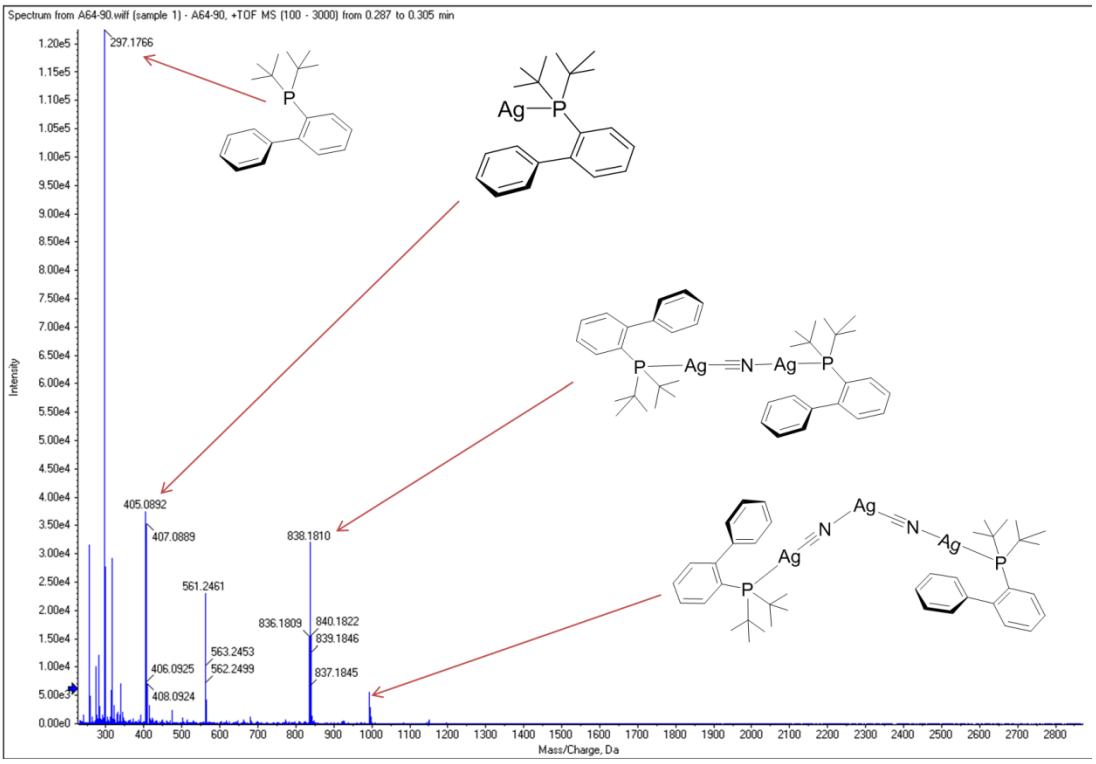

Magnification region from 200 to 460 Da:

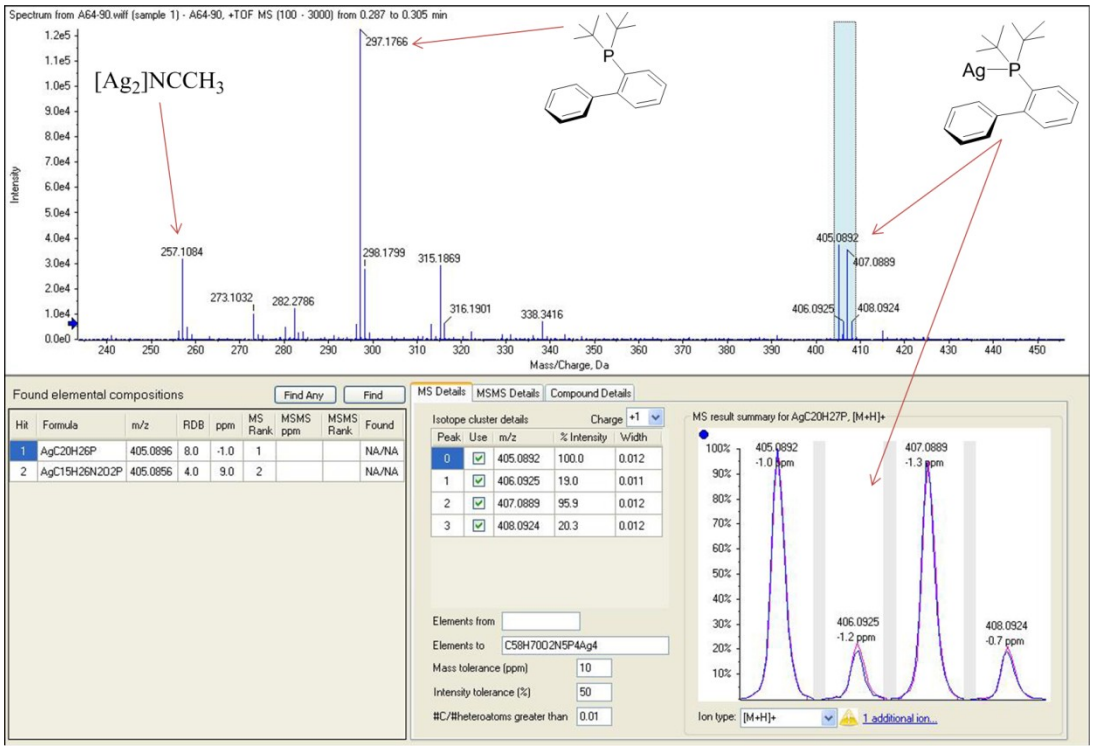

Fig. S47: HRESI-MS of cyanide bridged [(XPhos-Ag)$_2$(μ-CN)] complex after 360 laser shots:

- Peak at 838.1833 m/z expanded to show the cluster of ions composition:

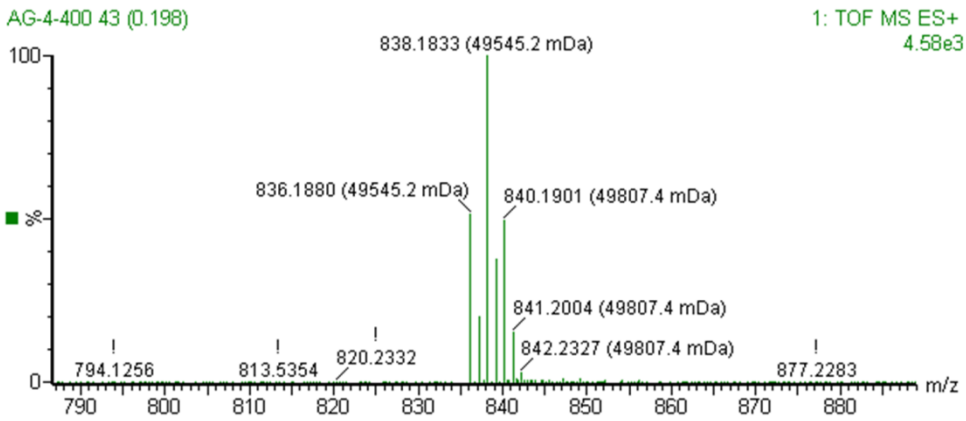

- Plot of the isotopic distribution for this $C_{41}H_{54}Ag_2NP_2$ chemical elements formula:

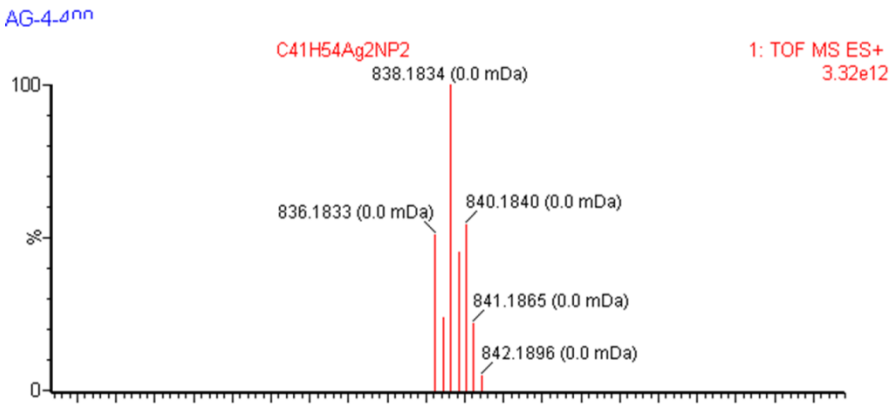

Fig. S48: HRESI-MS of cyanide bridged $[(XPhos\text{-}Ag)_2(\mu\text{-}CN)_2(\mu\text{-}Ag)]$ complex after 360 laser shots:

- Peak at 973.0960 m/z expanded to show the cluster of ions composition:

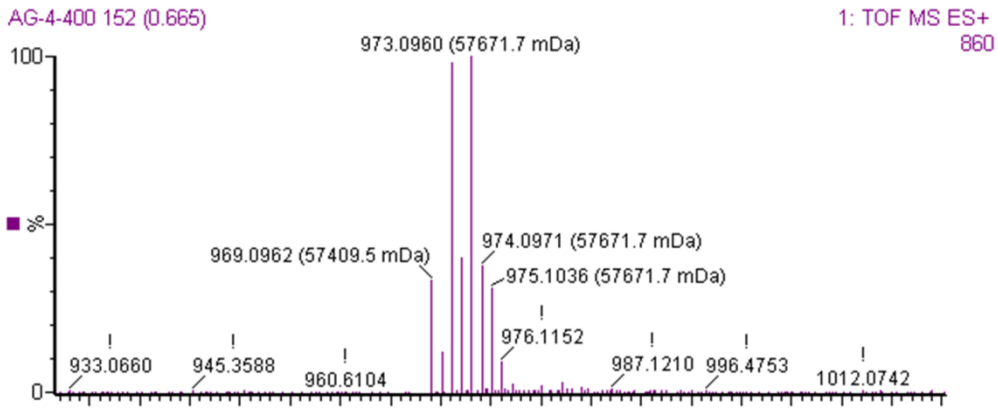

- Plot of the isotopic distribution for this $C_{42}H_{54}Ag_3N_2P_2$ chemical elements formula:

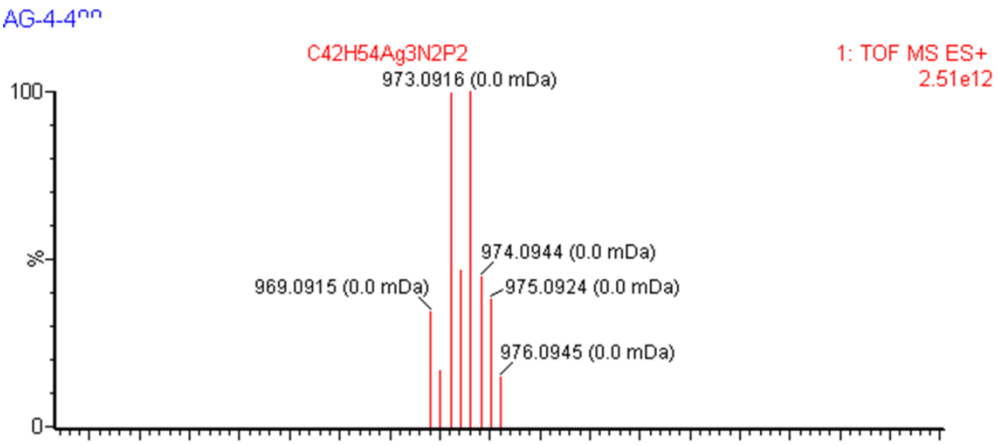

Fig. S49: HRESI-MS of cyanide bridged $[(XPhos\text{-}Ag)_2(\mu\text{-}CN)_3(\mu\text{-}Ag)_2]$ complex after 360 laser shots:

- Peak at 1106.0103 m/z expanded to show the cluster of ions composition:

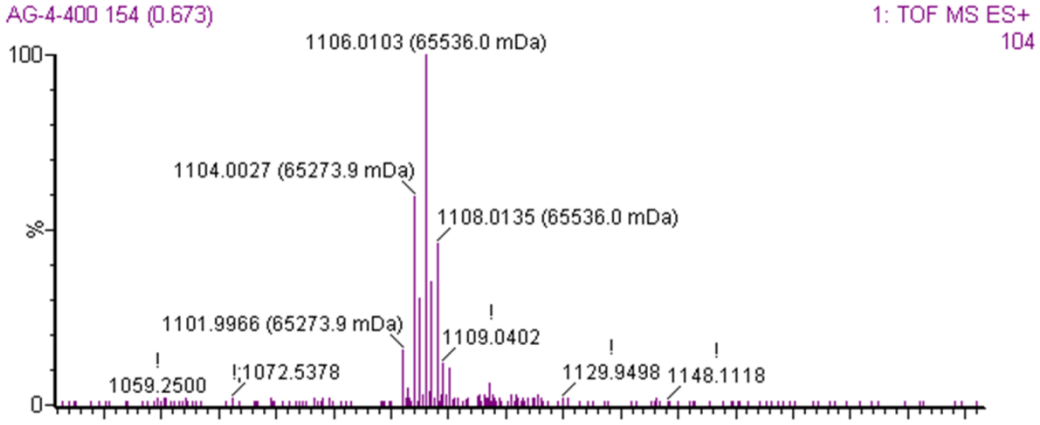

- Plot of the isotopic distribution for this $C_{43}H_{54}Ag_4N_3P_2$ chemical elements formula:

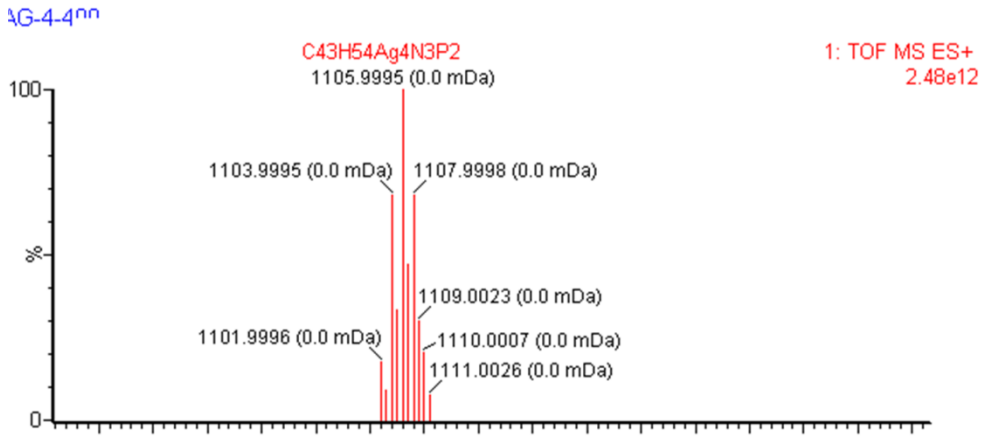

Fig. S50: HRESI-MS of cyanide bridged $[(XPhos\text{-}Ag)_2(\mu\text{-}CN)_4(\mu\text{-}Ag)_3]$ complex after 360 laser shots:

- Peak at 1238.9052 m/z expanded to show the cluster of ions composition:

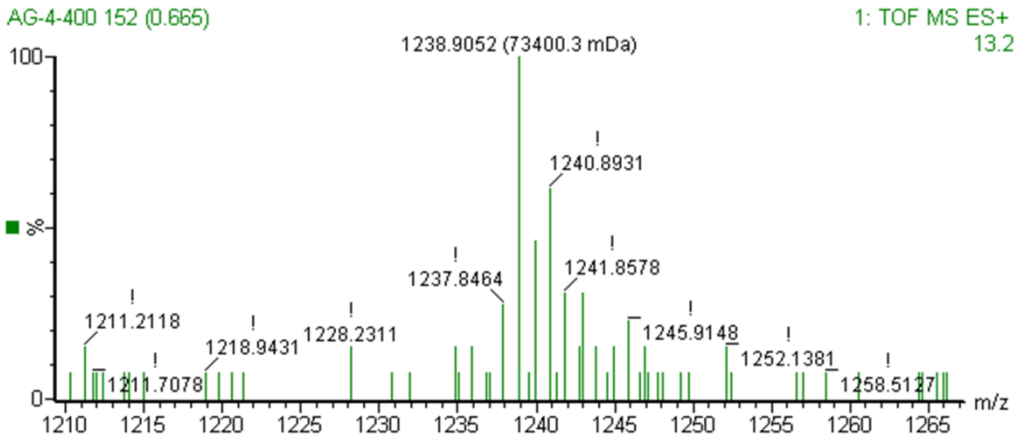

- Plot of the isotopic distribution for this $C_{44}H_{54}Ag_5N_4P_2$ chemical elements formula:

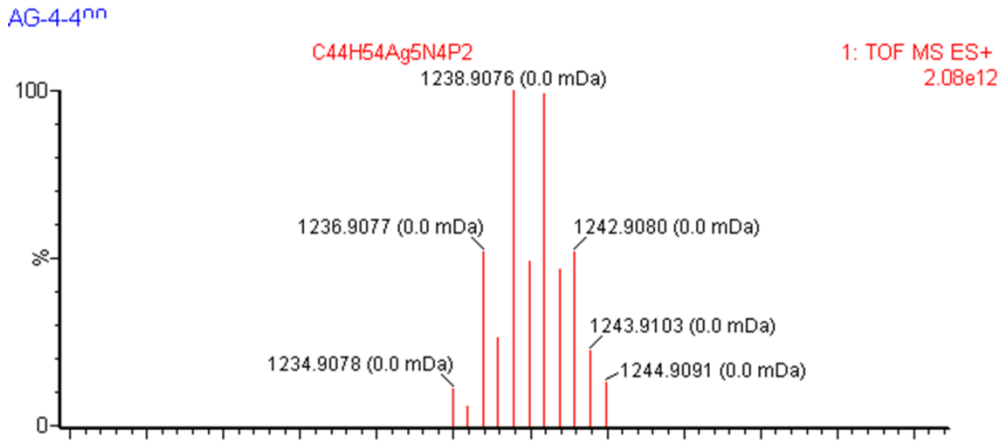

Fig. S51: Electrochemical behaviour of complexes **1**, **2** and **4**.

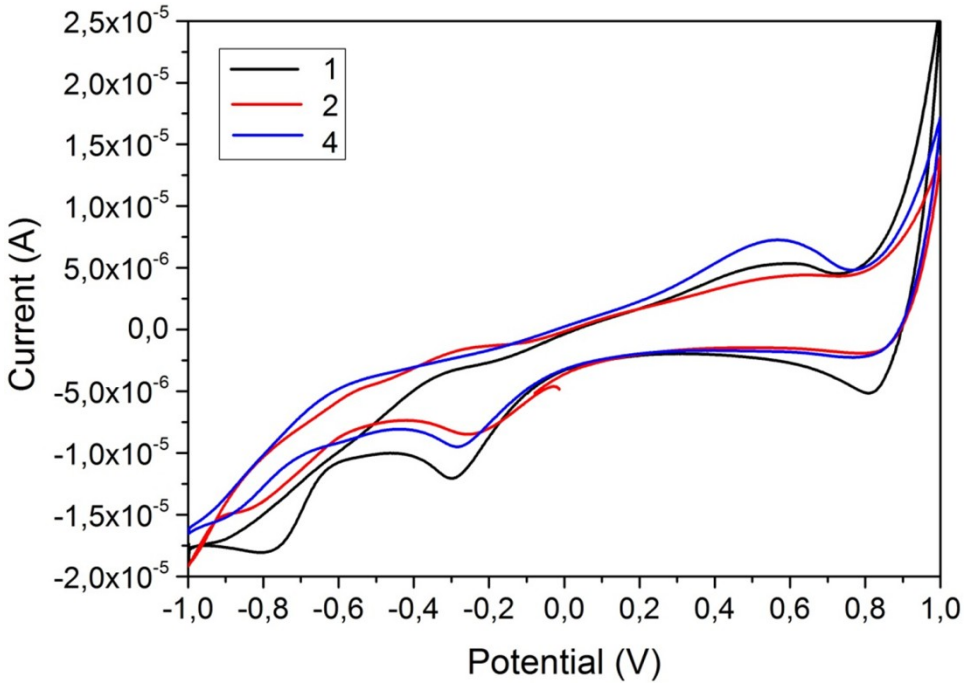

The electrochemical data for complex **1** shows two irreversible reduction waves at -0.30 and -0.80 V, respectively, that can be assigned to reduction of Ag and COT ligand.[1] In the case of complex **2**, a similar behaviour was observed with the two irreversible reduction waves appearing at -0.25 V and -0.79V that were also attributed to the reduction of Ag^+ and COT, respectively. In addition, for both complexes **1** and **2** a reversible oxidation wave attributable to the oxidation of Xphos ligand[2] at 0.70 V. The electrochemical data for complex **4** exhibited only a single reduction wave at -0.29 V attributable to the reduction of Ag^+ to Ag^0 in complex **4**. The peak corresponding to COT reduction previously recorded for complexes **1** and **2** was absent in the cyclic voltammogram of **4** probably because the electron density of COT is, in this case, too different to that of parent COT. The reversible oxidation wave at 0.68 V assigned to XPhos ligand oxidation[2] was also observed in this case.

[1] a) A. J. Fry, C. S. Hutchins and L. L. Chung, *J. Am. Chem. Soc.* **1975**, *97*, 591-595; b) R. D. Allendoerfer, *J. Am. Chem. Soc.* **1975**, *97*, 218-219.

[2] a) B. W. Smucker and K. R. Dunbar, *Dalton* **2000**, 1309-1315; b) M. G. Richmond and J. K. Kochi, *Inorg. Chem.* **1986**, *25*, 656-665; c) C. Gouverd, F. Biaso, L. Cataldo, T. Berclaz, M. Geoffroy, E. Levillain, N. Avarvari, M. Fourmigue, F. X. Sauvage and C. Wartelle, *Phys. Chem. Chem. Phys.* **2005**, *7*, 85-93.